

Determining the Contribution of Visual and Haptic
Cues during Compliance Discrimination in the Context
of Minimally Invasive Surgery

by

Evan Fakhoury

Submitted in accordance with the requirements
for the degree of Doctor of Philosophy

The University of Leeds
School of Mechanical Engineering

December 2015

The candidate confirms that the work submitted is his own, except where work which has formed part of jointly authored publications has been included. The contribution of the candidate and the other authors to this work has been explicitly indicated below. The candidate confirms that appropriate credit has been given within the thesis where reference has been made to the work of others.

In the paper listed below, the primary author completed all experimental studies, evaluation of data and preparation of publication. All authors contributed to proof reading of the articles prior to publication.

- E. Fakhoury, P. Culmer, and B. Henson, “**The Effect of Vision on Discrimination of Compliance Using a Tool,**” *International Journal of Human.-Computer Interaction*, vol. 30, no. 11, pp. 882–890, 2014.

Work was also disseminated through a conference presentation (oral). The following presentation contributed to the thesis:

- E. Fakhoury, P. R. Culmer, and B. Henson, “**The Effect of Indentation Force and Displacement on Visual Perception of Compliance,**” in *World Haptics Conference (WHC), 2015 IEEE*, 2015, pp. 88–93.

This copy has been supplied on the understanding that it is copyright material and that no quotation from the thesis may be published without the proper acknowledgement.

© 2015 The University of Leeds and Evan Fakhoury

The right of Evan Fakhoury to be identified as Author of this work has been asserted by him in accordance with the Copyright, Designs and Patents Act 1988.

Acknowledgements

First and foremost, I wish to express my deepest gratitude to my supervisors, Dr Brian Henson and Dr Pete Culmer. Brian, thank you for believing in me from day one. I would not be here today if it weren't for you. Your invaluable guidance along the way helped me grow as a researcher and a critical thinker. I could not have asked for a better advisor and mentor for my PhD. Pete, you've always been much more than a teacher to all of your students. Thanks for being a sharp supervisor when I was moving off track, a caring advisor when things got a little tough, and just a very good friend throughout.

I would also like to thank all the lab technicians who were happy to answer any of my questions or help me out when I needed it, in particular Mr. Abbas Ismail and Mr. Tony Weis.

This entire journey would not have been the same if it were not for great friends. In my opinion, a PhD is a difficult journey that is mentally, psychologically, physically and emotionally challenging. However, having friends around you who always support you, believe in you, and shake sense into you when you need it, really does make this whole process enjoyable. Nizar, thank you for being the best friend anyone can ask for, even from thousands of miles away. Zahra, James, Earle, you've helped me more than you'll ever know.

Last but certainly not least, I would like to thank my family: My father who has done the impossible just to provide me with all the opportunities he never had. Thank you for believing in me dad, I hope I always make you proud. My mom who still believes her son is the smartest man alive, and who am I to take that away from her! And of course, my sister Dona for her continuous support from day one. You guys believed in me even when I didn't believe in myself, and for that I am eternally grateful.

Abstract

While minimally invasive surgery is replacing open surgery in an increasing number of surgical procedures, it still poses risks such as unintended tissue damage due to reduced visual and haptic feedback. Surgeons assess tissue health by analysing mechanical properties such as compliance. The literature shows that while both types of feedback contribute to the final percept, visual information is dominant during compliance discrimination tasks. The magnitude of that contribution, however, was never quantitatively determined.

To determine the effect of the type of visual feedback on compliance discrimination, a psychophysical experiment was set up using different combinations of direct and indirect visual and haptic cues. Results reiterated the significance of visual information and suggested a visio-haptic cross-modal integration. Consequently, to determine which cues contributed most to visual feedback, the impact of force and position on the ability to discriminate compliance using visual information only was assessed. Results showed that isolating force and position cues during indentation enhanced performance. Furthermore, under force and position constraints, visual information was shown to be sufficient to determine the compliance of deformable objects.

A pseudo-haptic feedback system was developed to quantitatively determine the contribution of visual feedback during compliance discrimination. A psychophysical experiment showed that the system realistically simulated viscoelastic behaviour of compliant objects. Through a magnitude estimation experiment, the pseudo-haptic system was shown to be successful at generating haptic sensations of compliance during stimuli indentation only by modifying the visual feedback presented to participants. This can be implemented in research and educational facilities where advanced force feedback devices are inaccessible. Moreover, it can be incorporated into virtual reality simulators to enhance force ranges. Future work will assess the value of visual cue augmentation in more complicated surgical tasks.

Table of Contents

ACKNOWLEDGEMENTS	I
ABSTRACT	III
TABLE OF CONTENTS	IV
LIST OF FIGURES	VIII
LIST OF TABLES	X
ABBREVIATIONS	XI
1. INTRODUCTION.....	1
1.1. SURGICAL METHODS.....	2
1.1.1. <i>Open Surgery</i>	2
1.1.2. <i>Laparoscopic Surgery</i>	3
1.1.3. <i>Robotic Assisted Laparoscopic Surgery</i>	5
1.2. SURGICAL TRAINING	7
1.2.1. <i>Laparoscopic surgery training systems</i>	8
1.2.2. <i>Robotic surgery training systems</i>	8
1.2.3. <i>Haptic feedback devices for surgical simulation</i>	9
1.3. SUMMARY	10
2. LITERATURE REVIEW	12
2.1. INTRODUCTION	12
2.2. PERCEPTION	12
2.3. COMPLIANCE DISCRIMINATION.....	13
2.3.1. <i>Impact of haptic feedback using cutaneous information</i>	15
2.3.2. <i>Impact of haptic feedback using a tool</i>	17
2.3.3. <i>Impact of visual feedback</i>	18
2.3.4. <i>Cross-modal integration</i>	21
2.3.4.1. General cross-modal integration	21
2.3.4.1. Visio-haptic cross-modality during compliance discrimination	22
2.3.5. <i>Force feedback</i>	23
2.3.5.1. Effect of force feedback on compliance discrimination.....	23
2.3.5.2. Effect of force transmission ratio.....	24
2.3.6. <i>Pseudo-haptic feedback</i>	25
2.4. QUANTIFICATION OF SENSORY PERCEPTIONS.....	29
2.4.1. <i>Weber's law for compliance discrimination</i>	31

2.4.2.	<i>Psychophysical methods</i>	31
2.4.2.1.	Method of constant stimuli	31
2.4.2.1.	Method of limits	32
2.4.2.1.	The yes-no procedure.....	33
2.4.2.2.	The forced choice procedure.....	33
2.4.2.3.	The magnitude estimation ratio scaling procedure.....	34
2.5.	CONCLUSIONS	36
2.6.	OVERVIEW	37
2.7.	RESEARCH MOTIVATION.....	39
2.8.	AIM OF THE THESIS.....	41
2.8.1.	<i>Aim</i>	41
2.8.2.	<i>Objectives</i>	41
3.	STIMULI MODELLING	42
3.1.	BIOMECHANICS OF SOFT TISSUE.....	43
3.1.1.	<i>Viscoelasticity</i>	43
3.1.2.	<i>Viscoelastic models</i>	44
3.1.2.1.	Maxwell model	45
3.1.2.2.	Voigt model	46
3.1.2.3.	Kelvin model	46
3.2.	METHODS	48
3.2.1.	<i>Stimuli fabrication</i>	48
3.2.2.	<i>Compliance testing</i>	50
3.2.2.1.	Modular Universal Surface Tester (MUST)	50
3.2.2.1.	Custom Indentation Rig	50
3.2.2.2.	Mecmesin MultiTest 5-i	51
3.2.3.	<i>Viscoelastic model fitting</i>	51
3.2.3.1.	Maxwell model	52
3.2.3.2.	Voigt model	53
3.2.3.3.	Kelvin model	54
3.2.4.	<i>Regression Analysis</i>	54
3.3.	DISCUSSION	55
3.4.	SUMMARY	56
4.	THE EFFECT OF VISUAL CUES ON COMPLIANCE DISCRIMINATION	57
	ABSTRACT.....	57
4.1.	INTRODUCTION.....	58
4.2.	METHODS	59
4.2.1.	<i>Participants</i>	59
4.2.2.	<i>Stimuli</i>	59

4.2.3.	<i>Experimental design</i>	60
4.2.3.1.	Control task: Cutaneous feedback only	60
4.2.3.2.	Direct vision with touch through tool	60
4.2.3.3.	Indirect 2D vision with touch through tool	61
4.2.3.4.	Only touch through tool	61
4.2.3.5.	Only indirect vision	62
4.3.	EXPERIMENTAL ANALYSIS	63
4.4.	RESULTS	64
4.5.	DISCUSSION	66
5.	THE EFFECT OF INDENTATION DEPTH AND FORCE ON VISUAL COMPLIANCE DISCRIMINATION ..	69
	ABSTRACT	69
5.1.	INTRODUCTION	70
5.2.	METHODS	71
5.2.1.	<i>Participants</i>	71
5.2.2.	<i>Stimuli</i>	71
5.2.3.	<i>Experimental Set-up</i>	72
5.2.3.1.	Experiment condition: Maximum indentation depth	73
5.2.3.2.	Experiment condition: Maximum indentation force	73
5.2.4.	<i>Experimental Design</i>	74
5.3.	RESULTS	75
5.4.	DISCUSSION	76
6.	DEVELOPING AND VALIDATING THE PERCEPTUAL FIDELITY OF A NOVEL ROBOTIC PSEUDO-	
	HAPTIC FEEDBACK SYSTEM	80
	ABSTRACT	80
6.1.	INTRODUCTION	81
6.2.	METHODS	83
6.2.1.	<i>Pseudo-haptic system design</i>	83
6.2.2.	<i>Participants</i>	87
6.2.3.	<i>Stimuli</i>	87
6.2.4.	<i>Experimental design</i>	87
6.3.	EXPERIMENTAL ANALYSIS	91
6.4.	RESULTS	92
6.5.	DISCUSSION	94
7.	IDENTIFYING THE VISUAL ‘BOUNDARY OF ILLUSION’ USING A PSEUDO-HAPTIC FEEDBACK	
	SYSTEM	98
	ABSTRACT	98
7.1.	INTRODUCTION.....	99

7.2.	METHODS	99
7.2.1.	<i>Participants</i>	100
7.2.2.	<i>Stimuli</i>	100
7.2.3.	<i>Experimental design</i>	100
7.2.4.	<i>Experimental Procedure</i>	102
7.3.	EXPERIMENTAL ANALYSIS.....	105
7.4.	RESULTS	106
7.5.	DISCUSSION	ERROR! BOOKMARK NOT DEFINED.
8.	CONCLUSIONS.....	113
8.1.	SUMMARY	113
8.2.	ASSESSMENT OF RESEARCH OBJECTIVES	116
8.3.	GENERAL DISCUSSION.....	118
8.4.	FUTURE WORK.....	121
	REFERENCES.....	124
	APPENDIX A:	138
A.1.	CONSENT FORM.....	138
A.2.	CHAPTER 4 INFORMATION SHEET.....	139
A.3.	CHAPTER 5	140
A.4.	CHAPTER 6	141
A.5.	CHAPTER 7	142
	APPENDIX B: PROTOCOLS	144
B.1.	CHAPTER 6 EXPERIMENT PROTOCOL.....	144
B.2.	CHAPTER 7 EXPERIMENT PROTOCOL.....	145
	APPENDIX D: REGRESSION ANALYSIS DATA	148
	APPENDIX E: DISCUSSION ANALYSIS	149

List of Figures

Figure 1. OS (a,b) vs. LS (c)	3
Figure 2. Da Vinci robot set-up.....	6
Figure 3. Da Vinci console controllers used by surgeons to manipulate tools at the surgical site	7
Figure 4. The four experimental setups as presented by Freidman et al. [43]	16
Figure 5. Animation steps of the simulation of an elastic images using additional visual feedback [80] ..	29
Figure 6. A plot of the proportion ‘yes’ responses as a function of stimulus intensity.....	33
Figure 7. Spring-mass system (a) and damper-mass system (b) during tension	45
Figure 8. Schematics representing the (a) Maxwell, (b) Voigt, and (c) Kelvin models	47
Figure 9. Silicone tray used to cast the shapes of the samples	49
Figure 10. The 11 samples created for the psychophysical experiments	49
Figure 11. MUST rig (a) and custom indentation rig (b) during indentation of the samples	51
Figure 12. Force-displacement data from indenter (shaded grey) and fitted Maxwell function (solid black) for Sample # 6	53
Figure 13. Force-displacement data from indenter (shaded grey) and fitted Voigt function (solid black) for Sample # 6	54
Figure 14. RMSE when fitting the experimental indentation data to the Maxwell, Voigt and Kelvin models.....	56
Figure 15. D65 Daylight simulator, plastic sample frame and indenter tool used in the experiments.....	62
Figure 16. The 4 tasks performed by the participants: Direct vision with tool (a), indirect vision with tool (b), only tool touch (c) and only indirect vision (d)	63
Figure 17. Psychometric functions for all five 2AFC experiments	65
Figure 18. Standard deviations for the participants’ responses across all four experiments	65
Figure 19. Indentation rig holding the actuator and sensor during an indentation process	72
Figure 20. Participant positioning during the experiments.....	72
Figure 21. Light and video recording set-up during sample indentation	73
Figure 22. Psychometric functions plotted for the maximum indentation depth and force experiments, along with the averaged participants’ responses for each sample.	75
Figure 24. Standard deviations for the participants’ responses in both tasks	76
Figure 25. Visual variations at maximum indentation force and depth for samples 1, 6 (reference) and 11	79
Figure 26. Pseudo-haptic feedback system design and set-up	86
Figure 27. Schematic of indenter robot with the circular tray that holds all 11 samples	86
Figure 28. Experiment set-up: (1) indenter tool, (2) Omega.7 haptic feedback device, (3) computer monitor, (4) silicone sample observed during indentation, (5) speed & position indentation guide	88

Figure 29. Flow chart describing the process occurring within the pseudo-haptic system during an indentation task	89
Figure 30. Robotic system set-up: (1) indenter position, (2) HD webcam, (3) Rotating tray, (4) robot used for linear sample indentations, (5) robot used to rotate tray to one of 11 set positions, (6) robot used to mount camera	90
Figure 31. Participant performing a sample indentation	90
Figure 32. Flowchart describing the participant indentation procedure	91
Figure 33. Participant’s screen showing the physical sample on left and indentation illustration on right during the experiment	91
Figure 34. Psychometric function representing participants’ performance during the experiment. The JND value is the difference in stiffness between those corresponding to the ratings at 84% and 50%	93
Figure 35. Weber fractions for all twelve participant	94
Figure 36. Flow chart describing the process occurring within the pseudo-haptic system during an indentation task	102
Figure 37. (a) Participant’s screen showing the physical sample on left and indentation illustration on right during the experiment, (b) participant indenting stimuli using the haptic feedback device	105
Figure 38. Flowchart describing the participant indentation procedure	105
Figure 39. Distribution of Weber fractions and Steven’s power constants across all the participants, with the dotted lines representing the group means	108
Figure 40. Visual difference and perceived haptic difference in compliance between reference and test samples	108
Figure 41. Steven’s power function fitted to the participants’ softness ratings	109
Figure 42. Softness ratings vs compliance of the samples for $a = 0.18$ (obtained from the results), 0.42 and 0.8 (retrieved from [88]), plotted in log-log scale	110
Figure 43. Steven’s power law plotted for the power function obtained in this chapter, as well as for viscosity and tactual hardness obtained from the literature [88].....	112
Figure 44. Average Weber fractions along with the standard error for all nine experiments conducted throughout the thesis.....	150

List of Tables

Table 1. Specifications and prices of current commercially available force feedback devices [20].....	10
Table 2. Variations of cross-modal sensory interactions in virtual environments [59].....	23
Table 3. Stimuli intensities with their corresponding proportions detected	33
Table 4. Representative exponents of the power function relating subjective magnitude to stimulus magnitude [88].....	35
Table 5. A: B: Plasticizer ratios for making each of the 11 samples	49
Table 6. Stiffness and damping coefficients obtained via fitting indentation data to the Maxwell model	52
Table 7. Stiffness and damping coefficients obtained via fitting indentation data to the Voigt model	53
Table 8. Stiffness and damping coefficients obtained via fitting indentation data to the Kelvin model ...	54
Table 9. β values for all experiments with α and γ fitted using the logistic function.....	64
Table 10. α and β values for both tasks	75
Table 11. Omega.7 workspace, forces and resolution for all degrees of freedom	84
Table 12. Denso VS-068 specifications.....	84
Table 13. α and β values obtained by fitting participants' responses to $P(x)$	93
Table 14. Stiffness, theoretical softness rating and mean participant rating for each sample.....	107
Table 15. Visual stiffness and perceived haptic stiffness for each test sample compared to the reference sample.....	107
Table 16. Weber fractions and β values obtained in each psychophysical experiment	113
Table 17. Example of a full factorial pseudo-haptic experiment design	122
Table 18. R squared and root mean square error between model fits and experimental data for all samples	148
Table 19. Dunn's between-tasks post hoc tests with corrections.....	149

Abbreviations

2AFC	Two-alternative forced-choice
2D	Two-dimensional
3D	Three-dimensional
DoF	Degree of freedom
FDA	Food and drug administration
JND	Just noticeable difference
LS	Laparoscopic surgery
MIS	Minimally invasive surgery
MUST	Modular universal surface tester
OS	Open surgery
POE	Point of objective equality
PSE	Point of subjective equality
RALS	Robotic assisted laparoscopic surgery
RMIS	Robot-assisted minimal invasive surgery
SLS	Standard linear solid
VE	Virtual environment
VR	Virtual reality

1. Introduction

Contact mechanics, physiology, neuroscience, and psychophysics are all aspects that are required to understand the human haptic system [1]. We are continuously interacting with objects in our surrounding environments where visual, auditory, and haptic information are gathered and used. Surgeons use their hands or tools to perform complicated procedures. Visual information is either direct such as in open surgery (OS) or indirect such as in minimally invasive surgery (MIS). The ability to discriminate tissue compliance is critical in any surgical setting. Surgeons assess the mechanical properties of tissue using a combination of haptic and visual feedback. Finding means of enhancing the visual-haptic integration during basic surgical tasks such as palpation, a basic yet crucial method of tissue examination, could lead to improved performance during surgery and ultimately, to a happier patient.

In this introduction, the history and advancements of surgery as well as surgical training are discussed. In OS, surgeons use their fingers to manipulate tissue directly. Information regarding tissue properties such as compliance and texture are mostly obtained through cutaneous information which is any type of feedback related to the skin. Laparoscopic surgery (LS), a form of MIS, requires surgeons to use long slender tools to operate through small incisions. Haptic feedback is received indirectly through the mechanical elements of the instrument being held. While open surgical settings allow the surgeon direct visual access into the operating theatre, visual access in LS is restricted to a two-dimensional (2D) monitor relaying a direct camera feed. This reduced haptic and visual feedback weakens a surgeon's ability to accurately discriminate compliance of tissue which can lead to unintended tissue trauma such as scarring and internal bleeding [2].

Virtual reality (VR) laparoscopic simulators are being used more and more in training facilities and hospitals. These simulators create a virtual environment similar to that in a laparoscopic procedure. The aim of these simulators is to accelerate learning of challenging techniques and procedures and to introduce novice surgeons to LS without risking real damage to patients [3]. These systems have become very realistic and are used in several hospitals today to train both novice and experienced surgeons

on old and new surgical methods. These systems, however, are very expensive and not accessible to all hospitals or teaching universities [3].

On this basis, this research is an assessment of the contribution of visual, haptic and visio-haptic feedback during compliance discrimination of compliant objects simulating tissue palpation in MIS, RALS, or VR surgical training. By determining the contribution of visual and haptic feedback during such surgical tasks, it may be possible to enhance a surgeon's perceptual process, hereby reducing unintended tissue damage in MIS. Furthermore, a quantitative analysis of the contribution of visual and haptic cues could also be incorporated into future VR training simulators in order to enhance the training process both visually and haptically.

1.1. Surgical Methods

The ultimate objective of scientific medicine is to prolong human life and reduce suffering [4]. Surgery is an operation performed by a surgeon on a patient using specialized techniques and tools in order to investigate and/or treat a health condition such as disease or injury. Haptic feedback, which is any form of feedback involving touch, is a key aspect of surgery. Three sensory feedback channels govern haptic information processed during surgery: visual, kinaesthetic, and tactile feedback [5]. Visual feedback provides the surgeon with visual information regarding shape, colour, position, velocity, as well as tissue features. Kinaesthetic feedback provides surgeons with force, position, and velocity information as perceived through their arms via contact with the tissue. Tactile feedback relates physical tissue properties to the surgeon such as texture, temperature, and stiffness through direct contact with the tissue [5]. By degree of invasiveness, the two types of surgery are OS and MIS.

1.1.1. Open Surgery

OS is an invasive surgical procedure in which a large incision to the outer body is performed in order for the surgeon to access the targeted area (Figure 1) [6]. Surgeons rely on their gloved hands for haptic feedback and have direct visual access into the operating site. The advantages of OS include ensuring direct visual and haptic access for the surgeon during an operation. Surgeons have direct visual access to the surgical viewport and can manoeuvre around, palpate, and manipulate tissue using their

fingers. Moreover, force, position, and velocity information are directly perceived by the surgeon [5]. Previous research has shown that haptic information transmitted through the fingertips is more reliable than that using a tool [7], [8]. On the other hand, the disadvantages of OS include excessive invasiveness, longer patient recovery time, longer hospital stay and larger scar size left after operation completion [9].

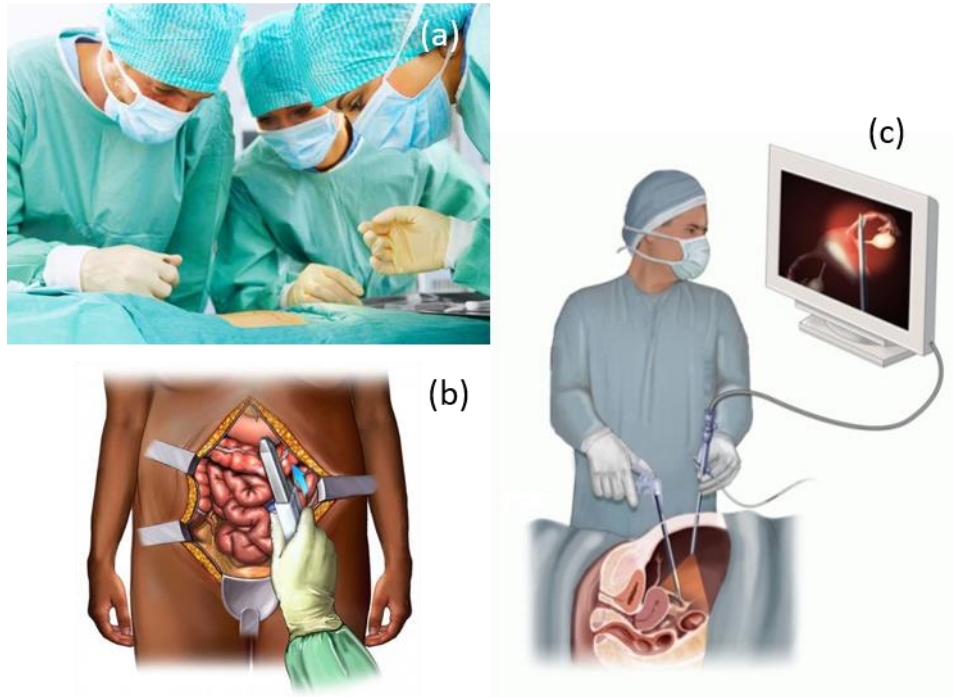


Figure 1. OS (a,b) vs. LS (c)

1.1.2. Laparoscopic Surgery

LS is a type of MIS in which entire procedures are performed through small incisions in the abdomen via slender tools (Figure 1). Surgeons use these tools to perform several tasks such as cutting, suturing, tying knots, and palpating tissue to check for tumours and unhealthy tissue [10]. Today, operations such as splenectomy and cholecystectomy are performed using LS [11]. LS has gained considerable popularity all over the world due to its significant advantages over OS which include shorter hospital stay, minimal invasiveness, reduced operating time, reduced patient trauma and blood loss, and quicker recovery time, less need for narcotic pain medicine [9], [12]–[14]. While LS has replaced OS in numerous procedures, it still poses some risks that are yet to be resolved. Surgeons rely on limited haptic feedback from tools

which are inserted into small incisions, making the process more difficult than OS [15].

Perhaps the greatest limitation in LS is the reduced haptic feedback translated to the surgeons where they are forced to rely on feedback from those long slender tools inserted into tiny incisions, as opposed to directly using their hands such as in OS [16]. Laparoscopic instruments can often result in excessive use of force leading to unintended tissue scarring [17]. Kazi [18] investigated the effect of force feedback in LS. Results showed that the introduction of force feedback could reduce the maximum exerted force by up to 40%. Bholat et al. [19] set up an experiment in which blindfolded surgeons were asked to identify shapes and analyse textures of objects via three methods of haptic feedback: direct contact, indirect contact using conventional instruments, and indirect contact using laparoscopic instruments. Results showed that while direct contact is superior to indirect contact during the shape identification tasks, laparoscopic instruments were superior to direct contact during texture analysis tasks. These findings suggest that laparoscopic instruments do in fact provide the surgeons with haptic feedback. Standard LS suffers from lack of cutaneous haptic feedback information to the surgeon. However, researchers have shown that standard laparoscopic tools actually amplify the haptic information available during tasks such as fine texture analysis [20].

In LS, visual information is provided to the surgeon through a 2D monitor display as opposed to direct vision in OS. The nature of LS means that surgeons rely primarily on visual cues to guide them through manoeuvres [15]. Gerovichev et al. [21] evaluated the effect of both visual and haptic feedback on human performance during needle insertion. Results showed that by introducing real-time visual feedback, user performance was improved by at least 87% highlighting the effect of visual cues during surgical tasks. It was suggested that the introduction of visual feedback provides greater improvement in performance than force feedback. Moreover, when both force and visual feedback were presented to the users, performance was improved by at least 43%. This suggests that while visual feedback may in some cases be superior to haptic feedback, the combination of both might be more effective in tasks such as needle insertion. Tavakoli et al. [22] showed that haptic feedback can be replaced with visual on-screen feedback during basic LS tasks in order to reduce the

exerted forces. Later chapters in this thesis aim to determine the role of visual feedback in MIS.

1.1.3. Robotic Assisted Laparoscopic Surgery

Robotic surgery emerged due to a need to improve the precision of surgical technologies [23]. Robotic platforms have been researched, designed, built, and optimised in order to improve the surgeons' performance during surgeries. Different robotic systems possess different degrees of freedom. The degree of freedom of a mechanical system is the number of independent parameters defining its configuration. Lanfranco et al. [24] produced a comprehensive summary of the history of surgical robotics. The first robot ever to have been used was PUMA 560 in the field of neuroscience, followed by the PROBOT for urology, ROBODOC for orthopaedics, and then Aesop (Computer Motion Inc., Goleta, CA) as a means of controlling the camera during LS. As part of the ninth NASA Extreme Environment Mission Operations (NEEMO) in their underwater laboratories, SRI International designed and successfully demonstrated a surgical robotic system allowing surgeons to remotely perform telesurgery during battlefield-based trauma. Zeus (Computer Motion Inc., Goleta, CA) was the first robotic system with the ability to be actively controlled by a surgeon via a remote console station. It was eventually phased out following the merger of Computer Motion and Intuitive Surgical in favour of the Da Vinci robot. These systems, however, were primarily designed and built for research and development purposes, and not for mass production and commercial use in hospitals.

Today, the da Vinci robot (Intuitive Surgical Inc., Sunnyvale, California) is the only Food and Drug Association (FDA) approved surgical robot currently on the market [23]. The da Vinci (Figure 2) is making its way slowly into more and more hospitals and research institutes around the world [25]. The 'master-slave' system consists of three parts: the surgeon's console, the video electronics tower, and the robotics tower which supports three robotic arms. The surgeon takes a seat at the console where he has visual access into the operation field via a binocular three-dimensional (3D) imaging system (Figure 3). The surgeon uses his or her feet to activate pedals adjusting the robotic arms and instruments. Using their hands to grasp and manipulate the robotic instruments, the surgeon can control the movement of the robotic arms

connected to the robotic tower. Disadvantages of this system include its considerably high cost, the lack of force feedback present for the surgeon, and the bulkiness of the arms and attachments needed [26].

Surgical robotic systems provide an improved 3D stereoscopic viewport as in the case of the da Vinci robot [25]. The effectiveness of force feedback in RALS has been investigated by several researchers. Byrn et al. [27] designed a study investigating the impact of 3D vision on the performance of surgeons using the da Vinci to perform basic surgical tasks such as knot tying, threading, and needle capping. Results suggested that using 3D vision as opposed to 2D vision reduces task completion time by 34%-46% and error rates by 44%-66%. Multi-million-pound robots such as the powerful da Vinci suffer from one major weakness: lack of haptic force feedback during an operation. Gwilliam et al. [28] investigated the effects of haptic and visual force feedback on teleoperated palpation. They discovered that direct haptic force feedback alone minimizes the forces applied, while a combination of haptic and visual force feedback minimized errors. Kazi [18] conducted experiments to study the effect of force feedback in LS. Results suggested that when force feedback was present, the maximum force exerted was reduced by up to 40%. The need to introduce force feedback into RALS remains debatable.



Figure 2. Da Vinci robot set-up

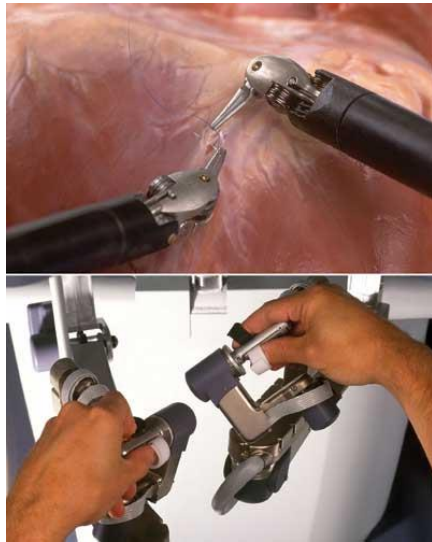


Figure 3. Da Vinci console controllers used by surgeons to manipulate tools at the surgical site

1.2. Surgical Training

Surgical training can be in the form of standard virtual laparoscopic training or robotic assisted laparoscopic training. The first trains the surgeon for standard LS. Virtual environments are used to simulate tissue and graspers are attached to haptic feedback devices in order to simulate tissue interactions. The latter is training for operators of robotic systems such as the da Vinci. Current robotic assisted surgical advancements are met with training and skill learning challenges. More and more complex skills are now required to perform minimal access procedures highlighting the need for training [20]. An inexperienced surgeon can unintentionally cause the patient complications or discomfort. Today, medical simulators are regarded as valuable tools for providing surgeons with the proper experience as well as specialized task training. One study, with twenty nine surgeons across seven hospitals on 4700 patients [29], reported that in order to perfect a laparoscopic procedure, surgeons needed to perform approximately 750 operations. However, these simulators are not only used for task training. Their computer simulation systems allow for skill analysis and detailed performance feedback allowing surgeons to improve their skills and also analyse, understand, and reduce their weaknesses and faults [3], [30].

1.2.1. Laparoscopic surgery training systems

Laparoscopic surgical tools enter the body through small incisions usually in the abdomen. This reduces the force feedback translated to the surgeon. Visual feedback is limited as well due to the use of 2D screens. Mastering orientation and tool manipulation is quite unintuitive due to the fulcrum effect [31] which is the perceived inversion of movement. Surgeons are forced to move a tool handle left in order to move the tool tip right and vice versa. For these reasons, training prior to performing operations becomes critical. Today, there are several simulators for laparoscopy which are commercially available.

The MENTICE VIST-Lab is a LS simulation system [24]. Designed for medical students, Immersion's CAE EndoscopyVR Surgical Simulator provides virtual training environments for bronchoscopy and gastrointestinal procedures [24]. The LAP Mentor III (Simbionix) offers haptic feedback allowing for simulation-based laparoscopic training. SEP Basic (SimSurgery®) is another surgical simulation system that contains exercises which are designed for learning and training basic and advanced skills and techniques. The LapSim System (Surgical Science) is a laparoscopic simulation system that allows surgeons and students to learn and practice old and new techniques. SIMENDO offer a certification program using a laparoscopic simulation system [24]. Some hospitals today are pushing certification systems forward so that medical students and residents learn all the skills necessary as part of their educational curriculum. The HystSim™ (VIRTAMED) is a training simulator designed for hysteroscopic procedures [24]. Ultimately, these simulators have two common goals which are to shorten the learning curves and provide seamless transfer of skills directly into the operating theatre. The problem with such systems is that they are expensive and task-specific.

1.2.2. Robotic surgery training systems

Today, many systems exist to provide surgeons with training and expertise in preparation for robotic surgery. The RobotiX Mentor (Simbionix) is an educational simulation system that allows surgeons to develop all the necessary skills needed to perform real operations [24]. RoSS™, or Robotic Surgery Simulator (Simulated Surgical Systems, LLC) is a portable stand-alone simulator designed for training and

teaching novice surgeons the skills required in order to operate the da Vinci® surgical robot. MIMIC® develops several simulation systems for surgical training such as the Xperience™ Team Trainer for laparoscopic training and the Maestro AR™ for robotic training [24]. The Maestro uses augmented reality to provide 3D interaction in virtual surgical environments [24]. The da Vinci Skills Simulator (Intuitive Surgical®, Sunnyville, CA) is a robotic system that utilizes a virtual environment to train and educate experienced and novel surgeons before they can operate using the da Vinci robot on living patients [24].

1.2.3. Haptic feedback devices for surgical simulation

Commercial force feedback devices are used today by research and industry in areas such as surgery, military, and gaming. The advantages of using off-the-shelf commercial force feedback devices are flexibility, variety, and relative ease of use. Today, these devices come equipped with intuitive user interfaces requiring a minimal amount of previous programming knowledge, making them more accessible. Depending on budget and needs, it is possible to choose a haptic feedback device which will be less costly and less complicated than designing and building a custom one [20]. These commercial feedback devices are controlled using available software drivers. In order to properly choose a force feedback device for a specific application, one must take into account desired workspace, degrees of freedom, force and torque output range and resolution, and available budget. Table 1 lists the most widely used commercial force feedback hardware manufacturers and devices currently available collated by [20]. These devices have been extensively used in research. Morris et al. [32] used a Omega.3 haptic feedback device to teach motor skills which required a specific force sequence. Dominjon et al. [33] used a PHANToM Premiere 1.0 to simulate the mass of virtual balls in a virtual environment. The PHANToM was also used to simulate virtual springs [34]. Wagner et al. [35] assessed the benefits of force feedback in robotic surgery. They examined the effect of force feedback on dissection tasks using a PHANToM haptic device. Wagner & Howe [36] set up an experiment using a PHANToM 1.5 to investigate whether or not force feedback improves performance.

Table 1. Specifications and prices of current commercially available force feedback devices [20]

Company	Devices	Degrees of Freedom	Degrees of Force Feedback	Workspace (mm)	Max Force (Nm)	Max Torque (mNm)	Stiffness (N/mm)	Price (€ X1000)
<i>SensAble Technologies</i>	Omni	6	3	160 x 120 x 70	3.3	0	1.02	2
	Desktop	6	3	160 x 130 x 130	7.9	0	1.7	11
	Premiere 1.0	6	6	127 x 178 x 254	8.5	0	3.5	18
	Premiere 1.5	6	6,3	191 x 267 x 381	8.5	515	3.5	24-51
	Premiere 3.0	6	6,3	406 x 584 x 838	22	515	1	53-51
<i>Force Dimension</i>	Omega 3,6,7	3,6,7	3	160 x 160 x 110	12	8	14.5	14-24
	Delta 3,6	3,6	3,6	360 x 360 x 300	20	200	15	22-40
<i>Novint</i>	Falcon	3	3	101 x 101 x 101	9	0	N/A	0.2
<i>Immersion Corp</i>	CyberForce	6	3	304 x 304 x 495	8.8	0	N/A	45
	CyberGrasp	5	5	Finger	12	0	N/A	
<i>Haption</i>	Virtuose 6D	6	6	129 x 120 x 120	10	500	2.5	30
	Desktop							
	Virtuose 3D15-25	6	3	500 x 644 x 350	15	0	2	25
	Virtuose 6D35-45	6	6	1080 x 900 x 600	35	3000	2.5	85
	Virtuose 6D40-40	6	6	400 x 400 x 400	100	10000	N/A	120
	INCA 6D	6	6	Variable	40	5000	N/A	80
<i>Mimic</i>	Mantis	6	3	325 x 270 x 260	15.2	0	5.5	10
<i>Quanser</i>	Mirage F3D-35	6	3	400 x 200 x 300	25	0	2	35
	HD2	6	5	530 x 300 x 500	19.7	1725	10	60-70
	Pantograph 2DOF	2	2	270 x 240	10.1	0	3	20
	Pantograph 3DOF	3	3	270 x 240	10.1	255	3	25
	Pantograph 5DOF	5	5	480 x 250 x 450	9	750	10	50
<i>Moog FCS Robotics</i>	HapticMaster	3	3	1000 x 400 x 360	250	0	10	43
<i>MPB Technologies</i>	Cubic 3	3	3	330 x 290 x 220	2.5	0	N/A	N/A
	Freedom 65	6	6	170 x 220 x 330	2.5	150	2	25
	F7S	7	7	170 x 220 x 330	2.5	150	2	29

1.3. Summary

Driven by a relentless desire to improve the comfort and wellbeing of patients, MIS has become standard practice in an increasing number of operations, replacing OS. Advancements in MIS have brought light to improved LS equipment as well as continually evolving RALS systems, which consequently resulted in the conception

and development of MIS training systems. LS and RALS training simulators are used today to provide experienced and novice surgeons with crucial training for standard as well as novel surgical procedures. RALS was initially designed to improve a surgeon's accuracy, reduce errors, and improve efficiency during MIS procedures. These systems benefit from improved visual cues by using 3D stereoscopic vision and enhanced instrument manipulation [26]. However, disadvantages of RALS systems such as the da Vinci are that they offer no haptic feedback, are very expensive, require continuous maintenance and training, and are bulky. LS is also faced with several drawbacks for both the surgeon and the patient. Reduced haptic and visual feedback could cause unintended tissue damage. With the current rate of advancement in surgical technologies, it is clear that there is a need to further assess the contribution of visual and haptic feedback as well as the cross-modality between vision and touch during all the modes of surgery available in an attempt to enhance the surgeon's sensory experience in current and future surgical environments. Such an assessment would highlight the impact of each modality to the entire sensory process, allowing for enhancement of the sensory modality with the greatest contribution.

2. Literature Review

In Chapter 1, the history, advancements, advantages and disadvantages of surgical methods were evaluated. This chapter is a review of the impact and contribution of the visual and haptic cues used when judging the compliance of tissue or tissue-like objects during surgical tasks such as palpation.

2.1. Introduction

By definition, surgery is the act of curing through bodily invasion [37]. Humans have been developing surgical techniques ever since they learned how to manufacture and operate tools. It was not until the industrial revolution that surgeons were able to overcome the three biggest hurdles in surgery: pain, infection, and bleeding [38]. Advancements in managing and reducing those hurdles have led to significant advancements in surgery such as MIS. Different methods of surgery provide surgeons with different combinations of visual and haptic cues. In all surgical settings, however, visual information is crucial. Surgeons combine haptic feedback with direct or indirect visual access into the patient's body to assess tissue health. While the progression from OS to MIS has seen a reduction in patient hospital stay and costs as well as patient invasiveness, MIS suffers from reduced haptic and visual feedback [15]. In this review, the effects of haptic feedback, visual feedback, and the integration of the two during compliance discrimination within the modes of surgery available are documented. The literature review focuses on compliance discrimination performance during a simple surgical method of examination: palpation. The ability to discriminate mechanical properties of tissue such as compliance during palpation is critical for assessing tissue for abnormalities [15]. Finally, a general summary of the methods used to design, analyse, and interpret psychophysical experiments are documented.

2.2. Perception

Perception is the acquisition and processing of sensory data in order to feel, see, hear, taste, or smell objects in the world around us [39]. According to Kosslyn & Sussman [40], 'there is no such thing as immaculate perception'. Although the act of perception comes naturally to us, and it happens so quickly, analysing and fully understanding

the reasons behind our decisions is an extremely complicated task. Perception is the end result of several complex processes referred to as the perceptual process [41]. The order in which these processes are arranged determines how we experience and react to a stimulus in the environment. This perceptual process can be divided into four categories: stimulus, electricity, experience and action, and knowledge [41]. Stimulus, or cue, refers to whatever captures our attention and stimulates our receptors. It could be anything from a scent, a sight, a touch, a flavour, or a sound. These receptors create electric signals which are transmitted to the brain. The desired outcome, to be able to perceive the stimulus, is referred to as experience and action. Knowledge refers to the information used in the perceptual situation.

Haptic perception is the recognition of an object of this world through touch. It can be cutaneous (related to skin), kinaesthetic (related to limb movement), or proprioceptive (related to body position) [42]. Haptic perception is not solely linked to the sense of touch. Many factors come into play when about to touch an object and perceive its material properties and characteristics including visual cues and muscle memory. In a surgical context, surgeons use a combination of visual and haptic cues in order to manipulate the tissue, assess its health and perform complicated procedures. These cues are used to estimate properties of the tissue. An instrumental mechanical property used by surgeons is the stiffness or the compliance of tissue. Softness is the subjective assessment of a physical stimulus with known compliance. “An object is classified as soft if it conforms to the body and hard if the body conforms to it” [43]. A compliant object is one that deforms in an elastic, viscoelastic, or non-elastic manner when an input force is applied on it.

2.3. Compliance discrimination

In any given surgical environment, a surgeon performs tasks such as palpating, probing, grasping, cutting and suturing [44]. Palpation is a basic yet crucial method of physical examination using the fingers or hands [10]. The process of palpation follows a specific order: Hand positioning, tissue deformation, gathering tissue information using haptic and visual feedback available, obtaining information feedback, and finally assess the tissue in an attempt to establish an educated guess regarding its mechanical properties. Health care providers assess a patient’s body for

size, texture, location, compliance, or consistency of an organ or body part. In a surgical context, palpation provides essential haptic feedback information regarding tissue compliance, stiffness, size, texture, elasticity, and consistency in order to assess tissue health during an operation. Palpation is especially vital for the detection of tumours [15]. For instance, pyloric tumours in infants with sizes from a few millimetres to 20 cm in the liver can be detected through palpation [10]. In OS, surgeons palpate an organ or area in the body by exploration using their hands, usually looking for abnormalities or tumours [45]. Even with the presence of advanced imaging equipment such as CT and MRI scans, the human hand is still considered a very useful tool for tissue assessment [15]. In MIS, however, surgeons are forced to use tools to perform all their tasks. In this case, surgeons manipulate and palpate tissue using those tools.

While there are numerous properties that can describe the behaviour of tissue during palpation, the compliance of tissue is highlighted in this thesis as it informs the surgeon regarding the softness or hardness of the tissue, which in turn allows the surgeon to critically assess the health of that tissue [45]. While compliance is a mechanical property relating the exerted force onto an object to the observed displacement due to that force, softness is the subjective assessment of the compliance of an object.

A vast amount of research has gone into visual and haptic feedback and the information they provide during compliance discrimination tasks. Variations in visual and haptic feedback include direct contact and visual access such as in the case of OS as well as indirect contact and visual access such as in the case of MIS. The following is a comprehensive review of the literature regarding compliance discrimination using haptic information, visual information, and a combination of both.

The review begins with a summary of the literature focused on the impact of cutaneous information during compliance discrimination tasks. In MIS, cutaneous feedback is replaced with haptic feedback using tools. Although this thesis is primarily focused on compliance discrimination in MIS, it is necessary to review and assess performance through cutaneous cues before moving on to performance in MIS. Next, research pertinent to the impact of haptic feedback on compliance discrimination performance is assessed followed by that of visual information in MIS. After reviewing how haptic

and visual cues affect performance independently, the integration of both during compliance discrimination tasks is assessed. This is followed with a review of the impact of force feedback on compliance discriminability. Finally, the power and uses of visual information during compliance discrimination tasks are discussed.

2.3.1. Impact of haptic feedback using cutaneous information

Cutaneous information is any sensory information obtained through direct contact with the skin. While this thesis is focused on compliance discrimination in MIS, RALS, and surgical training, it is necessary to begin by showcasing previous on compliance discrimination prior to the introduction of minimally invasive surgical methods. In OS, surgeons use their fingers to obtain valuable information regarding tissue properties. Tissue stiffness is a useful property used by surgeons and clinicians to assess tissue health.

Researchers have made a distinction between the sensation caused by the displacement of the finger due to the stiffness of the material and the sensations of the fingertip when touching the deformed surface of a compliant material. In an experiment by Friedman et al. [43] seen in Figure 4, subjects were asked to scale softness of silicone rubber disks using 4 different methods: active tapping with the finger pad (A), active tapping with a 2-finger tool (B), active tapping with a 1-finger tool (C), and passive pressing of the finger (D). Participants labelled objects as soft if the objects' compliance exceeded that of the human finger. An analysis of the results revealed that the softness function had a steeper slope when participants actively indented using their finger than when actively or passively indenting using a tool. Results also showed that although cutaneous information could be sufficient when discriminating between two objects, compliance discrimination was impaired when kinaesthetic information was absent. Kinaesthetic cues are the self-awareness of the body's position with respect to itself and its surroundings [46]. In summary, these findings reinforce the idea that cutaneous information is indeed superior to information obtained using a tool or stylus during compliance discrimination tasks. The results also highlight the importance of kinaesthetic information during direct indentation tasks.

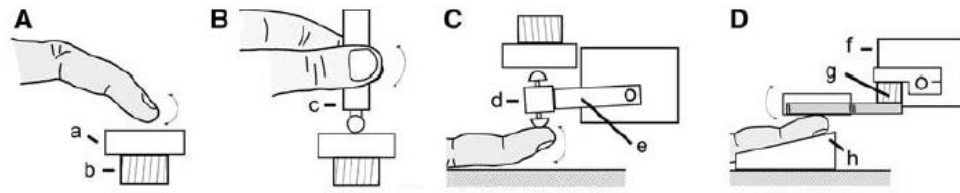


Figure 4. The four experimental setups as presented by Freidman et al. [43]

Compliant objects can be classified as one of two types of objects: deformable objects with rigid surfaces (typewriter keys, piano keys, car brake pedal), and deformable objects with deformable surfaces (rubber, foam, fruit) [47]. Srinivasan & LaMotte [47] investigated the ability of humans to discriminate the compliance of objects having either deformable or rigid surfaces under active and passive touch conditions. Ones with deformable surfaces were fabricated from transparent rubber while those with rigid surfaces consisted of a rigid plate attached to a spring, fitted inside a hollow cylinder. A pairwise discrimination experiment showed that for compliant specimen with deformable surfaces, tactile information was found to be sufficient, regardless of force and velocity applied. The effect of force on compliance discrimination using a tool, however, such as in the case of MIS is yet to be investigated. Chapter 5 addresses this research need.

Bergmann Tiest & Kappers explored the roles of force-displacement and surface deformation cues during compliance discrimination using cutaneous information [48]. They conducted 2AFC experiments in which recruited participants grasped compliant rubber stimuli between their thumb and index finger. Results suggested that most of the information obtained originated from stimuli surface deformation cues. It was observed that 90% of the information cues come from surface deformation cues, whereas only 10% comes from force-displacement cues. Moreover, it was shown that using cutaneous cues, compliance can be perceived directly without the necessity to subconsciously calculate the ratio of force increase to finger displacement. Den Boer et al. [49] investigated the sensitivity of laparoscopic dissectors when in contact with a simulated arterial pulse. Results suggested that the overall sensitivity obtained using the instrument was low compared to using bare fingers.

2.3.2. Impact of haptic feedback using a tool

Using a handheld tool, the softness of a compliant object can be assessed by actively tapping, pressing, or palpating [50]. LS Surgeons palpate tissue using tools in order to evaluate the elasticity, hardness, toughness and compliance of that tissue, which allows them to make a judgement regarding the tissue health state followed by a diagnosis [15]. LS require sensing and evaluating these mechanical properties from the tissue, transmitted through the tool, and finally to the surgeon's hands. The added separation between the assessor and the object as well as the additional force required to maintain a stable grasp of the tool while assessment result in a compliance assessment task that is without doubt more challenging than direct assessment or palpation using cutaneous feedback [8].

Friedman et al. [43] conducted a series of magnitude estimation experiments investigating people's ability to estimate the softness of silicone disks having different levels of compliance. In one of the experiments, participants used a stylus to actively indent each specimen either by tapping the stylus with one finger or by holding it with two fingers in a precision grip (Figure 4). Results suggested that kinaesthetic and vibratory cues are used while judging softness using a tool. It is therefore essential to use such cues in LS for improved performance as well as implement them in RALS and RALS simulators for a more realistic experience.

While haptic feedback is indeed reduced when palpation is performed using a handheld tool [2], [8], [15], [19], [45], some research has found compliance discrimination via tool to be viable [19], [50]. LaMotte [50] set up an experiment investigating the abilities of humans to discriminate softness of compliant rubber objects using a handheld tool. This experiment was a softness ranking experiment with three modes of contact: active tapping using the finger pad, passive tapping using a stylus controlled by a torque motor, and active tapping using an unconstrained stylus held with two fingers. When the tapping velocity was maintained constant, subjects were able to discriminate compliance using a tool to a similar degree of accuracy as when using their finger pads. Bholat et al. [19] explored tactile feedback presence during MIS. Results showed that while direct palpation using the finger pad provided the highest accuracy for shape discrimination tasks, palpation using a conventional and laparoscopic instruments, in fact, do provide surgeons with haptic feedback

regarding texture, shape and consistency. In some cases, the laparoscopic instruments magnified the available haptic information.

The use of tools in MIS and RALS is unavoidable. For the time being, there is no way of getting around using graspers in LS. The extent of the reduced haptic feedback as a result of using a tool instead of the hands remains unclear. It is therefore critical to explore the impact of visual and haptic feedback variations on compliance discrimination performance during a basic surgical task such as palpation. Chapter 4 aims to address this issue.

RALS systems such as the da Vinci do offer a more realistic experience by allowing surgeons to control slender robotic arms housing slender instruments in real time using their hands, wrists and fingers via a 3D image output console. While such a system brings forward improved manoeuvrability and accuracy, it lacks force feedback leaving surgeons relying more on visual information to assess tissue compliance. Visual cues are therefore critical in MIS and RALS, often more so than haptic cues.

2.3.3. Impact of visual feedback

The nature of MIS compels surgeons to be aware of the forces they exert on soft tissue in order to minimize any damage that might occur. Experienced MIS surgeons develop learning skills in which they compensate for the limited haptic feedback by relying mostly on visual cues obtained via the 2D screen in the case of LS, or through the 3D stereoscopic viewport in the case of RALS [42].

In his 1979 book about visual perception, Gibson [51] wrote: “seeing and touching are two ways of getting the same information” (p.258). While meant to be merely an attention grabber, this claim clearly communicates the power of visual information. Srinivasan et al. [52] investigated the impact of visual information on the haptic perception of stiffness in virtual environments. Using a haptic interface, they were able to simulate the sensation of stiffness of on-screen springs. The relationship between haptic and visually displayed springs was obtained using mathematical equations which are based on Hooke’s law. As the mismatch between visual and haptic information increased, vision information dominated causing an increased misconception of stiffness. Subjects disregarded hand positioning during the

indentations and based their judgements on the visual cues observed on screen as well as the force feedback cues created by the haptic device. A sensory discrepancy was introduced between the visual and haptic information relayed to the subjects. The results indicated that visual information greatly influenced the ability to perceive stiffness. While the authors investigated the impact of visual information on the ability to perceive stiffness of virtual springs, a system more complex than Hooke's law needs to be designed and investigated in order to explore visual dominance within a surgical context. Properties such as viscoelasticity need to be accurately modelled and investigated in a compliance discrimination task using some sort of tool similar to MIS.

Perreault & Cao [42] set up a within-subject 2AFC experiment examining the effects of vision and masking friction on compliance discrimination of silicone mixtures simulating tissue during active probing. In the no-vision compliance discrimination task, more errors, higher thresholds, and longer detection times by the participants were observed. Results also show that the introduction of visual information resulted in a reduced mean applied force onto the samples. The authors concluded that while both visual and haptic feedback sources were equally important during compliance discrimination of tissue-like objects, the presence of visual information reduced detection times, errors and threshold values. Hence, not only does visual information seem to dominate during visio-haptic interactions, it also provides benefits such as error and discrimination time reduction.

Drewing et al. [53] investigated multisensory visual-haptic softness perception using deformable objects. Participants judged the magnitude of softness of the stimuli under direct vision-only, haptic-only cutaneous feedback, and visual-haptic conditions. In the vision-only condition, participants directly watched as another person palpated the deformable objects with their index finger. Results suggest that participants could infer the softness of the objects under all three conditions relatively well. Moreover, the integration of visual and haptic feedback was biased more towards vision than touch. Kuschel et al. [54] focused on the integration of vision and touch during compliance perception. It was speculated that the sense with the highest reliability present contributes most to the perception of compliance. If the reliability of a sense was reduced, its relative contribution to perception of compliance is automatically

reduced. This was confirmed by Johnson et al. [55] who set up an experiment investigating visually induced feelings of touch. Their results showed that when haptic perception is distorted or weakened (such as in LS) we tend to rely more on incoming visual information than we do on tactile information. In other words, when haptic feedback is not reliable, visual feedback could potentially be used as a viable substitute during visio-haptic compliance discrimination tasks. No such work has been done for MIS palpation tasks using a tool. Chapter 7 will further assess the reliability of visual feedback when haptic feedback is distorted or diminished in MIS.

Although not focused on compliance, Rock & Victor [56] set up a psychophysical experiment investigating the roles of vision and touch during object identification. Participants were presented with objects that were visually different from their tactual shape. They were asked to grasp the objects while viewing them and then match their impression of the shape to another object. Results suggested that visual information was dominant during shape identification tasks, with participants completely unaware of any sensory conflict taking place. Participants somehow ‘felt what they saw and not what they touched’, which once again highlights the power of visual information. Morris et al. [32] used haptic, visual, and visio-haptic training in a study exploring the role of haptic feedback in motor skill learning. Results showed that while the training combining both visual and haptic information was more accurate than the vision-only or haptic-only training, haptic training alone was shown to be inferior to visual training alone, emphasizing the power of visual feedback while learning a sequence of forces. The authors suggested that such skill learning methods which combine visual and haptic feedback in an optimum fashion can be used in surgical training.

From the literature, it is clear that visual information can affect and change how we perceive softness of compliant objects. It is necessary, however, to investigate the scope of this visual dominance, especially in compliance discrimination tasks requiring the use of a tool such as the case of LS and RALS. This will be evaluated in Chapter 4. The literature has shown that in the event of a discrepancy between visual and haptic cues present, humans tend to rely more on visual cues to judge the softness of compliant objects. The next step would ideally be to investigate the extent to which this discrepancy can be maintained before a sensory mismatch becomes obvious to observers. This will be further evaluated in Chapter 7.

2.3.4. Cross-modal integration

2.3.4.1. *General cross-modal integration*

Object recognition is a complicated process that is usually performed to a surprisingly high level of accuracy due to the combined use of visual, haptic and even memory cues [57]. In MIS, haptic feedback is used in the form of shape, size, texture and compliance through a tool [15]. Haptic feedback is combined with visual cues such as colour, texture, elasticity and shininess available to the surgeon through a 2D screen. Coupled with a search through memory for cues such as colour, smoothness, translucency and temperature, a surgeon can have a good idea regarding the properties and health of the tissue at hand. When judging an object novel unique object, visual and haptic cues both provide sensory information for estimation of the properties of that object [58]. Researchers have investigated the way these sensory modes work together or at times dominate one another, in numerous types of haptic discrimination tasks. There are many types of cross-modal interactions. Cross-modality could be used to transform one sensory channel into another such as auditory-to-visual or visual-to-haptic. It could also be used to enhance the stimulus perceived from one channel using another sensory channel. Initially described by Biocca et al. [59], Table 2 illustrates all types of cross-modal interactions as well as their definitions and uses.

Wu et al. [60] showed that in a visio-haptic setup, visual and haptic information often compensate for one another in such a way that sensory information received from haptic and visual channels are optimally merged. Norman et al. [61] evaluated participants' ability to compare the shapes of 3D objects using visual feedback, haptic feedback, or vision-haptic cross-modal feedback. Results showed that participants were able to identify 3D objects with reasonably high accuracy in all three tasks. However, performance was slightly better when cross-modal feedback was presented. The authors theorized that touch and vision do overlap but are not necessarily equivalent during 3D object identification.

Biocca et al. [59] set up an experiment exploring the contribution of cross-modal sensory integration to simulating an illusion of presence in a virtual environment. More specifically, their work investigated the potential of visual information for generating cross-modal illusions without the presence of any haptic feedback. Results

suggest that due to the visual displays present, participants sometimes experienced haptic feedback when in reality, none was present. It was hypothesized that visual cues simulating physical resistance helped produce this illusion.

2.3.4.1. Visio-haptic cross-modality during compliance discrimination

Cross-modal interactions are constantly taking place in our daily lives. Perhaps the most common cross-modal interaction is that between vision and touch. Lecuyer et al. [62] investigated the interaction between visual and haptic cues in a virtual environment. Using a spaceball to simulate stiffness, results suggested that perceived stiffness was significantly influenced by the provided visual information. Kuschel et al. [54] focused on the perceptual integration and combination of vision and haptic information during compliance discrimination. They speculated that the modality with the highest current reliability contributes most to perception of compliance. If the reliability of one modality was reduced, its relative contribution to the bimodal perception automatically decreases. Courousse et al. [63] speculated that perceptual judgement is the same in haptic only and in visual-haptic conditions. However, they believed that visual feedback did modify and influence movement parameters. For instance, when visual feedback was present, manipulation speed decreased. When visual feedback was not present and subjects relied solely on haptic feedback, manipulation speeds increased, possibly in an attempt to increase the amount of haptic information. Drewing et al. [53] set up a study investigating softness perception of deformable objects through multisensory visual-haptic feedback. Participants judged the softness magnitudes of the stimuli under haptic-only, vision-only, and visio-haptic conditions. Participants used their index finger to judge the softness of the samples when haptic feedback was allowed. Visual feedback was simply direct visual access to the stimuli. Their results showed that softness discrimination was possible under all three conditions. Moreover, participants were reliably able to judge softness under vision-only conditions. Finally, their results suggested that the integration of haptic and visual feedback during softness discrimination was not optimised, and was biased more towards vision. The need to fully understand and optimise the cross-modality occurring between vision and touch during compliance discrimination tasks is quite apparent and necessary.

Table 2. Variations of cross-modal sensory interactions in virtual environments [59]

Cross-modal sensory interactions in VEs	Descriptions	Examples
Amodal mapping	Use of VE or other representational system to map abstract or amodal information (e.g., time, amount, etc.) to some continuous or discrete sensory cue (e.g., color, size, depth, etc.).	The use of color mapping and relative size in graphics and scientific visualization to represent money, time, etc.
Cross-modal mapping	Use of a VE to map one or more dimensions of a sensory stimulus to another sensory channel. Typical mappings are auditory-to-visual, visual-to-haptic. The mapped cues may be simultaneous and redundant (e.g., beeping sound and flashing light) or a replacement (e.g., sound source, such as a beep, mapped and experienced as a visual analog, such as a flashing light).	An oscilloscope. Auditory stimuli are transformed to oscillations of a line. The user benefits from the analytical and pattern-perception capabilities of the visual system to analyze the properties of sound.
Intersensory biases and adaptations	Stimuli from two or more sensory channels may represent discrepant/conflicting information about a virtual object, e.g., its spatial location. As the users attempt to perceptually integrate the discrepant information, they may experience immediately (1) sensorimotor illusions usually biased towards one sensory modality, e.g., incorrect distance judgments; or, over time, (2) simulation sickness or other discomfort, and/or (3) adaptation/recalibration of a sensory or motor modality.	“Ventriloquism effect” when spatially discrepant audio and visual cues are experienced as colocalized with the visual cue. In immersive VR systems, lag in visual update rate may be experienced as a potentially nauseating conflict between the visual and proprioceptive systems (i.e., the world appears to “swim” back-and-forth around the head).
Cross-modal enhancement or modification	Stimuli from one sensory channel enhances or alters the perceptual interpretation of stimulation from another sensory channel. Interactions might include changes in detectability, perceived intensity, perceived fidelity, or some other perceptual quality of the stimuli from another sensory channel.	Increased perceived visual fidelity of display as a result of increased auditory fidelity. Changes in the perceived location or intensity of a haptic force based on changes in visual cues. Increased ability to hear and process speech as result of seeing synchronized lip movement.
Cross-modal transfers or illusions (synesthesia)	Broadly, all environments: Stimulation in one sensory channel leads to the illusion of stimulation in another sensory channel. Narrowly, virtual environments: Stimulation from one sensory display, leads to the illusion of stimulation in a sensory channel not connected to a display.	Experience of visual sensations (e.g., colored or pulsating lights) when hearing sounds. Illusion of haptic sensations from a visual cue.

2.3.5. Force feedback

2.3.5.1. *Effect of force feedback on compliance discrimination*

Force feedback is often presumed to improve performance in MIS and RALS [35]. Using a telerobotic system, Wagner et al. [35] investigated the effects of force feedback on a blunt dissection task. It was hypothesized that force feedback was valuable during the task due to the difference in stiffness between the artery being

dissected and the surrounding tissue. This suggests that force feedback is useful when a difference in stiffness at the operating site is found. Wagner et al. [36] attempted to reduce human error and improve performance by introducing force feedback to a palpation task using a stylus attached to a haptic feedback device. The presence of force feedback resulted in an error reduction of 80% compared to when no force feedback was present, highlighting the potential of force feedback in robotic surgery.

Kazi et al. [18] set up an experiment mimicking tissue hardness detection via palpation with and without force feedback. Results suggested that the introduction of force feedback caused a reduction in the forces exerted on the simulated tissue. Gwilliam et al. [28] evaluated the benefits of force feedback on performance during teleoperated palpation of simulated soft tissue using a da Vinci surgical system coupled with a custom control system that provides force feedback. Results suggested that haptic force feedback was shown to reduce forces exerted on the tissue.

Tholey et al. [64] investigated the role of force feedback in MIS. A custom laparoscopic grasper with force feedback capabilities was developed and used to set up softness ranking experiments. Vision-only, force-only and a combination of vision and force setups were implemented in an effort to evaluate the role of force feedback during tissue characterisation. Results showed that a combination of vision and force feedback provides better tissue discriminability when vision or force feedback were presented separately. It is necessary to understand the weight of each sensory modality in order to improve the cross-modal integration taking place during compliance discrimination in MIS.

2.3.5.2. *Effect of force transmission ratio*

In OS, surgeons have the ability to quickly adjust their pinch forces when presented with a sudden high load force such as a tumorous tissue to avoid tissue slippage while at the same time avoiding excessive forces [65]. During LS, surgeons are no longer in direct contact with the tissue but rather with handles for laparoscopic graspers referred to as grippers. Apart from visual cues, force and position transmitted from the tip of the grasper to the handle are the only means of information accessible regarding the pinch forces applied. Unaware of frictional forces between the tissue and the gripper, surgeons are forced to ‘over-grip’ in an attempt to eliminate slippage, often leading to severe tissue damage [66]. Depending on the grasper type and manipulation action,

the transmitted forces are often limited or disturbed. Disruptions include trocar friction, abdominal wall resistance, scaling factors, mechanical construction of the grasper and its efficiency [67]. Westebring-van der Putten et al. [67] investigated the effect of laparoscopic force transmission ratio on grasp control under indirect visual access conditions. Participants were asked to lift tissues with varying stiffness levels barehanded, with tweezers, or with laparoscopic graspers. Results suggested that lifting with a laparoscopic grasper requires 4.5 to 14.5 times as many practice sessions as lifting barehanded. Pinching force was 26 to 60% greater when lifting using graspers than when barehanded. As the stiffness of the tissue being lifted increased, more slips occurred. Results also suggested that it is more difficult to anticipate slippage when lifting tissues with varying stiffness levels using laparoscopic graspers as opposed to direct skin-tissue contact. Sjoerdsma et al.[68] stated that the pinching force on the hand ought to be a reliable representation of the grasping force at the jaws of the laparoscopic grasper. They set up experiments evaluating the transmission of information from the jaws to the hands. They found that the transmitted information was ‘far from ideal’ due to mechanical friction losses as well as inconsistent force transmission variation.

2.3.6. Pseudo-haptic feedback

The effect of visual information on haptic discrimination tasks has been investigated by several researchers [52], [56], [60], [69]. In Section 2.3.3, visual feedback was found to be dominant during haptic compliance discrimination tasks. In this section, a relatively new technique which uses this visual dominance to substitute for distorted or absent haptic feedback is introduced.

In 1996, Srinivasan et al. [52] investigated the impact of visual information on the haptic perception of stiffness in virtual environments. Using a force reflective haptic interface, they set up 2AFC experiments in which participants pressed pairs of virtual springs and were asked to choose which virtual spring felt stiffer. While haptic information was provided using the force feedback device, visual feedback was represented graphically on a computer monitor. Visual representations of the springs were presented side by side on the screen. By modifying a visual scaling parameter added to Hooke’s law, they were able to modify the degree of registration between physical and visual spring stiffness. In other words, they were able to create and

control discrepancies between what participants saw and what they felt. The results showed a dominance of visual information during virtual spring deformation. More importantly, the results indicated the presence of a haptic ‘illusion’: a distortion of haptic stiffness which increased as the mismatch between visual and haptic feedback increased. It was suggested that such illusions can be exploited in the future in order to overcome haptic interface limitations as well as enhancing the range of haptic experiences. However, the authors did not realize that these illusions could also be used to simulate new sensations and not just enhance existing ones.

It was not until Lecuyer et al. [70] simulated the sensation of friction in a virtual environment in the year 2000 that pseudo-haptics became known [71]. The term ‘pseudo-haptics’ consists of two parts. ‘Pseudo’, meaning false or not genuine, and ‘haptics’, meaning any form of touch interaction. The power of visual information is significantly used in pseudo-haptics. Pseudo-haptics is the generation, augmentation, or deformation of haptic sensations by information coming from other sensory modalities [62]. More specifically, it is the process of simulating a haptic sensation by manipulating the visual information available. So far, pseudo-haptics has been used to simulate various haptic properties such as stiffness of a virtual spring [72], texture of an image [73], friction in a virtual passage [74], mass of a virtual object [33], torque feedback [75] and shapes of different objects [76]. It has not, however, been used to simulate viscoelasticity of compliant objects, such as the case of human tissue.

Lecuyer et al. [72] studied the phenomenon of sensory illusion occurring while using a pseudo-haptic feedback system. Subjects were presented with pairs of virtual springs which they were able to compress using a haptic device and were asked to decide which spring they thought was stiffer. Within each pair, one was a realistic spring with matching visual and haptic stiffness while the other was visually and haptically augmented. They connected the PHANTOM desktop which is a force feedback device to a monitor display in order to simulate spring stiffness. Spring stiffness was haptically simulated using Hooke’s law described in Equation (1). The force translated to the force feedback device is simply the simulated spring coefficient multiplied by the displacement (x) made by the PHANTOM end effector. Visually, piston-like renderings were displayed on a computer screen in order to simulate spring

stiffness. Similar to haptic stiffness control, visual stiffness was controlled by modifying Hooke's law to incorporate a visual stiffness as shown in Equation (2).

$$F_d = K_h \cdot x_h \quad (1)$$

Where F_d is the force sent back to the user from the haptic device, K_h is the simulated haptic stiffness, and x_h is the displacement of the PHANToM end effector.

$$x_v = \frac{F_u}{K_v} = \frac{K_u}{K_v} \cdot x_h \quad (2)$$

Where F_u is the force applied by the user onto the PHANToM haptic device, K_u is the simulated haptic stiffness, K_v is the simulated visual stiffness, and x_v is the visual displacement of the piston.

The ability to separately manipulate visual and haptic stiffness allowed for independent sensory augmentation. Their experiment used 4 haptic stiffness values (210N/mm, 280N/mm, 380N/mm, and 600N/mm) and 12 visual stiffness values (varying from the reference spring stiffness by -70, -60, -50, -40, -30, -20, -10, 0, 10, 20, 30, and 40 percent) in a 2AFC experiment using the method of constant stimuli. Within every trial, participants were asked to compare the stiffness of the reference spring with that of the pseudo-haptic test spring. Both the haptic and visual stiffness values of the reference spring were identical at 210N/mm. They were then asked to select the 'stiffer' of the two springs. The aim of this experiment was to study the phenomenon referred to as 'boundary of illusion' which describes the moment when a sensory illusion occurs using pseudo-haptics. On average, the boundary of sensory illusion, represented by the point of subjective equality (PSE) between the two springs, was found to be -24% increasing monotonically with the haptic difference between the springs. This suggests that greater visual deformation was required to compensate larger haptic differences. Moreover, it further qualified the notion of visual dominance in stiffness perception. The variability in the results, however, possibly imply that further exploration into pseudo-haptics within stiffness discrimination is necessary. The authors discussed a current need to simulate properties such as viscoelasticity using an appropriate pseudo-haptic feedback system. This need will be addressed in Chapter 6.

With a focus on tumour identification during palpation, Li et al. [77] set up an experiment in which pseudo-haptics was used to generate haptic sensations. Visual information and force feedback were combined to allow for exploration of a virtual tissue model which contains stiffer tumorous tissue. Pseudo-haptic feedback was in the form of cursor speed augmentation which simulates resistance to motion. Participants moved the on-screen cursor using a stylus input connected to the haptic device. As the cursor approached a virtual tumour, the speed of the cursor becomes slower than the participants' expectations thus creating the illusion of increased stiffness. The three detection methods used were forced feedback only, pseudo-haptic feedback only, or a combination of force feedback and pseudo-haptic feedback. Results showed that the introduction of pseudo-haptics increased discrimination sensitivity by 5% and decreased detection time by 48.7% suggesting great potential for the development and use of pseudo-haptics in RALS and medical simulators. While the authors showed that pseudo-haptics enhances discrimination performance during palpation of simulated tissue, the extent of its effect is not yet determined. This issue will be addressed in Chapter 7.

Some researchers augmented the position, speed and size of an on-screen cursor in order to simulate haptic sensations. Lecuyer et al. [74] set up a pseudo-haptic experiment in which they modified the speed and size of an on-screen cursor in order to simulate the sensation of bumps and holes. Using a pseudo-haptic feedback system, Li et al. [78] showed that visual information can be used to correctly identify virtual tumours. By manipulating the speed and size of an on-screen cursor, they were able to simulate varying stiffness levels. Bibin et al. [79] introduced a medical simulator designed for training in anaesthesia procedures. In such procedures, the anaesthesiologist first palpates the patient's body prior to inserting a needle and stimulating the nerve. Palpation is essential as it allows the anaesthesiologist to locate the patient's organs underneath the skin in order to find the most suitable location for the needle to be inserted. A spherical cursor was manipulated by the anaesthesiologist using a computer mouse. Pseudo-haptics was applied to the cursor visually to simulate bumps and hollows matching the organs and arteries beneath the skin. Argelaguet et al. [80] introduced a method for perception of elasticity of images using pseudo-haptics. Without using a haptic feedback device, they were able to simulate elasticity using visual deformation. Participants used a standard computer mouse to interact

with the images (Figure 5), which visually deformed according to their associated elastic properties. Shadows and creases were also simulated to amplify stiffness perception. The issue with such feedback systems is that while effective, they all rely on changes in physical characteristics of a cursor based on the behaviour of the user. In medical simulators, no such cursors exist as trainees actively palpate and manipulate simulated tissue using haptic feedback devices. Pseudo-haptic feedback needs to be incorporated into existing medical simulators without the use of cursors.

To conclude, pseudo-haptics has been used to generate various haptic sensations often without the need for active haptic feedback devices. In Chapter 7, pseudo-haptics will be used as a tool to quantitatively determine the extent of the contribution of visual feedback during haptic compliance discrimination.

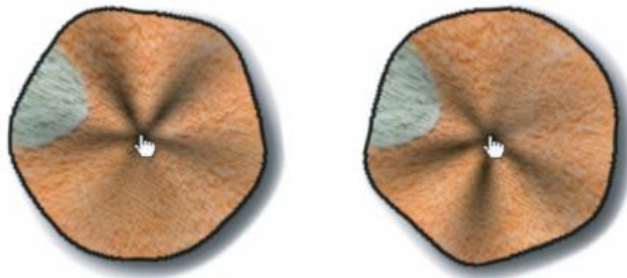


Figure 5. Animation steps of the simulation of an elastic images using additional visual feedback [80]

2.4. Quantification of sensory perceptions

“From a computer’s point of view, perceiving a scene is more difficult than playing world championship chess [41].” Perception is the result of a series of complex processes described in Section 2.2. It is necessary, however, to use a quantitative method of measuring subjective responses in order to obtain usable concrete data and results. This section explores methods of measuring and analysing subjective data. This is crucial as all experiments conducted in this thesis rely on observations made by human participants.

Psychophysics is the use of quantitative methods to calculate the relationship between stimulus intensity (physics) and perception (psycho) [41]. This method was first introduced by Fechner in the mid nineteenth century and has been used since as a

scientific means of measuring sensations [81]. This approach related the physical stimuli (Φ) to the sensations (Ψ) which are in the psychological domain.

A sensory threshold is described as the weakest detectable stimulus intensity. In other words, it is the critical point after which a sensation is detected. Weber and Fechner investigated the sensory thresholds of the human sensory organs [81]. The two main types of thresholds are the absolute threshold and the difference threshold. The absolute threshold is defined as the minimum amount of energy needed to induce a sensation [82]. When presented with a stimulus greater than the absolute threshold, the intensity of this stimulus must be modified by a specific amount before it is possible to detect a sensory change from the absolute threshold. The difference threshold is then defined as the minimum required amount of change in stimulus ($\Delta\Phi$) in order to produce a sensation that is just noticeable; a Just Noticeable Difference (JND) [81]. For instance, using stiffness as the sensory stimulus, if the stiffness of a spring is 100N/m and it has to be increased to 112N/m in order to just notice a change in stiffness, then the JND would be 12N/m.

While the JND provides information regarding a specific sensory reference point, the Weber's law is a more comprehensive measure of performance as it takes into account both the difference in sensation as well as the reference stimulus. German physiologist E. H. Weber was investigating the discrimination of weights being lifted when he found out that the heavier the weights, the greater the JND was [81]. Heavier weights seemed to be more difficult to discriminate than light weights. Weber realized that there was a linear relationship between the physical and the perceived stimulus intensity in which a single JND value acted as the gradient of that sensory relationship. This experiment resulted in what is now known as Weber's law [Equation (3)]. Weber's law is therefore defined as the relationship between the stimulus intensity level (Φ) and the magnitude of the difference threshold ($\Delta\Phi$) through a constant fraction (c) [83]. Weber's law will be used throughout this thesis to compare compliance discrimination performance across various setups.

$$\Delta\Phi = c \Phi \tag{3}$$

According to Weber's law, the value of the fraction (c) should remain constant as the intensity level is varied, meaning that $\Delta\Phi/\Phi$ remains constant.

2.4.1. Weber's law for compliance discrimination

Weber's law has been used in the literature to analyse performance during compliance discrimination tasks. Tan et al.[84] (1995) conducted several psychophysical experiments designed to measure the compliance JND as well to explore the roles of mechanical-work and force cues during compliance discrimination tasks. An apparatus consisting of a moving plate and a fixed plate was used by participants to discriminate compliance. Participants grasped the two plates between their index finger and thumb and squeezed the plates together. A resistive force was manipulated through a control algorithm which simulated various compliance levels.

In a study by Dhruv & Tendrick [85], participants used a PHANToM haptic interface to perform active compliance discrimination tests of virtual samples with 2, 4, and 8 mm/N base levels of compliance. With 14-25% Weber fractions during compliance discrimination, it was suggested that participants were relatively sensitive to changes in compliance.

Nicholson et al. [86] found the mean Weber fraction to be 7.7% in an experiment in which participants used their index finger and thumb to squeeze a mechanical rig that simulates various levels of non-biological stiffness using metal springs. Participants were blindfolded, however, and hence did not have access to any visual information while performing the tasks.

2.4.2. Psychophysical methods

Several methods are used for measuring perceptual sensitivity, the simplest being presenting a person with a stimulus and asking them if they are able to perceive it. In reality, this method is not quite effective due to our nature to often react differently in various occasions. There was a necessity for developing threshold measurement techniques and so scientists developed several methods to measure sensory thresholds. The most widely used methods are documented below.

2.4.2.1. *Method of constant stimuli*

In this method, the same stimuli are used throughout the entire experiment. The threshold lies somewhere within the range of stimuli available. This method is used when only a finite number of stimuli are available for the experimenter. At the lower

end of the spectrum, stimuli are almost undetectable whereas at the upper end, stimuli should almost always be easily detectable. This experiment requires each stimulus to be presented repeatedly in a random order. For each stimulus presented, a response, usually from recruited participants, is required as to whether or not that stimulus is detectable. This method will be used throughout the experiments in this thesis. A set of sample stimuli intensities and their corresponding proportions detected are tabulated below (Table 3). In this example, each stimulus was presented 100 times. Responses are recorded as ‘yes’ (stimulus detected) or ‘no’ (stimulus not detected) and then stored as a proportion detected (%) and then plotted against the stimulus intensities. This plot is referred to as the psychometric function; a model describing the relationship between a physical stimulus and the subjective responses corresponding to that stimulus [81]. The absolute threshold is then the stimulus intensity corresponding to the proportion response of 0.5 (50%) on the psychometric function (Figure 6).

2.4.2.1. Method of limits

A far less time consuming and perhaps the most widely used method for determining sensory thresholds is the method of limits [82]. Using this technique to measure the absolute threshold, a stimulus is first presented well above or well below the threshold. The intensity of stimulus is then slightly changed on each successive trial until the sensory threshold is attained. This method can be performed either ascending or descending series. In ascending, the participant or observer is presented with a very weak stimulus to begin with. Then, the stimulus intensity is increased by a small amount over each trial until the participant or observer notices a sensation. Alternatively, in descending, participants are first presented with a stimulus with relatively high intensity which is slowly reduced until the participant can no longer report its presence. This method cannot be used when dealing with a limited number of stimuli. For instance, if only 20 deformable objects with different levels of stiffness are available, the smallest increment would simply be the stiffer or less stiff sample. If the difference in stiffness between consecutive samples is significant, then smaller increments are needed to obtain the absolute threshold, meaning it would difficult to use the method of limits with sensations that have stimuli with discrete values.

2.4.2.1. *The yes-no procedure*

The yes-no procedure is mostly used to find the absolute threshold [82]. Observers undergo a series of trials in which they report whether or not they perceive any stimulus. Participants are asked to judge the presence or absence of a stimulus within a series of trials. While useful to estimate the value of the absolute threshold, this procedure is not widely used to calculate the Weber fraction often due to contamination from the fluctuation in participants' responses.

Table 3. Stimuli intensities with their corresponding proportions detected

Stimulus intensity (Φ)	Proportion detected (%)
4	4
6	7
8	13
10	31
12	55
14	66
16	78
18	93
20	98

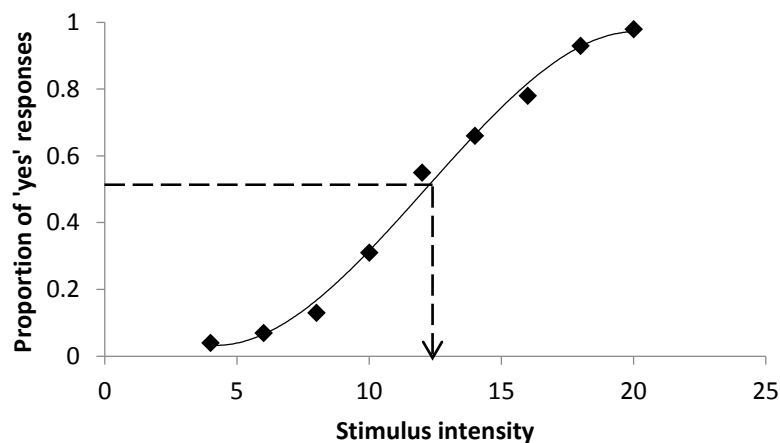


Figure 6. A plot of the proportion 'yes' responses as a function of stimulus intensity.

2.4.2.2. *The forced choice procedure*

This procedure is the most widely used method of measuring detection or discrimination thresholds [82]. Observers are presented with two or more stimuli at

the same time and are asked to indicate which of the stimuli is the greatest based on the perceptual difference between the reference stimulus and the test stimuli [87]. In this procedure, the threshold is located usually at the 75% or 84% correct responses mark [81]. This method is more accurate than the method of adjustment as it relies on binary decisions as opposed to numeric signal decisions which are sometimes biased. It is also superior to the Yes-No method due to the greater amount of information present during each trial. Observers are presented with two or more stimuli at once and are forced to select a certain stimulus resulting in improved performance. Consequently, this method will be used throughout this thesis to measure compliance discrimination thresholds.

2.4.2.3. The magnitude estimation ratio scaling procedure

The magnitude estimation technique requires observers to judge the difference between stimuli magnitudes and make numeric estimations regarding that sensory difference. This technique is useful as it not only shows the relationship between the stimuli intensity and perceived intensity, but associates numeric values to different intensities making it possible to estimate the stimulus that doubles or triples sensation for instance [81]. Usually, a reference stimulus with a specified numeric value associated with its sensation intensity is presented to the observer. Other stimuli are then presented to the observer with various sensations. Based on the reference, the observers are asked to associate numeric values to these stimuli based on the value allocated to the reference. Using this procedure, it is possible to formulate a mathematical model highlighting the relationship between sensation magnitude and the physical magnitude of a stimulus. This relationship is illustrated using Stevens' Power Law [41], [82]. The magnitude estimation procedure will be used in Chapter 7.

Stevens' power law

Over the past few centuries, researchers, scientists, psychologists, and mathematicians have tried to formulate a psychophysical law that can be used to understand human behaviour in social environments. In 1738, Bernoulli investigated the psychological worth of money [88]. He believed that the value of any asset, commodity, or utility decreased as its physical amount increased. In dollars, the subjective value of a dollar decreases if you have more of them. A dollar for a beggar is not the same as that for

a billionaire. Bernoulli proposed a logarithmic relationship between the utility of money and the actual amount of money. In 1850, Fechner realized a relationship between stimulus sensation and intensity. This became known as Fechner’s law. Then in 1953, S. S. Stevens questioned Fechner’s law and managed to find irregularities in his experimental findings. His brightness and loudness psychophysical experiments did not match with Fechner’s logarithmic law but were instead proportional to the cubic root of the stimulus intensity. This sparked the era of ‘new psychophysics’; the measurement of sensation through comprehensive methods. After extensive experimentation to validate his function, Stevens proposed a new relationship between stimulus intensity and sensation magnitude to replace Fechner’s logarithmic law. This function was referred to as the power law [Equation (4)], where Ψ is the sensation magnitude, Φ is the stimulus intensity, k is a constant which determines the scale unit, and a is the power exponent which varies depending on the stimulus sensory type.

$$\Psi = k \Phi^a \tag{4}$$

Stevens set up psychophysical experiments for various sensory stimuli and managed to accumulate the power exponents for several senses and stimuli (Table 4). These exponents are still used today to estimate stimuli intensities and sensation magnitudes for various continua. This table continues to expand as more and more types of stimuli thresholds are measured and quantified.

Table 4. Representative exponents of the power function relating subjective magnitude to stimulus magnitude [88]

Continuum	Measured exponent	Stimulus condition
Loudness	0.67	Sound pressure of 3000-Hz tone
Vibration	0.95	Amplitude of 60 Hz on finger
Vibration	0.6	Amplitude of 250 Hz on finger
Brightness	0.33	5° target in dark
Brightness	0.5	Point source
Brightness	0.5	Brief flash
Brightness	1.0	Point source briefly flashed
Lightness	1.2	Reflectance of grey papers
Visual length	1.0	Projected line
Visual area	0.7	Projected square
Redness (saturation)	1.7	Red-grey mixture
Taste	1.3	Sucrose
Taste	1.4	Salt

Taste	0.8	Saccharine
Smell	0.6	Heptane
Cold	0.1	Metal contact on arm
Warmth	1.6	Metal contact on arm
Warmth	1.3	Irradiation of skin, small area
Warmth	0.7	Irradiation of skin, large area
Discomfort, cold	1.7	Whole body irradiation
Discomfort, warmth	0.7	Whole body irradiation
Thermal pain	1.0	Radiant heat on skin
Tactual roughness	1.5	Rubbing emery cloths
Tactual hardness	0.8	Squeezing rubber
Finger span	1.3	Thickness of blocks
Pressure on palm	1.1	Static force on skin
Muscle force	1.7	Static contractions
Heaviness	1.45	Lifted weights
Viscosity	0.42	Stirring silicone fluids
Electric shock	3.5	Current through fingers
Vocal effort	1.1	Vocal sound pressure
Angular acceleration	1.4	5-sec rotation
Duration	1.1	White noise stimuli

2.5. Conclusions

The main advantage of OS over MIS is the ability for surgeons to use their hands to manipulate tissue and perform tasks. Cutaneous cues have been shown to provide better feedback than haptic cues using a tool, such as in the case of MIS or RALS. However, tactile feedback is still present in MIS. MIS instruments have been shown to possess the ability to interpret texture, shape and consistency of objects [19]. With the current shift to reduced patient trauma and discomfort, MIS is becoming standard practise in numerous types of operations previously only possible via OS [15]. Consequently, the work conducted throughout this thesis is an investigation of compliance discrimination performance in MIS. With the use of tools in MIS being inevitable, perhaps a shift in direction of research focus from tool optimisation to visio-haptic integration enhancement is necessary.

The literature shows that the combination of visual and haptic feedback provides improved accuracy, reduced errors and an overall more reliable sensory experience. Since visual and haptic information are continuously merged during MIS, the visual-haptic cross-modality during compliance discrimination in MIS is in need of investigation. It is necessary to explore the integration of these two senses in a controlled setting in which haptic feedback is provided using a handheld tool and visual feedback is provided through a 2D display, mimicking a MIS setup. Moreover, with the transition from OS to MIS, reduction in haptic feedback forces surgeons to rely more on visual cues. Researchers have demonstrated the dominance of visual feedback in compliance discrimination tasks [52]. It is necessary, however, to determine the scope of that dominance within MIS.

Force feedback has been shown to improve performance and reduce errors in MIS tasks. The introduction of force feedback into RALS has, in some cases, shown benefits. Modifying robotic systems to incorporate force feedback might be tedious, time consuming and expensive. Perhaps the solution for a more realistic force feedback experience is vision-driven rather than force-driven. A simpler, less expensive and less time consuming method might be to simulate force feedback by modifying the visual feedback available. This is referred to as pseudo-haptics [71]. Visual feedback can potentially be used through a unique visio-haptic mismatch in such a way that this mismatch simulates a viable substitute for the reduced, absent or distorted haptic feedback. On-screen visual modifications in position, velocity, shape or size of an object resulted in haptic sensations. Stiffness simulation is the furthest pseudo-haptics research has reached in terms of applications within surgery. Tissue stiffness is critical during manual assessment. However, the mechanical properties of human tissue are more complicated than a simple spring modelled using Hooke's law. Pseudo-haptics can then be used to quantitatively determine the contribution of visual information during a simple surgical task such as palpation.

2.6. Overview

Palpation is a basic yet critical task in any surgical setting. Surgeons assess tissue health either using their hands in OS or slender tools in LS and RALS. Extensive research has gone into the impact of both visual and haptic information on the ability

to discriminate basic haptic properties such as compliance. Both sources of sensory information have been shown to be instrumental during compliance discrimination tasks. While some research such as Friedman et al. [43] showed that cutaneous information is the most reliable source of feedback during compliance discrimination, other such as Bholat et al. [19] found laparoscopic tools capable of providing sufficient haptic feedback. In any case, the drive to reduce patient discomfort as well as improve cost and performance has resulted in the rapid development and implementation of MIS methods recently. This thesis will be targeted at the specific task of compliance discrimination with a specific focus on MIS, which can be LS, RALS, or even robotic training. Finally, psychophysical methods have been widely used in this area of research to calculate sensory thresholds and evaluate performance and are hence suitable for use in this thesis.

Visual information, be it direct or indirect, has been shown to dominate in situations where both vision and touch are available [52], [61], [63]. Haptic stiffness has been found to be significantly dependent upon the visual cues presented in a virtual environment [62]. A cross-modal integration between visual and haptic cues has already been established in the literature [59], [60], [89]. In a sensory situation in which both visual and haptic cues are present, these two cues compensate for one another when necessary, resulting in an optimal merging of information [59], [60]. With so many variations in visual cues available today in surgery, a study that explores the significance of each with all surgical methods would prove useful and would help formulate a greater understanding of the cross-modality between vision and touch.

The power of visual information has been used to simulate various haptic sensations such as friction, stiffness, torque, mass and texture through pseudo-haptics [35]. To the best of the author's knowledge, no previous research has attempted to use pseudo-haptic feedback in order to simulate viscoelastic behaviour of tissue-like materials as of yet. Such a system would be used to quantitatively determine the impact of visual cues on haptic compliance discrimination. This system can then potentially be used to reduce error and improve the force range of inexpensive haptic feedback systems for LS and RALS training.

2.7. Research Motivation

Our ability to haptically perceive different levels of stiffness, texture, size, weight, and shape depends on a multi-sensory process involving information gathered from touch, vision, and even memory [46], [57], [90]–[93]. Extensive research has been conducted investigating a visual-haptic cross-modal integration of sensory information during haptic perception processes [52], [57]–[59], [90], [93].

Put into a surgical context, haptic and visual feedback are essential for gathering information regarding tissue properties such as compliance. Open surgery is an invasive surgical technique that allows surgeons to use their own hands to assess tissue and perform tasks. While this method of surgery provides the surgeon with the greatest amount of haptic information [43], its disadvantages include a longer hospital stay for the patient, a larger scar, excessive invasiveness, longer operating duration leading to increased costs for both the patient and the hospital [15]. Over the past few decades, LS has grown in popularity to become an industry standard in several operations [94]. As effective as it is, this minimally invasive type of surgery is faced with obstacles such as reduced haptic and visual feedback. The use of counterintuitive graspers along with indirect visual access into the operating theatre reduces the surgeon's ability to discriminate material properties of tissue such as stiffness, size, and colour.

Research has gone into the integration of visual and haptic information during LS. While both types of feedback are important in compliance discrimination tasks, it has been shown that visual information is indeed dominant during such discrimination tasks [7], [52]. RALS has emerged from the need to improve the accuracy, precision, and performance of surgeons during LS [95]. Surgeons use robotic systems such as the da Vinci robot to perform entire procedures. The da Vinci utilizes HD stereoscopic visual access into the operating theatre which leads to reduced human error and improved performance. However, the da Vinci offers no force feedback. The surgeon performs entire operations without any force feedback whatsoever, relying mostly on visual information provided by the stereoscopic binoculars to perform any and all assessments regarding tissue properties and health. The da Vinci is another example of the power of visual information during haptic feedback tasks. Aside from its high cost which can be considered the biggest obstacle by itself, disadvantages of the da

Vinci are mainly its large size which could create manoeuvrability issues in a small operating workspace, the cost of maintenance of such a high-end system, and the cost to recruit and train surgeons and nurses with the necessary skills in order to safely operate it [96].

Surgical technologies continue to advance. Advancements in MIS mean that it is here to stay, at least for now. The introduction of RALS has seen great results and continues to develop. Plenty of research has gone into investigating whether or not the introduction of force feedback into RALS is the ‘future’ of robotic assisted surgery. While the degree of usefulness of force feedback remains controversial, there is no debate regarding the significance and even dominance of visual feedback in compliance discrimination tasks [7], [52], [71], [93]. Nonetheless, the relative contribution of visual information during compliance discrimination tasks particularly in MIS, RALS, and surgical training is yet to be fully determined. With extensive literature emphasizing the dominance of visual feedback during haptic compliance discrimination tasks, there is a need to quantify the extent of this visual dominance in an effort either to substitute for absent, weakened, or distorted haptic feedback; or to enhance a surgeon’s sensory experience during MIS and surgical training.

2.8. Aim of the Thesis

2.8.1. Aim

The aim of the research is to evaluate the contribution of visual information during compliance discrimination tasks within a surgical context by characterizing the differences between the tactile feel of computer simulated compliant materials compared to real ones and assessing the impact of visual and haptic cues on performance using psychophysical methods.

2.8.2. Objectives

1. Create an array of samples mimicking real tissue softness, with similar stress-strain behaviour to a known soft tissue organ such as the liver.
2. Link the physical compliance of the samples to viscoelastic parameters such as stiffness and viscosity coefficients using suitable mathematical models.
3. Determine the effect of the type of visual cues available during modes of surgery on the ability to discriminate compliance of soft samples using psychophysical experimentation methods.
4. Assess the effect of indentation force and displacement on the ability to visually discriminate compliance through a monitor.
5. Develop a pseudo-haptic feedback robotic system capable of independently manipulating visual and haptic feedback.
6. Validate the pseudo-haptic system's ability to simulate viscoelastic behaviour of compliant objects.
7. Determine the extent to which visual feedback augmentation can generate realistic sensations of haptic compliance via a psychophysical experiment such as magnitude estimation.

3. Stimuli Modelling

LS and RALS training simulators used today use virtual environments to simulate numerous surgical scenarios [97]. As a result, realistic visual and haptic soft tissue rendering is critical. Soft tissue biomechanics is studied and combined with computer-graphics simulations to mimic realistic haptic and visual tissue deformation. The human body is primarily composed of soft tissue [97]. Hence, accurate modelling of the behaviour of tissue is vital for medical training as well as tissue characterization [98]. Understanding how human tissue behaves during loading, relaxation, and unloading is critical for numerous industries including the consumer products industry, physical therapy, and digital human modelling in general [98].

In this thesis, psychophysical methods were used to conduct experiments in which human participants performed medically relevant tasks such as palpation of simulated tissue. Soft tissue is known to behave in a nonlinear manner and is difficult to use and experiment on while maintaining consistency across all participants. Therein lays the need to develop compliant objects with similar behaviour to human tissue. The advantages of using fabricated samples from materials such as silicone include improved reliability, repeatability and consistency during testing [99]. Soft tissues and elastomers are considered to behave in a nonlinear manner since they undergo large deformations exhibiting time dependent behaviour [100]. Linear models, however, have been used in previous research to simulate the behaviour of tissue [99], [101]–[104]. In this chapter, these models will be assessed and one will be selected to model the behaviour of the fabricated samples in each psychophysical experiment.

The experiments conducted in this thesis assess compliance discriminability of humans under various combinations of visual and haptic feedback. Surgeons palpate tissue either using their hands (OS) or slender tools (MIS) to determine tissue health [15]. Tissue characterisation is a complicated process involving the use of mathematical models to simulate the behaviour of tissue during all deformation stages: loading, relaxation and unloading. Participants will be asked to palpate the samples at a relatively rapid rate. Since the rate of recovery of the samples will always be less than the recovery speed of the participants' palpations, the work carried out is primarily focused on tissue deformation during the loading section of palpation.

3.1. Biomechanics of soft tissue

Biomechanics refers to the analysis of dynamic systems within the field of biology [105]. More specifically, it is the study of the mechanics of living things. On the surface, surgery might appear to be unrelated to mechanics but patient treatment and rehabilitation rely heavily on tissue stress and strain. Biological tissues generally exhibit nonlinear history dependent stress-strain behaviour. Predicting nonlinear force-displacement and stress-strain behaviour of tissue has been investigated extensively in the literature. Mathematical models can and have been used to simulate tissue behaviour during loading, unloading, and relaxation under various loading conditions [99], [102], [104], [106]. Soft tissue refers to any structures surrounding bone and cartilage such as organs, muscle, skin, nerves, and blood vessels. With the human body being primarily made up of soft tissue, soft tissue modelling is considered vital for developing next generation medical simulators for several medical purposes such as minimally invasive surgery, heart surgery, and plastic surgery [97]. Human soft tissue is known to exhibit viscoelastic characteristics [106].

3.1.1. Viscoelasticity

A viscoelastic material possesses both viscous and elastic characteristics during deformation [107]. The three features that define viscoelasticity are creep, hysteresis, and relaxation [107]. A sudden stress followed by a constant maintained strain thereafter is referred to as relaxation. In this phenomenon, the stresses created in the body decrease with time [107]. A sudden applied stress that is maintained constant thereafter while the body continues to be deformed is referred to as creep. During a cyclic loading, hysteresis is the relationship between the stress and the strain during loading and unloading [105]. Unlike purely elastic materials, viscoelastic materials lose energy due to the viscous component during loading and unloading creating a state of hysteresis. Most soft tissues combine elastic and viscous properties and hence are referred to as viscoelastic [97]. Viscoelastic behaviour is typically predicted by fitting stress-strain experimentation data to mathematical models.

3.1.2. Viscoelastic models

Viscoelastic behaviour of tissue is often predicted using mechanical models under various loading conditions. The three general mechanical models of material behaviour are the Maxwell model, the Voigt model, and the Kelvin model. More complex models can be made by combining two or more of these models together. The Maxwell and Voigt models are often used to describe the viscoelastic response of soft tissue [99], [102]. The Maxwell model been used to describe the stress relaxation behaviour of food matrices such as agar gel [104]. Taylor et al. [99] successfully applied a Voigt viscoelastic model to stress-strain experimental data of bovine tissue. Lopez-Guerra and Solares [108] modelled viscoelasticity in atomic microscopy simulation using several models including the Maxwell model, the Voigt model and the Kelvin model. Nobile et al. [104] used the generalized Maxwell model to describe stress relaxation of solid-like foods including ripened cheese and meat. Results showed that the model was successful at fitting to the data for the five food types used. Leeman & Peyman [102] used a Maxwell model to describe the acoustical properties of human soft tissue.

These models are composed of different combinations of linear springs and damper coefficients. Deformation resulting from a linear spring is position dependent whereas that resulting from a damper is velocity dependent. A tensile force applied onto a spring would be of the form:

$$F = Kx \quad (5)$$

Where F is the force applied, x is the measured displacement of the object due to the force applied and K is the spring constant.

While a force applied onto a damper would be of the form:

$$F = \eta \frac{dx}{dt} = \eta \dot{x} \quad (6)$$

Where η is the damping coefficient and \dot{x} is the velocity of the object on which the force was applied.

The Young's modulus of a spring is another measure of the stiffness of an elastic object such as a spring. It is defined as the ratio of the stress applied (σ) and the strain (\mathcal{E}) along an axis, as follows:

$$E = \frac{\sigma}{\mathcal{E}} \quad (7)$$

For a unit cross-sectional area, the Hooke's law spring constant (K) is the Young's modulus of elasticity (E) of a spring since any displacement is assumed to be longitudinal [109]. Throughout this thesis, a unit cross-sectional area is assumed for simplicity. Hence, the constant E used is a representation of both the spring constant as well as the Young's elastic modulus.

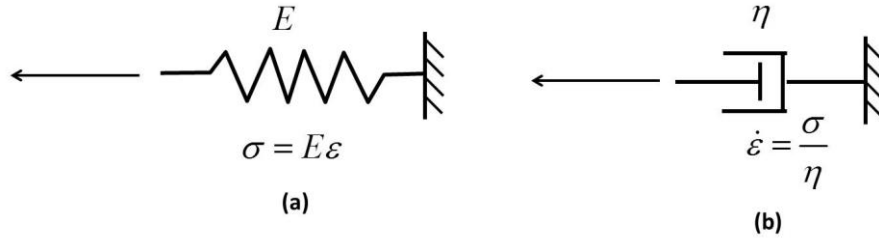


Figure 7. Spring-mass system (a) and damper-mass system (b) during tension

3.1.2.1. Maxwell model

The Maxwell model (Figure 8) is simply a spring and a damper connected to one another in series [102]. The same stress is transmitted from the spring to the damper ($\sigma_S = \sigma_D$). This stress produces a spring displacement as well as a damper velocity. The total strain is the sum of the strain acting on the spring and damper ($\mathcal{E}_{Total} = \mathcal{E}_S + \mathcal{E}_D$). Deriving the strain with respect to time, we obtain the following:

$$\frac{d\mathcal{E}_{Total}}{dt} = \frac{d\mathcal{E}_D}{dt} + \frac{d\mathcal{E}_S}{dt} = \frac{\sigma}{\eta} + \frac{1}{E} \frac{d\sigma}{dt} \quad (8)$$

In dot notation, the general Maxwell equation becomes:

$$\dot{\mathcal{E}} = \frac{\dot{\sigma}}{E} + \frac{\sigma}{\eta} \quad (9)$$

For a constant applied stress, the general Maxwell equation becomes:

$$\varepsilon = \varepsilon_0 \left(1 + \frac{Et}{\eta} \right) \quad (10)$$

Alternatively, put under constant strain, the stresses of a material under the Maxwell model gradually relax. The main disadvantage of this model is its inability to predict creep (constant stress) accurately [110]. The Maxwell model for creep suggests that strain linearly increases with time. In reality, polymers generally show that the strain rate actually decreases with time [110].

3.1.2.2. Voigt model

In the voigt or (Kelvin-Voigt) model, a spring and a damper are connected in parallel and so have the same strain (Figure 8). The Voigt model is usually used to describe creep (constant stress applied) [110]. The total stress is the sum of the stress of each component:

$$\sigma = E \cdot \varepsilon + \eta \frac{d\varepsilon}{dt} \quad (11)$$

The total force, shown below in dot notation, is the sum of the individual forces applied on the spring and damper [Equation (8)]

$$F = Ex + \eta \dot{x} \quad (12)$$

The Voigt model is known for its ability to describe creep compliance, but not for its ability to describe stress relaxation [108]. Applying a constant stress to a Voigt material, the deformation would approach that of a purely elastic material ($\frac{\sigma}{E}$) with an exponentially decaying difference. The Voigt equation then becomes:

$$\varepsilon = \frac{\sigma}{E} \left[1 - e^{-\frac{Et}{\eta}} \right] \quad (13)$$

3.1.2.3. Kelvin model

The Kelvin model (Figure 8) is composed of a Maxwell model having a spring constant E_1 and damper viscosity coefficient η , in parallel with a spring with spring constant E_2 [103]. Since the Maxwell spring-damper system and the second spring are connected in parallel, the total stress is the sum of that of the Maxwell model and the spring, whereas the total strain is the same across both. The total stress consists of a

rate dependent stress component in spring 1 and rate independent stress component in spring 2. Substituting into a general equation:

$$\frac{d\varepsilon}{dt} = \frac{\frac{E_1}{\eta} \left(\frac{\eta}{E_1} \frac{d\sigma}{dt} + \sigma - E_2 \varepsilon \right)}{E_1 + E_2} \quad (14)$$

The Kelvin model can also be represented as:

$$F + \tau_\varepsilon \dot{F} = E_2(x + \tau_\sigma) \quad (15)$$

where

$$\tau_\varepsilon = \frac{\eta_1}{E_1}, \quad \tau_\sigma = \frac{\eta_1}{E_2} \left(1 + \frac{E_2}{E_1} \right)$$

The Kelvin model is used when the simpler models do not provide a good enough fit. While the Kelvin model allows for fitting a greater range of polymers and materials, it necessitates fitting an additional parameter which makes it more complicated than the Maxwell or Voigt models. In this model, a spring with stiffness E_1 is in parallel with a spring with stiffness E_2 which is attached in series to a damper with a viscosity coefficient η . Solving the general model for σ at equilibrium, the equation becomes:

$$\sigma = \left(E_1 + E_2 \exp\left(\frac{-E_1 t}{\eta}\right) \right) \cdot \varepsilon \quad (16)$$

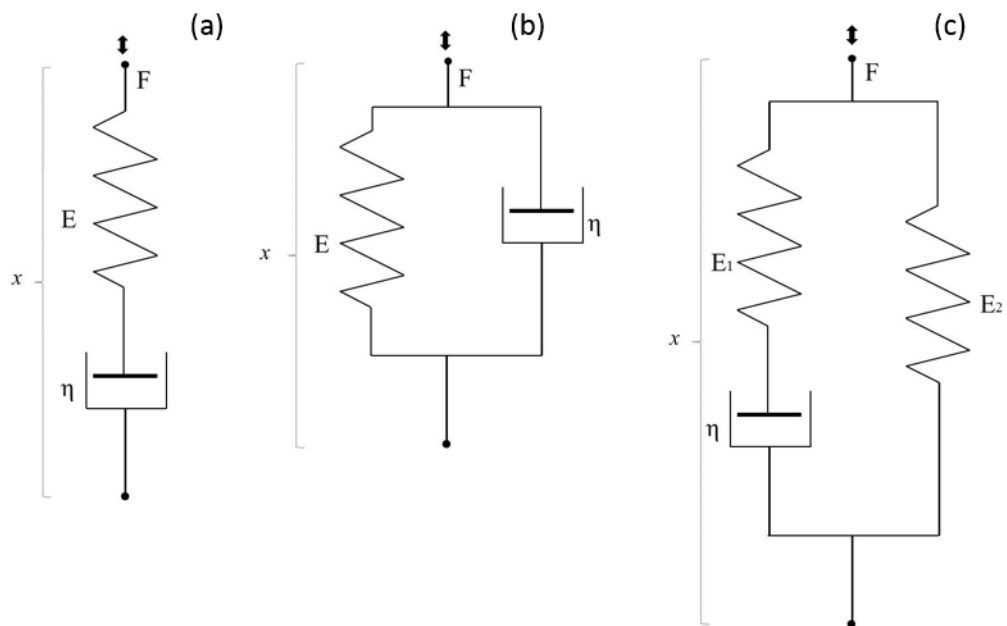


Figure 8. Schematics representing the (a) Maxwell, (b) Voigt, and (c) Kelvin models

3.2. Methods

11 silicone samples were fabricated. In compliance discrimination literature, the number of samples used has often ranged between 10 and 12 samples [47], [50]. These samples were used throughout this thesis in all experiments. However, it should be noted that new samples were fabricated and tested for each experiment to eliminate any sample ageing or variability in their mechanical properties. Stress-strain functions of each sample were obtained using specialized indentation rigs. The stress-strain data was fitted to the models described in Section 3.1.2 to obtain stiffness constants and damping coefficients for the samples.

3.2.1. Stimuli fabrication

The samples were fabricated using a two-part silicone-based gel polymer (Plastil, Mouldlife) with a plasticizer in different ratios to obtain the desired compliance levels. Mixing these materials has been proven useful in tissue modelling exhibiting biological variability [111]. Seen in Table 5, Plastil gel 10 parts A and B were mixed with the plasticizer in a ratio of A: B: plasticizer ranging from 1:1:2.6 (least compliant) to 1:1:4 (most compliant) to create 11 unique samples. To maintain simplicity and reduce variability during indentation, sample indentation was to be performed only using one finger or tool tip. Moreover, tumour detection can range from a few millimetres beneath the tissue surface to over 20 cm in the liver [10]. Hence, tissue palpation depth has a large range. A silicone mould tray (Figure 9) was used to cast each sample. Each tray cup was 5cm wide and 2cm deep with a truncated conical shape. The size of a liver, for instance, ranges from 6 to 15 cm [112], so this sample size was selected as it fell in that range. Prior to pouring the silicone mixtures, each cup were encapsulated three times with a thin polyurethane coating to prevent sticking and to maintain the same adhesion and friction properties across all the samples. The coatings were sprayed onto the moulds using an airbrush. After allowing the coatings to dry for approximately 15 minutes, a unique ratio of Plastil gel 10 parts A, B, and plasticizer for each sample were poured into plastic containers and mixed thoroughly before pouring into the silicone tray cups. A skin coloured pigment was also added into each mixture without affecting the material properties to mask visual cues from slight colour variations of each sample. The silicone samples were left for 24 hours to

set and then coated with a layer of thin polyurethane coating to prevent the surface from sticking to any object after removal. Samples were then carefully removed from the mould tray and were ready to be tested (Figure 10). To avoid wear and tear of the samples, a new set of samples was fabricated for each psychophysical experiment in this thesis.



Figure 9. Silicone tray used to cast the shapes of the samples

Table 5. A: B: Plasticizer ratios for making each of the 11 samples

Sample	1	2	3	4	5	6	7	8	9	10	11
A	1	1	1	1	1	1	1	1	1	1	1
B	1	1	1	1	1	1	1	1	1	1	1
Plasticizer	2.6	2.8	3.0	3.1	3.2	3.3	3.4	3.5	3.6	3.8	4.0



Figure 10. The 11 samples created for the psychophysical experiments

3.2.2. Compliance testing

The compliance of the samples was tested using three indentation rigs for data validation and consistency. The three rigs were the Modular Universal Surface Tester (MUST), a custom-built indentation rig, and the Mecmesin MultiTest 5-i indenter. Initially, the MUST was used to collect stress-strain data for all the samples which were used to estimate the stiffness and damping coefficients following model fitting. The custom-built rig was primarily designed and assembled for the experiment in Chapter 5. Finally, the Mecmesin MultiTest 5-i indenter was used in Chapters 6 and 7 to re-test the compliance of the samples at variable speeds. The samples were tested without any side constraints during axial compression as during stiffness measurement, samples are best kept unconstrained laterally [113].

3.2.2.1. *Modular Universal Surface Tester*

The compliance of each of the fabricated samples was characterised using a MUST (Compass Instruments) (Figure 11). A hemispherical uPVC (unplasticized polyvinyl chloride) rigid tip with an 8 mm diameter was attached to the MUST indenter tip and used to indent the samples at a rate of 0.2mm/s until reaching a force of 500 mN. The force-displacement profile of the indentation was recorded at 100 Hz. Each sample was tested five times for improved data consistency. The average force and displacement values across the five repeats were calculated and used for model fitting.

3.2.2.1. *Custom Indentation Rig*

An indentation rig (Figure 11) was designed and assembled using a linear actuator (SMAC Inc. USA, LCA50-025-7) coupled with a 6 degree-of-freedom (DoF) force transducer (ATI, Nano17). This rig was designed and built specifically for an experiment described in Chapter 6 where controlling indentation rate and depth was necessary. Aluminium framework (Bosch Rexroth) was used to assemble the rig. Force and position data were controlled and measured using a LabVIEW (National Instruments, TX) program. A hemispherical uPVC (unplasticized polyvinyl chloride) rigid tip with an 8 mm diameter indented the stimuli at a rate of 10mm/s until reaching a depth of 10 mm into the stimuli. Since the rig was controlled using LabVIEW, a higher loop rate was possible. Hence, the force-displacement profile of the indentation was recorded at 1 kHz. Each sample was tested five times for improved data

consistency. The average force and displacement values across the five repeats were calculated and used for model fitting.

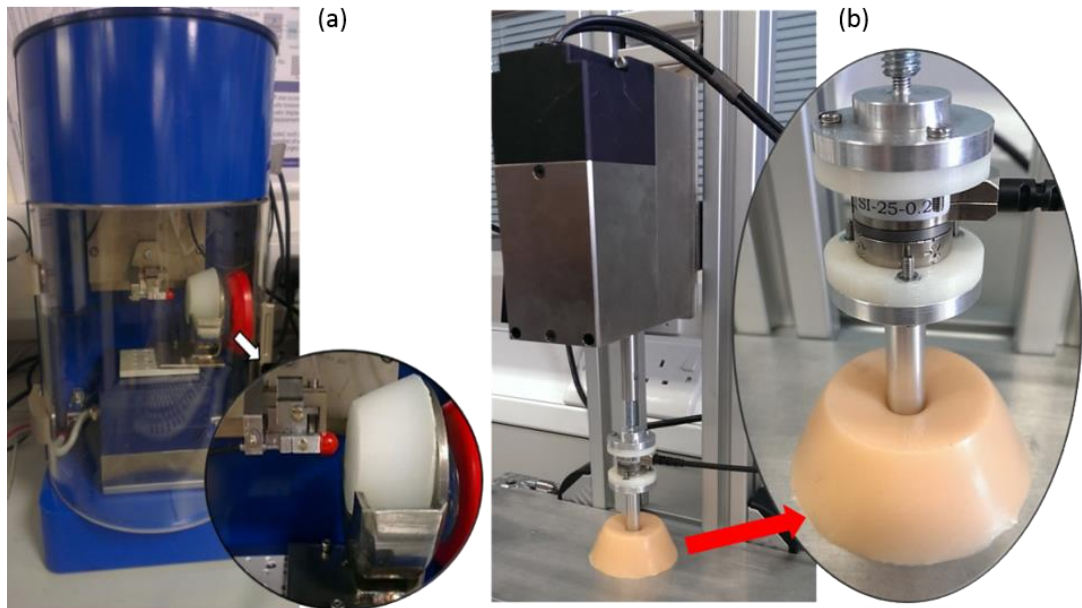


Figure 11. MUST rig (a) and custom indentation rig (b) during indentation of the samples

3.2.2.2. *Mecmesin MultiTest 5-i*

This is a computer-controlled tensile and compression testing system for force measurements up to 10N that was used to obtain the stress-strain data for the samples during compression. The system has a maximum load capacity of 5 KN, with a load resolution of 1:5000, a load accuracy of $\pm 0.1\%$ of full scale, and speed range of 1-1000mm/min. This system was used to conduct stress-strain tests on the 11 samples. The same 8mm diameter hemispherical tip previously used in the MUST and the custom indentation rig was attached as an indentation fixture. Samples were indented at a speed of 2mm/s for a depth of 10mm. Each sample was tested five times for improved data consistency. The average force and displacement values across the five repeats were calculated and used for model fitting.

3.2.3. Viscoelastic model fitting

The force-displacement data collected from the MUST were normalized and fitted to the Maxwell, Voigt, and Kelvin mathematical models.

3.2.3.1. Maxwell model

This model is used in Chapter 4 where applied stress is varied since sample indentations are performed manually by participants and hence cannot be controlled. The stiffness and damping coefficients extracted for all samples are presented in Table 6. Although the damping coefficient influences the viscoelastic behaviour of the samples, the stiffness coefficient, or Young's modulus of elasticity, has been frequently used in the literature to showcase the mechanical properties of biological tissues during loading and unloading [10], [111].

Table 6. Stiffness and damping coefficients obtained via fitting indentation data to the Maxwell model

Sample	Stiffness coefficient (N/mm ²)	Damping coefficient (N.s/mm)
1	0.160	0.0250
2	0.156	0.0240
3	0.151	0.0229
4	0.139	0.0192
5	0.130	0.0164
6 (Reference)	0.127	0.0160
7	0.120	0.0131
8	0.115	0.0129
9	0.113	0.0121
10	0.103	0.0110
11	0.100	0.0101

Figure 12 shows the force-displacement data obtained for the reference sample using the indenter along with the Maxwell model fit during loading. Visually, the Maxwell model appears to provide a good fit for the viscoelastic behaviour of the samples during loading.

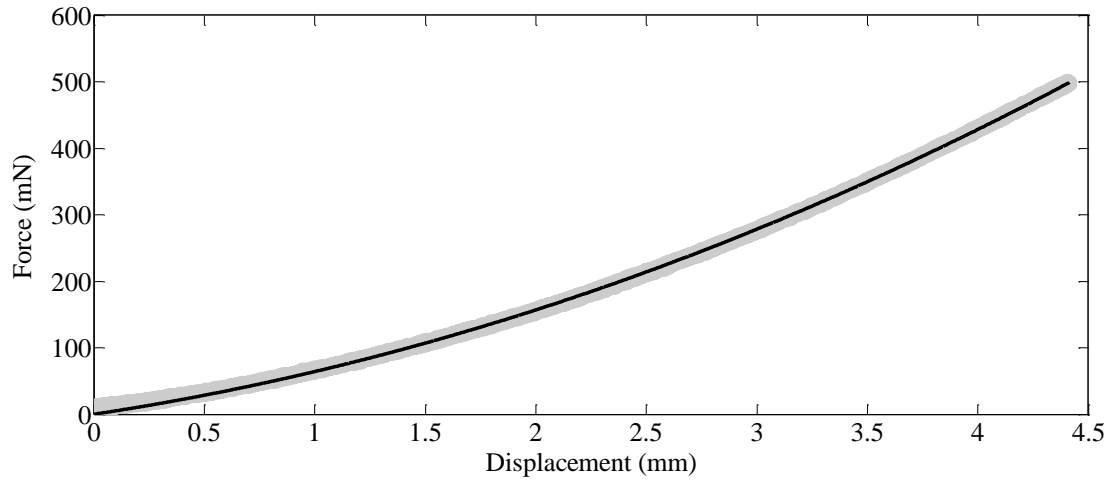


Figure 12. Force-displacement data from indenter (shaded grey) and fitted Maxwell function (solid black) for Sample # 6

3.2.3.2. Voigt model

Force and position data for all samples obtained during the indentation tests were fitted to the Voigt model (Table 7).

Table 7. Stiffness and damping coefficients obtained via fitting indentation data to the Voigt model

Sample	Stiffness coefficient (N/mm ²)	Damping coefficient (N.s/mm)
1	0.298	0.323
2	0.278	0.228
3	0.257	0.100
4	0.246	0.0854
5	0.266	0.0784
6 (Reference)	0.231	0.0732
7	0.220	0.0652
8	0.210	0.0570
9	0.200	0.0443
10	0.186	0.0353
11	0.179	0.0313

Figure 13 shows the force-displacement data obtained for the reference sample using the indenter along with the Maxwell model fit during loading.

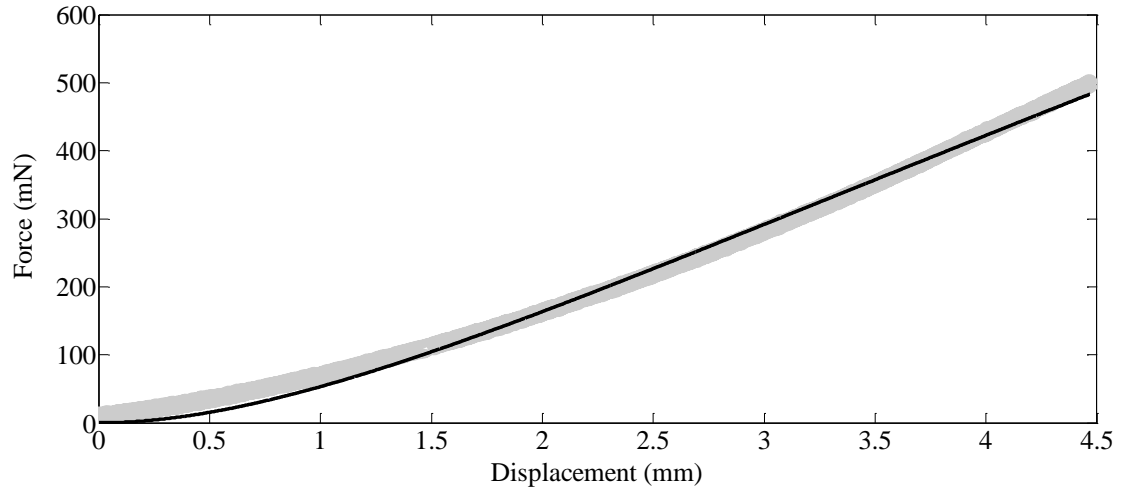


Figure 13. Force-displacement data from indenter (shaded grey) and fitted Voigt function (solid black) for Sample # 6

3.2.3.3. Kelvin model

Force and position data for all samples obtained during the indentation tests were fitted to the Kelvin model as well, and the resulting two stiffness coefficients as well as the damping coefficient are shown in Table 8.

Table 8. Stiffness and damping coefficients obtained via fitting indentation data to the Kelvin model

Sample	Stiffness coefficient 1 (N/mm ²)	Stiffness coefficient 2 (N/mm ²)	Damping coefficient (N.s/mm)
1	0.0738	2.94	74
2	0.0821	1.77	36
3	0.0771	1.27	26
4	0.0714	1.39	31
5	0.0654	1.14	26
6 (Reference)	0.0565	1.84	44
7	0.0589	1.19	33
8	0.0590	1.14	30
9	0.0552	0.966	24
10	0.0476	0.821	21
11	0.0468	0.505	13

3.2.4. Regression Analysis

Values of the R-squared (R^2) and the root mean square error (RMSE) were determined for all the fits of the models to the data (Appendix D). These are commonly used

statistical method that is a good indicator of how well the data fits a statistical model [114]. RMSE values for each sample measured using the Maxwell, Voigt and Kelvin models are shown in Figure 14.

3.3. Discussion

There are numerous mathematical models that can be used to predict the behaviour of tissue or tissue-like materials [97], [99], [102], [103], [106], [108], [115]–[117], the simplest being the Maxwell, Voigt and Kelvin models. Although these models have disadvantages, they are known to provide a good fit for tissue during loading and unloading. Both the Maxwell and Voigt models appear to provide good fits for the viscoelastic behaviour of the samples during loading (Figure 14). Moreover, all calculated values of R^2 were greater than 0.99 and all RMSE values were less than 5%, suggesting that all three models are good fits for the sample indentation data. However, while the Kelvin model provides a good fit, it introduces an added spring into the system which increases complexity.

Young's modulus of elasticity has been frequently used in the literature to describe and characterize tissue stiffness. A greater Young's modulus implies stiffer tissue, which could indicate the presence of a tumour [10], [118]. In this chapter, a silicone mixture sample range was fabricated to be used in compliance discrimination experiments. Although simplified, these samples were designed to simulate the behaviour and mechanical properties of tissue. The literature has shown that the stiffness of tissue ranges between 0.014MPa and 0.28MPa and fluctuates depending on type, location, size, and health [119]. Consequently, the stiffness coefficients obtained using the mathematical models align with those obtained in the literature, which validates the use of the samples in future experiments investigating compliance discrimination.

Throughout this thesis, the Maxwell and Voigt models will be used to obtain fits for the stress-strain data during loading for all the samples. These models were selected due to their simplicity, their history of use in similar situations throughout the literature, and their ability to accurately predict the behaviour of the samples used in this thesis.

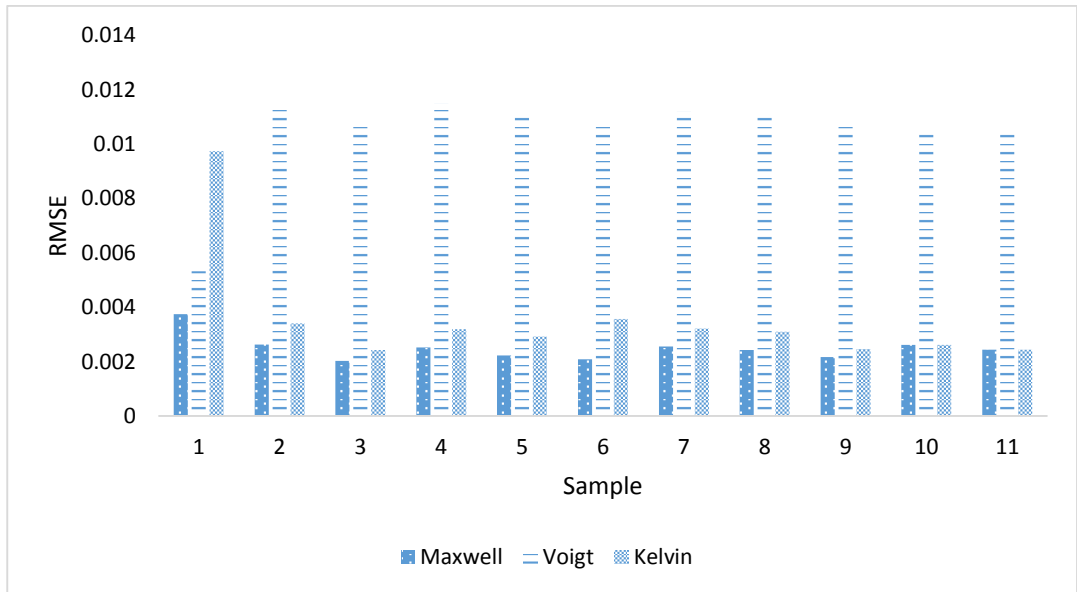


Figure 14. RMSE when fitting the experimental indentation data to the Maxwell, Voigt and Kelvin models

3.4. Summary

In this chapter, soft silicone samples which mimic the viscoelastic properties of human tissue were fabricated. Indentation tests were performed on these samples to obtain the stress and strain data during loading. Maxwell, Voigt and Kelvin models were fitted to these data sets to provide each sample with stiffness and damping coefficients. These coefficients are used throughout this thesis in all experiments to characterize the viscoelastic properties of the samples. The Maxwell model is used in Chapter 4 while the Voigt model is used in the remaining chapters.

4. The Effect of Visual Cues on Compliance Discrimination

Abstract

This chapter describes an assessment of the impact of the source of visual information on the ability to discriminate softness of compliant objects with a specific focus on tool-operated palpation. Twelve participants took part in four two-alternative forced-choice (2AFC) compliance discrimination tasks which represent different modes of surgery. In the first task, participants had direct visual access to the samples during palpation, which was performed using a tool. In the second task, tool-operated palpation was coupled with indirect visual information using a webcam and a monitor. In the third task, haptic feedback via a tool was the only source of feedback available to participants. In the fourth task, visual information was the only source of feedback available. Participants observed as the samples were indented by someone else and displayed on the monitor. As a control task, participants performed discriminations using their index finger without any visual cues present. Results showed that participants performed best during the control task followed by that involving a combination of direct visual access coupled with haptic feedback using a tool. Moreover, the task using only indirect vision without any haptic information presented similar compliance discriminability to that using only touch through a tool without any visual information. The results suggest that compliance discrimination is most reliable when cutaneous information is present. While participants were able to discriminate softness using either indirect vision only or haptic tool-operated touch only, performance was enhanced when a combination of both cues was used. This highlights the significance of visual information in palpation tasks and suggests a visio-haptic cross-modal integration occurring during compliance discrimination, with key implications for the development of new surgical tools and training systems capable of optimising this cross-modality.

4.1. Introduction

To understand the motivation behind these experiments, a brief summary of the literature concerning the link between visual and haptic feedback during simulated surgical palpation is presented. Palpation is a very powerful examination method used by clinicians to detect irregularities and tumours [10]. Surgeons assess tissue health to locate potentially cancerous tumours [45], by palpating (pressing or tapping) the tissue surface using a combination of haptic and visual information [15]. Abnormal tissue typically has distinct mechanical properties (such as compliance) from healthy tissue [116], thus allowing the surgeon to discriminate by evaluating changes in those properties. In LS, surgeons use slender tools to palpate tissue and perform tissue evaluations. While some research found that the use of LS graspers reduces the surgeon's ability to discriminate softness of tissue [8], others found compliance discrimination using a tool to be, in some cases, as informative as using one's finger [50]. The increasing use of MIS as a replacement for OS suggests that tool operated feedback is necessary for the time being. Perhaps a shift in focus from haptic feedback development to visual feedback optimisation is needed.

Visual information in any surgical environment has been shown to play a significant role during compliance discrimination [42], [52], [71], [120]. According to the literature, visual feedback dominates during compliance discrimination tasks where both visual and haptic feedback are present [52]–[56]. Srinivasan et al. [52] found a visual dominance during stiffness discrimination tasks within a virtual environment. Their set-up, however, did not use real physical stimuli such as in LS. Kuschel et al. [93] proposed that when both visual and haptic feedback are available, the modality with the highest reliability contributes the most to compliance discrimination. Their experiment also used virtual samples felt using a haptic feedback system and seen as graphically-rendered samples on a computer screen. Perreault & Cao [42] found that vision and touch are equally important for tissue compliance differentiation. However, their results were based on only three virtual tissues each with a specific compliance value. It would be beneficial to conduct similar palpation tasks exploring the impact of visual information on compliance discrimination using a greater range of physical complaint samples, in various scenarios simulating different modes of surgery. Thus,

both visual and haptic sources of information would not be prone to inaccuracies that arise from virtual visual and haptic simulations.

A 2AFC psychophysical experiment was set up using the method of constant stimuli in order to determine the effect of vision on compliance discriminability of deformable objects. Primarily, this work focused on how well people are able to discriminate softness of compliant objects under different conditions such as open and LS. Understanding the effect direct and indirect visual and haptic feedback have on the ability to discriminate compliance as well as how they differ from one another is essential for improving and developing visual and haptic feedback systems that can be used in surgical training systems and RALS procedures. The outcomes of the research are relevant to researchers in LS, RALS, tactile displays and human computer-interaction as they link current computer interfaces in LS and state of the art surgical robotic systems (such as the DaVinci) to the psychophysics behind compliance discrimination specifically in surgical palpation tasks.

4.2. Methods

Along with a control task, four 2AFC tasks were designed and conducted. The tasks were performed under different visual and haptic conditions. Participants performed compliance discrimination tasks for each of the conditions across the range of compliance levels. The method of constant stimuli was implemented in these psychophysical experiments since a finite number of physical stimuli was used.

4.2.1. Participants

Twelve participants (nine male and three female) were recruited for this study. Participants were students at the University of Leeds with ages ranging from 18 to 34. None of the participants had any known hand or eyesight impairments according to a completed questionnaire (Appendix A.1). Finally, ethical approval was obtained before conducting the experiment.

4.2.2. Stimuli

Eleven samples having different levels of compliance were fabricated for this experiment. The fabrication, testing, and modelling of the samples was described in Chapter 3. For this experiment, the mechanical properties of the samples were

obtained using the MUST tester. Stress and strain data were fitted to a Maxwell model which was found to be an appropriate fit for modelling soft tissue parameters during loading [103], in order to obtain stiffness and damping coefficients governing the viscoelasticity of each sample. These coefficients are tabulated in Section 3.2.3.

4.2.3. Experimental design

Participants performed 2AFC compliance discrimination tasks. They were presented with pairs of samples and were asked to compare the softness of these samples. Each pair consisted of a reference sample and a test sample. In total, 10 test samples were used in this experiment. The stiffness of the reference sample was located at the centre of the sample stiffness range (sample #6). The positions of the test and reference sample were randomly switched and the order of the trials was counterbalanced for each participant according to a 4x4 Latin Square Design [121]. This method of counterbalancing was used to prevent any learning effects from impacting the results. Due to the nature of this 2AFC experiment, the reference sample was subject to a greater number of indentations during each experiment. To account for wear and tear of the reference sample, a new reference sample was fabricated for each participant. This allowed for an even indentation number for all samples, eliminating any property changes.

4.2.3.1. *Control task: Cutaneous feedback only*

In the control task, cutaneous information alone was used to judge the softness of samples without any visual aid present. Participants performed 2AFC tasks on the sample pairs using their dominant index finger. They were asked to palpate both samples within each pair and state which of the two samples they thought was softer. There was no specified time limit on each discrimination task.

The four remaining tasks were under the following conditions: direct visual access with tool using a tool, indirect 2D visual access with touch using a tool, indirect 2D visual access with no touch, and no visual access with touch using a tool.

4.2.3.2. *Direct vision with touch through tool*

Participants were seated in front of a D65 daylight simulator. According to the International Commission on Illumination, the daylight simulator (Figure 15) provides standard illuminant D65 which imitates standard illumination conditions at

open-air. The daylight simulator was used to maintain controlled and consistent lighting conditions throughout all experiments. Participants were allowed direct visual access into the daylight simulator and hence could directly view the samples. Participants were given standardised introductions and were asked to follow a defined protocol (Appendix A.2). They inserted their dominant hand into the daylight simulator and were presented with a reference sample and a test sample positioned side by side inside the daylight simulator. The sample pairs were placed inside a frame with centres 10 cm apart to guide the participants, reduce location errors, and maintain experimental consistency. The frame, the samples and the tool used can be seen in Figure 15. Using the provided tool, participants were asked to judge the compliance of both samples subjectively stating which sample felt softer. Since discrimination with a tool is unaffected by the number of fingers the tool was controlled by [50], participants were asked to hold the tool using three fingers, similar to how they would hold a pen, keeping the tool in a vertical position. This represents a common, simple and consistent grip that novice participants are likely to be familiar with. Participants were given the freedom to go back and forth between the test and reference sample as often as needed until a decision had been made. There was no specified time limit on each discrimination task. This task is illustrated in Figure 16.

4.2.3.3. *Indirect 2D vision with touch through tool*

Participants did not have direct visual access into the daylight simulator but could view the samples inside the daylight simulator through a 19 inch HD compatible display monitor (Dell) positioned 15 degrees below eye level which is a standard laparoscopic screen setting [122]. The screen displayed a live feed of a high definition webcam (Microsoft Lifecam Cinema) shooting at a resolution of 720p with a frame rate of 30 fps at which there was no observable video latency. The webcam was positioned inside the daylight simulator in such a way that the viewing angle is similar to directly viewing the samples (Figure 16). With the daylight simulator obstructed by a dark curtain, participants performed the same 2AFC compliance discriminations looking at the screen and indenting the samples with the provided tool.

4.2.3.4. *Only touch through tool*

Participants did not have visual access to the samples during compliance discrimination (Figure 16). Using a tool, participants were asked to judge the

compliance of both samples subjectively stating which sample felt softer, relying solely on haptic feedback from the tool. A dark curtain was placed between the participants and the samples. Participants slid their dominant hand underneath the curtain and located the samples. The 3D printed frame was used in this task as it simplified locating where each sample was within each pair simplifying the indentation process as well as allowing it to be standardized and repeatable.

4.2.3.5. *Only indirect vision*

Participants judged the softness of the samples without touching any themselves but rather by observing the samples being indented using a tool on a 2D display by someone else. This setup is similar to that conducted by Drewing et al. [53]. Seated in front of a screen, participants were played 30-second recordings of sample pairs being indented. All clips were recorded using the same discrimination techniques such that they provided the participants with the necessary information to discriminate compliance. In each 30-second clip, each pair was indented three times at increasing indentation speed so that the participants would observe the behaviour of samples with time. The speeds were roughly 5mm/sec, 10mm/sec, and 20mm/sec. This experiment is illustrated in Figure 16. Participants were once again asked to judge the compliance of both samples, subjectively stating which sample felt softer. Each recording was repeated as many times as needed until a decision had been made.

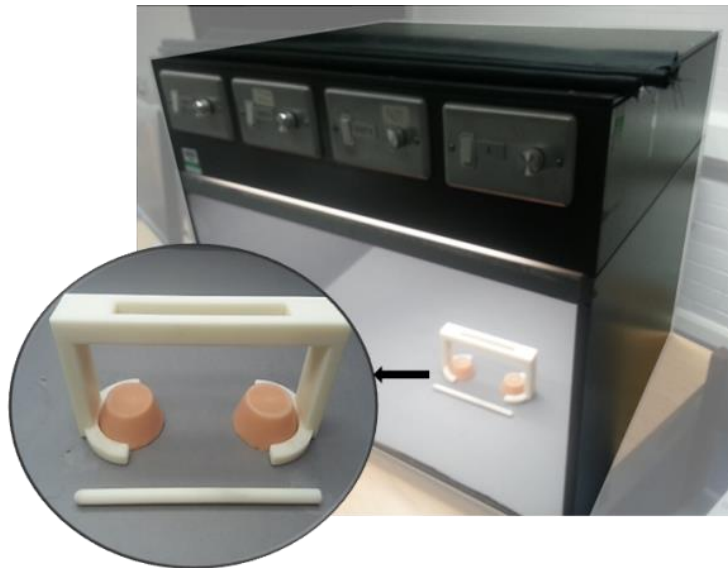


Figure 15. D65 Daylight simulator, plastic sample frame and indenter tool used in the experiments

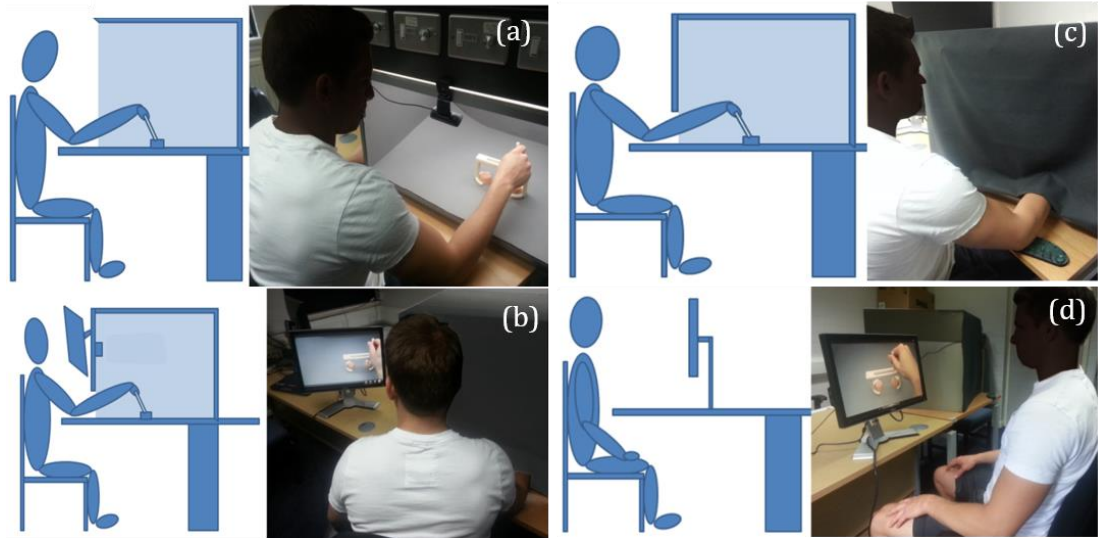


Figure 16. The 4 tasks performed by the participants: Direct vision with tool (a), indirect vision with tool (b), only tool touch (c) and only indirect vision (d)

4.3. Experimental analysis

Participants' responses were collated and fitted to a psychometric function referred to as the modified logistic function. A psychometric function is a measure of the relationship between some physical stimulus and the observer's forced-choice response at that stimulus [123]. In other words, it is the relation between a stimulus and an observer's ability to detect that stimulus. Sensory stimuli include weight, velocity, brightness, softness, roughness, wetness, loudness, and so on. In this experiment, psychometric functions were constructed to illustrate the relation between the compliance of the samples and the participants' ability to accurately judge them.

The results of the tasks were fitted with a parametric function referred to as the modified logistic function [Equation (17)] which was found to be a good fit for psychometric functions in previous research [123]–[127]. Using an iterative least squares method, the data collected from the participants was fitted to a logistic psychometric function $P(x)$ using a mathematical modelling package (Mathworks, Matlab vR2011b).

$$P(x) = \gamma + (1 - \gamma) \cdot \left(\frac{1}{1 + \left(\frac{x}{\alpha}\right)^{-\beta}} \right) \quad (17)$$

Where γ is the probability of being correct by chance, β is the steepness of the function, and α is the stimulus intensity at the halfway point.

The values on the x-axis corresponded to the spring stiffness of each sample, while the y-axis corresponded to a count of the number of times the reference sample was considered less compliant (stiffer) than the test stimulus, expressed as a percentage of the entire population of responses. The slope of a psychometric function can be seen as a measure of performance. A steeper psychometric function resembling the form of a step function represents a higher slope, and consequently more accurate discriminability. Hence, a higher β implies that participants were better able to discriminate compliance correctly.

4.4. Results

All twelve participants completed the study successfully and without incident. Results were used to plot psychometric functions for each experiment. Those functions were plotted (Figure 17) and compared in order to observe any significant difference in compliance discrimination performance between them. The curves represent the model fits for all data points across the tasks performed. The relative gradient of the curves indicate the ease with which the participants could distinguish between the samples; a steeper curve indicates more superior compliance discriminability by the participants.

The values for β and α for each task obtained by fitting the participants' responses to the logistic function are seen in Table 9. The value of γ , the probability of being correct by chance, was set to 0.5. Figure 18 shows the standard deviation from the mean for the samples across the five tasks.

Table 9. β values for all experiments fitted using the logistic function

	Finger pad only (Control task)	Direct vision + tool	Indirect 2D vision + tool	2D vision only	Tool touch only
β	96.3	69.3	27.8	19.0	19.8
α	0.225	0.227	0.224	0.221	0.227

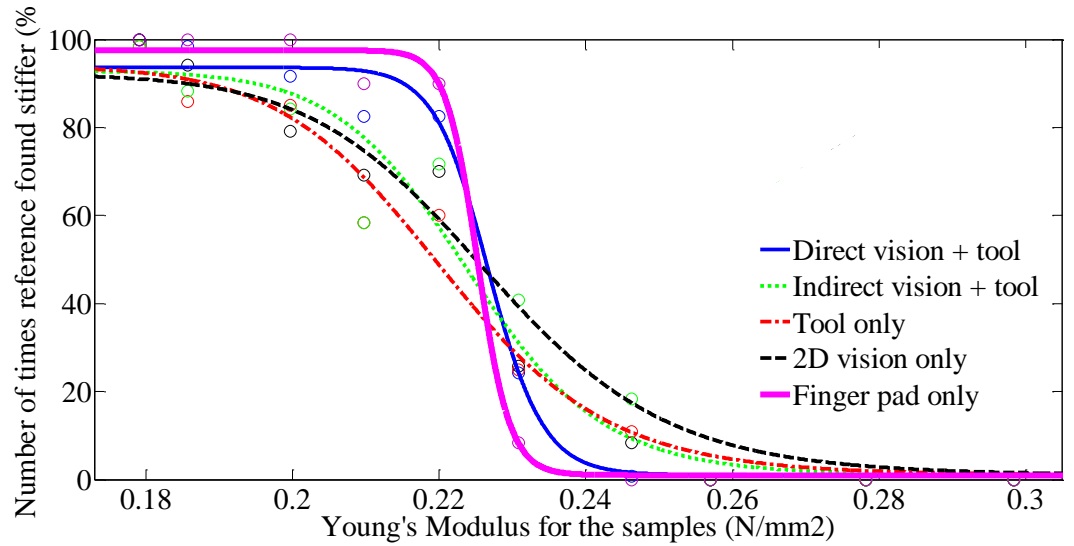


Figure 17. Psychometric functions for all five 2AFC experiments

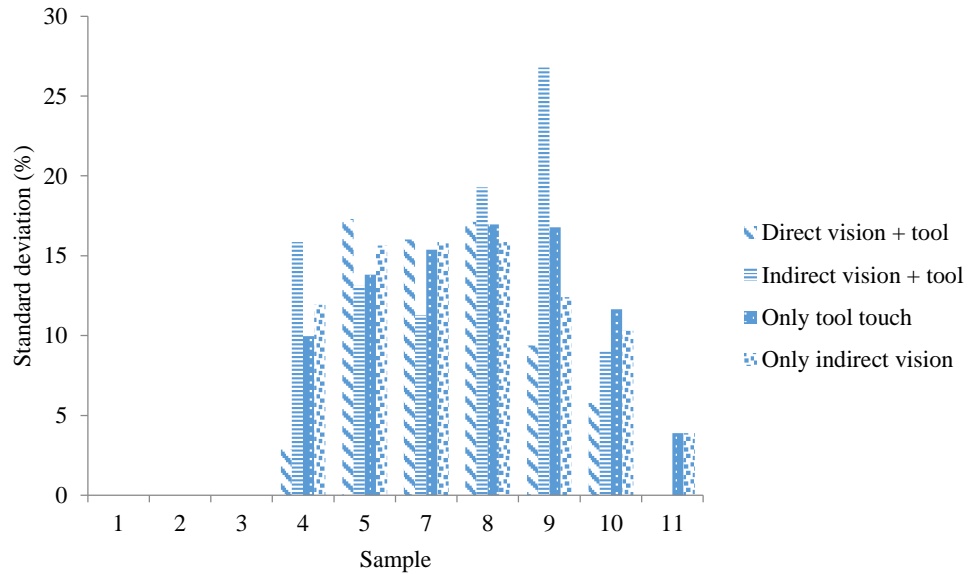


Figure 18. Standard deviations for the participants' responses across all four experiments

Table 10. β values and their corresponding standard deviations obtained after fitting individual participant responses to the logistic function

	Finger pad only (Control task)	Direct vision + tool	Indirect 2D vision + tool	2D vision only	Tool touch only
β	94.5	61.8	35.8	15.9	13.8
SD	11.1	9.8	5.2	4.3	3.8

4.5. Discussion

Table 10 shows the β values obtained after fitting the responses of each participant separately. These values were compared to the ones obtained in Table 9, where all responses were collated before model fitting. This comparison would reveal any participant outliers, bias, or trends. The tables indicate that overall, participants performed similar to the median.

Table 10 shows the slope values (β) across the four tool indentation tasks. The standard deviation presented for each task is a measure of how widely the values of β are dispersed from the average of all 12 participants' fits. It is observed that the direct vision with touch using a tool task holds the highest β value, indicating better compliance discriminability than the remaining tasks. A two-way ANOVA showed that the direct vision with tool touch task proved more accurate at discriminating compliance than the indirect vision with tool touch task ($p=0.035$), the tool touch only task ($p=0.0024$), and the indirect vision only task ($p=0.0016$). Moreover, the indirect vision with tool touch task showed better compliance discriminability than the indirect vision only task ($p=0.027$). An analysis between the vision only and touch only tasks revealed a p-value of 0.26, implying that we cannot explicitly judge which task has performed better, indicating that the two tasks demonstrate similar performance.

With the reference sample located at the centre of the compliance range, each pair presented different levels of discriminatory difficulty. In the pair having Sample 1 and Sample 6 for instance, it was relatively easy to find the less compliant sample due to the larger compliance gap between the two samples. For pairs with samples having similar levels of compliance, however, it was much more challenging for the participants to detect the less compliant sample. This causes the staircase shape of the psychometric curve.

Figure 18 is an illustration of the standard deviations for the participants' collated responses across all four experiments. Participants performed with 100% precision and accuracy when comparing the reference sample with the one of the three least compliant samples. As the difference in compliance between the reference and test sample got smaller, the standard deviation increased, which is to be expected. When the reference was compared to the softest test samples, i.e. Samples 8, 9, and 10, the

standard deviation gradually decreased as the difference in compliance between the samples increased. However, it can be observed that participants performed better when the difference in compliance between the test and reference sample increased, which is in agreement with Weber's law [83].

The highest performing discrimination task was for the condition of cutaneous touch without vision ($\beta = 96.3$). Results show a high rate of accuracy in discriminating compliance (98%). These results agree with previous literature suggesting that direct cutaneous feedback provides the most reliable information during compliance discrimination [43], [47], [128]. This indicates that there is possibly a need to translate cutaneous information into haptic feedback devices in order to achieve more accurate compliance discriminability. A haptic feedback system designed to simulate cutaneous as well as kinaesthetic feedback could be beneficial for the surgical and medical training community.

Participants performed similarly during the tool-operated haptic feedback only ($\beta = 19.8$) and the 2D visual feedback only ($\beta = 19.0$) tasks. This emphasizes the power of visual feedback when attempting to discriminate compliance of soft materials using a tool. The task that used a combination of these two sensory stimuli, i.e. the task in which participants had indirect 2D visual access coupled with touch using a tool ($\beta = 27.8$), showed superior compliance discriminability to when each sensory stimulus was available on its own. This suggests that while both indirect vision and direct tool touch provide reliable information regarding the compliance of objects, a combination of both is indeed more effective suggesting that a cross-modal integration of information between the two sensory modes is present. In the future, a haptic feedback system that is capable of optimising this cross-modality between vision and touch could be used by surgeons and physicians to improve performance, precision and accuracy in MIS as well as accelerate learning in virtual laparoscopic training simulators. Moreover, by modifying or augmenting the haptic and visual information relayed to the user, it may be possible to substitute for insufficient or distorted haptic feedback in LS or RALS.

During the vision-only task, participants were watching the samples being indented by someone else through a computer monitor. A post-experiment survey revealed that participants used specific cues in order to visually estimate the softness of the samples.

Apart from the bulginess and speed of recovery of the samples after indentation, participants seemed to use visual cues from the person performing the indentations. Fingertip colour change, deformation and flexibility during indentation were also used to assess the softness of the samples. The next experiment described in Chapter 5 will assess the impact of visual information during compliance discrimination tasks while utilizing a controlled indentation setup that is not influenced by the variability of a human finger. Indentation force, speed and position will be independently isolated in an effort to find the greatest source of information during compliance discrimination.

5. The Effect of Indentation Depth and Force on Visual Compliance Discrimination

Abstract

This chapter is an assessment of the effect of maximum indentation force and depth on people's ability to accurately and precisely discriminate softness of compliant objects using indirect visual information only. Twelve participants took part in two psychophysical 2AFC experiments in which they were presented with pairs of samples being indented on a 2D monitor and then were asked to determine which sample appeared 'softer'. In the experiments, the 2D monitor output video recordings of a computer-actuated tip indenting the sample pairs to one of two conditions: maximum depth (10mm) or maximum force (4N). This simplified one-dimensional indentation process simulates tool operated palpation performed by surgeons using tools in LS. Responses were used to plot psychometric functions which are a measure of precision and accuracy of compliance discriminability. The results indicated that while performance was best when the indentation process was limited to a maximum force value of 4N, participants were able to discriminate softness in both experiments. This not only emphasizes the impact of force and position control on softness discrimination tasks when only visual cues are used, but also further demonstrates the importance of visual information during compliance discrimination tasks. These findings will inform future work on designing a haptic feedback system that utilizes the power of visual information during softness discrimination tasks. Such a system with the ability to independently manipulate visual and haptic cues while controlling indentation force and depth could be useful for compliance discrimination performance enhancement as well as development of RALS training systems.

5.1. Introduction

The literature has shown the importance of visual information during haptic perception tasks such as compliance discrimination [7], [47], [52], [54], [120]. This chapter paper builds on previous work by highlighting the impact of visual cues during compliance discrimination. The work focuses on the visual discrimination of compliant samples that are indented in a controlled environment using either a maximum indentation force or depth. In one of the tasks in Chapter 4, participants watched video recordings of someone else indenting the samples using a tool. While indentation rate and depth as well as applied force were not controlled, participants were still able to judge compliance relatively well. In this chapter, visual cues such as applied force and depth during indentation are isolated in an effort to determine which cues are dominant during visual compliance discrimination.

Tan et al. [129] conducted psychophysical experiments in an effort to find the manual resolution of compliance. Their aim was to characterize, understand, and model our ability to recognize and manipulate objects manually. They performed forced-choice experiments in which participants actively squeezed a movable plate towards a fixed plate using cutaneous and proprioceptive cues. In their experiments, they compared the performance of participants for roving displacement and fixed displacement. For the fixed displacement task, while the resistive force of the moving plate was controlled using algorithms, the displacement the moving plate was allowed to reach was fixed for every trial regardless of the resistive force applied. For the roving displacement task, displacement of the moving plate was varied with equal a priori probabilities for each trial. Results suggested that by randomizing the allowable displacement of the moving plate, the Weber's fraction increased from an average of 8% (fixed displacement) to 22%. In this chapter, a follow up to this work was attempted by using force and displacement cues in an effort to quantify their impact on compliance discriminability using visual information only.

Srinivasan & LaMotte [47] showed that the force applied during indentation and the velocity of indentation do not affect the ability to discriminate compliance using cutaneous information. This finding is useful for tasks such as open surgery where surgeons are in direct contact with the tissue using their fingers. The effect of force,

velocity and position on compliance discriminability using a tool, however, such as the case of MIS, is yet to be investigated. The following experiments isolate force and position cues in an attempt to understand their effect on the ability to accurately and precisely judge softness of compliant objects using a tool. While vision has been shown to dominate during compliance discrimination tasks [52], [54], [69], [120], the effect of force and position cues during indentation is yet to be determined in a MIS context.

The aim of this experiment was to determine the effects of maximum force and displacement cues on people's ability to accurately discriminate softness of compliant objects using indirect visual feedback only. Understanding the impact of force and position control on visual discrimination of compliance could help enhance the fidelity of visual cues during haptic compliance discrimination. Moreover, it could potentially be translated into RALS systems in order to improve performance and reduce unintended tissue damage.

5.2. Methods

Participants took part in two 2AFC experiments; one where maximum indentation force was fixed and the other where the indentation distance was fixed. The method of constant stimuli was implemented since a finite number of physical stimuli were used to conduct the experiments.

5.2.1. Participants

Twelve participants (nine male and three female) took part in this study. To avoid learning effects, one of the participants have taken part in any of the previous studies. All participants were postgraduate students at the University of Leeds with ages between 23 and 34. Participants had no eyesight impairments according to a completed questionnaire (Appendix A.1). None of the participants had any medical or surgical background. Ethical approval was acquired prior to the experiment.

5.2.2. Stimuli

Eleven silicone-mixture samples were used in this study. Sample fabrication, testing, and modelling were described in Section 3.2. For this experiment, the mechanical properties of the samples were obtained using the custom rig indenter. Stress and

strain data were fitted to a Voigt model to obtain stiffness and damping coefficients governing the viscoelasticity of each sample as shown in Section 3.2.3.

5.2.3. Experimental Set-up

We set up an indentation rig (Figure 19) using a linear actuator (SMAC Inc. USA, LCA50-025-7) coupled with a 6-DoF force transducer (ATI, Nano17) as described in Chapter 3. The two experiments utilized video recordings of the samples being indented by the custom rig either to a maximum force or depth into the samples. Using a high definition webcam (Microsoft Lifecam Cinema), each sample indentation was recorded at an angle typical of a person's line of sight while seated under constant lighting conditions (Figure 21).

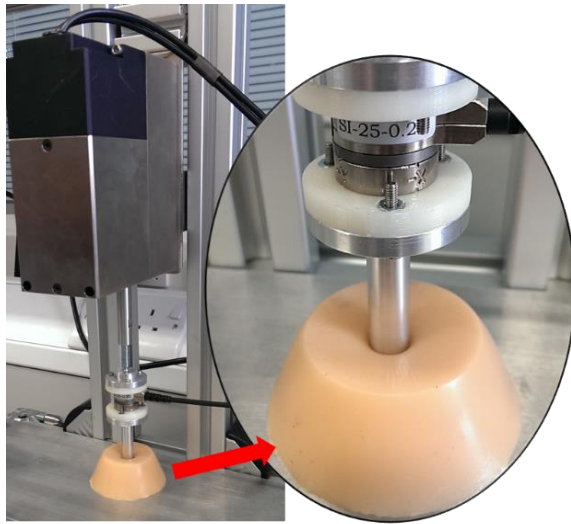


Figure 19. Indentation rig holding the actuator and sensor during an indentation process

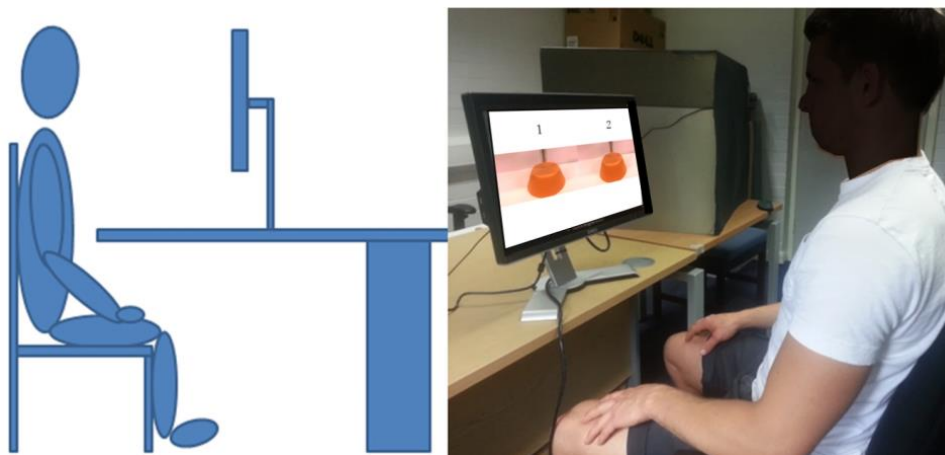


Figure 20. Participant positioning during the experiments

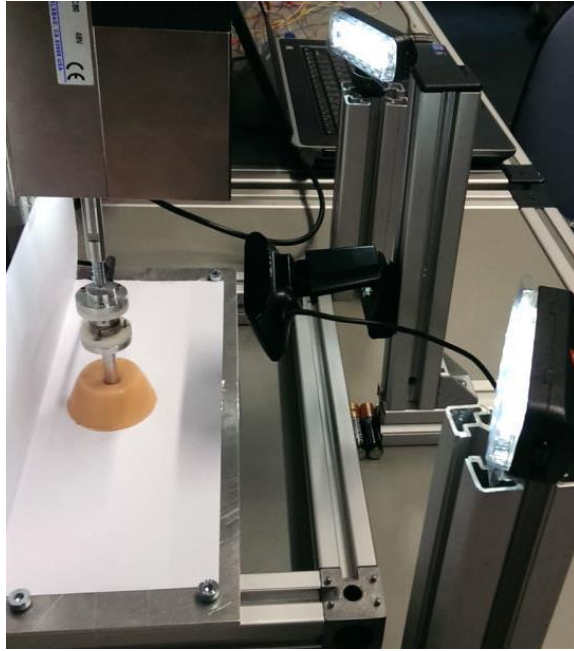


Figure 21. Light and video recording set-up during sample indentation

5.2.3.1. *Experiment condition: Maximum indentation depth*

The actuator was programmed to indent the sample at a constant rate of 10 mm/s until a maximum indentation depth of 10mm into the sample was reached, regardless of the force required to reach that depth. This indentation rate was considered appropriate as it most accurately mimicked the rates applied by participants in Chapter 4 during direct indentation of the samples using a tool. Most tumour sizes range from a few millimetres to 20 cm [10], so palpation depth is quite variable depending on the type and size of the tissue being palpated. Consequently, this thesis works under the assumption that a depth of 10mm is sufficient to obtain mechanical properties of a simulated tissue. The 11 samples had different compliance values and hence required different forces to reach the 10mm required depth.

5.2.3.2. *Experiment condition: Maximum indentation force*

The actuator was programmed to indent the sample at a constant rate of 10 mm/s until a desired indentation force of 4N was reached, which is in line with forces exerted onto tissue in the literature [118]. Using the load cell to measure the vertical loading force, values were communicated to the actuator which in turn indented the samples until that predetermined maximum force was reached. The actuator indented the samples until a maximum force of 4N is applied, regardless of the depth of indentation into the sample.

5.2.4. Experimental Design

Participants were seated in front of an HD monitor display (Dell P2214H) as shown in Figure 20. Participants were given a written document describing the experiment procedure and protocol (Appendix A.3) which they were asked to read. Participants were presented with two samples side by side on the computer screen. They were asked to observe as the tip of the actuator indented the two samples one at a time within each pair, and clearly state which of the two was, in their opinion, the ‘softest’. Since this was a 2AFC experiment, a response was always necessary. If unsure or needed more time to make a decision, participants were allowed as many repeats as necessary. To account for wear and tear of the reference sample, a new reference sample was fabricated for each participant. This allowed for an even indentation number for all samples, eliminating any property changes.

Each participant was presented with a total of 200 recorded clips of sample pairs being indented. These 200 clips consisted of 100 fixed force clips and 100 fixed depth clips. For each of the fixed force and fixed depth experiments, 10 unique recorded video clips were created. Each clip consisted of a reference and a test sample. Ten test samples were used in this experiment. Each of these clips was presented 10 times in random order resulting in a total of 100 clips per experiment per participant. In order to prevent extraneous factors from unknowingly affecting our results, the positions of the test sample and the reference sample were randomly altered and the order of all runs was counterbalanced for each participant using a 4×4 Latin Square Design [121]. This method of counterbalancing was used to prevent any learning effects from impacting the results. To prevent participants from obtaining cues about the nature of the fixed force and fixed depth conditions, the two were randomly interleaved within the experimental procedure. The 200 trials were presented to participants in two sessions to reduce boredom and keep the participants engaged and responsive. Each session took 40 to 50 minutes to complete depending on the participant.

The duration of each clip was 30 seconds in which the samples within each pair were indented three times in alternating order at a constant speed of 10mm/s. The rate of indentation was identical in both fixed force and fixed depth conditions. In any given recording or run, one of the two samples presented side by side as seen in Figure 20 was the reference sample; located at the centre of the sample compliance range

(sample 6). The other sample which was continually changed was the test sample. Participants were not informed about the conditions of the experiments (fixed force or depth) to eliminate any strategy formation.

5.3. Results

The results of the two tasks were fitted to a modified logistic function similar to that in Section 4.3. This function was found to be a good fit for psychometric functions in the literature [123], [125], [126]. The standard deviations for participants' responses are observed in Figure 23. The estimated values of α and β are shown in Table 11.

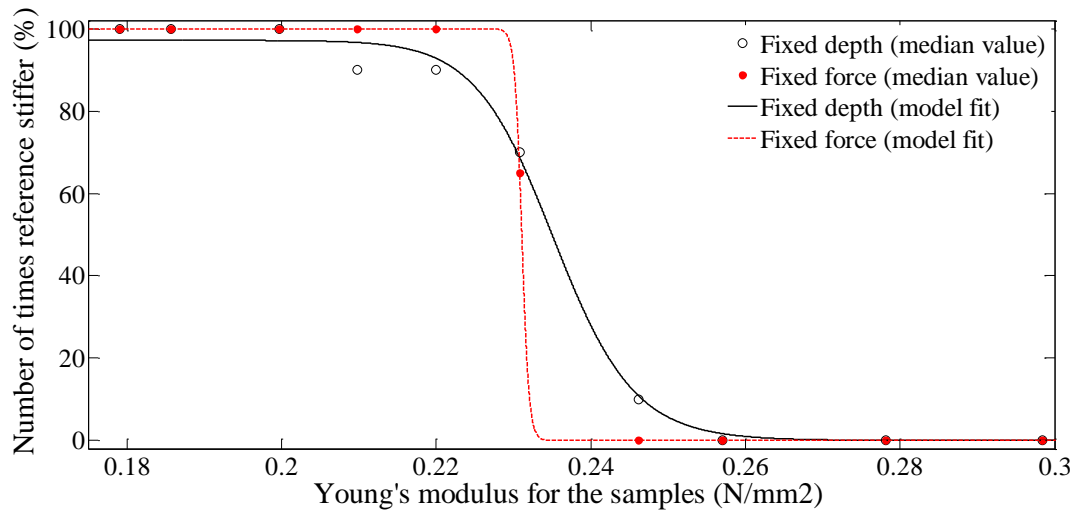


Figure 22. Psychometric functions plotted for the maximum indentation depth and force experiments, along with the averaged participants' responses for each sample.

Table 11. α and β values for both tasks obtained by fitting collated participants' responses

	β	α
Fixed force	60.1	0.231
Fixed depth	45.7	0.235

Table 12. β values and their corresponding standard deviations obtained for both tasks obtained from fitting the responses for each participant separately

	β	SD
Fixed force	91.8	16.3
Fixed depth	59.4	13.1

The x-axis represents physical stimuli in order of increasing stiffness (decreasing compliance). The y-axis represents the medians of participants' responses, displayed as a percentage correct proportion.

The slope (β) of a psychometric function at the halfway point is an indication of performance. The more a psychometric function resembles a step function, i.e. the greater its slope at the halfway point (50% correct), the better participants are at discriminating compliance. A t-test reveals that the psychometric functions show statistical difference between responses obtained in the two tasks ($p=0.0023$), indicating that participants performed better when they were asked to visually judge compliance of samples being indented by the rig up to a set force of 4N than up to a set depth of 10mm ($\beta_{FF} = 60.1 > \beta_{FD} = 45.7$)

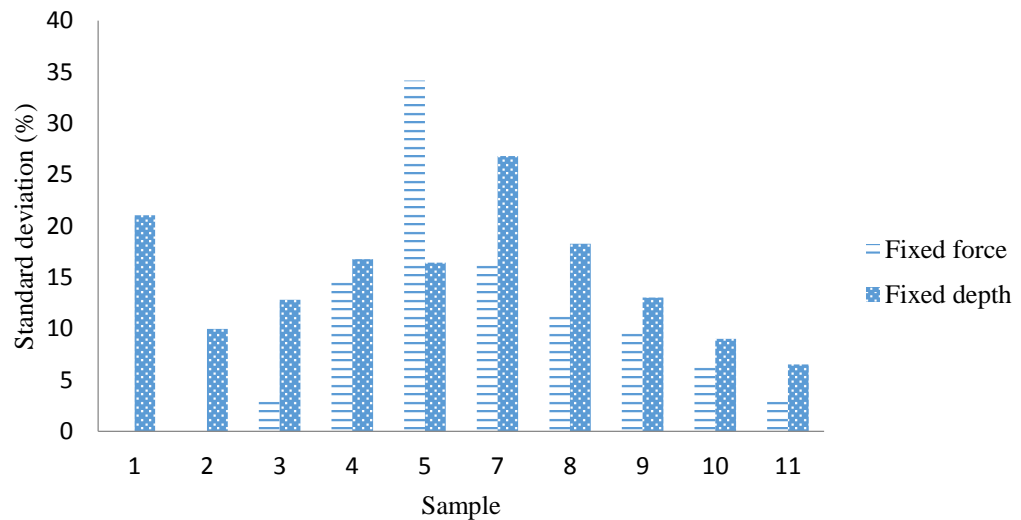


Figure 23. Standard deviations for the participants' responses in both tasks

5.4. Discussion

Psychometric functions are a way of analysing perceptual performance. These functions are often used to extract absolute thresholds and difference thresholds. The psychometric plots suggest that 2D visual compliance discrimination using maximum indentation force is superior to that using maximum indentation depth. In other words, visually judging the indentation of compliant materials up to a set force provides better compliance discrimination performance than when samples are indented to a set depth. Participants were not informed about any indentation force or depth restrictions

prior to the experiment and so they were naïve to the experimental conditions in both experiments. In the force controlled experiment, all the samples were indented until 4N was attained, disregarding indentation depth into each sample. Since the maximum force was fixed for all samples, the indenter tip travelled a longer distance into the more compliant samples than in the less compliant ones. This can be observed in Figure 24. When participants were watching clips of samples being indented, they developed their own strategies to decide regarding the compliance properties of the samples. In the position controlled experiment, all the samples were indented down to the same depth and so participants were forced to change strategies for this experiment. A post-experiment survey revealed that participants found this experiment more difficult than the fixed force experiment. A possible explanation for this phenomenon might be that in the fixed force experiment, participants unknowingly linked the variation in indentation depth with sample compliance. In the fixed depth task, however, participants were forced to focus on other cues such as the bulging of the sample edges, and the time it took for the samples' surface to reach its initial position after maximum indentation. Figure 23 shows the standard deviations for both tasks. It can be observed that participants were less precise and hence found the tasks most challenging as the difference in compliance between the test and reference stimuli decreased. The least compliant sample - Sample 1 - was difficult to judge during the fixed depth experiment. Visual cues and strategies used to judge the remaining samples were not effective in this case. One explanation might be that for lower compliance levels, visual cues previously used such as sample edge bulging or surface recovery speed after indentation show minimal variation. Some participants, however, had no such problems, which suggests that variations in judgement strategies play a significant role during visual compliance discrimination.

The point of subjective equality (PSE), parameterized by α , is estimated from fitting the participants' responses to the logistic function. At the point of objective equality (POE), the test stimulus physically matches the reference stimulus ($\alpha = \text{POE} = 0.23$). The closer the value of α is to the POE, the more accurate people are at matching physical stimuli to their corresponding stiffness values at the centrepoint. From Table 11, we can see that $\text{POE} < \alpha_{\text{FF}} < \alpha_{\text{FD}}$ indicating that the fixed force experiment allowed the participants to more accurately judge compliance than in the fixed depth experiment. This result sheds light on how controlling force can influence our decision

making process during compliance discrimination. The results further demonstrate the impact of visual information on compliance discrimination which has been shown in previous literature [7], [52]. Moreover, results show that the force exerted and the depth reached during indentation of compliant objects can influence our ability to accurately and precisely discriminate compliance.

In LS, surgeons use slender instruments to grasp and manipulate tissue while receiving haptic feedback via grasper handles. In RALS such as the DaVinci, surgeons remotely operate using graspers without the presence of any force feedback. The results in have shown that by implementing a maximal force and indentation position, visual compliance discrimination was enhanced. Providing an on-screen visual force feedback during LS and RALS that displays a theoretical maximum force beyond which tissue damage would occur might reduce tissue scarring and improve surgeons' ability to discriminate the compliance of tissue.

To summarize, the effect of indentation force and depth on our ability to discriminate compliance using only visual information was investigated. Previous work has shown the significance of visual cues during haptic discrimination [7],[52],[8]. Our results suggest that by controlling the force applied during indentation, it is possible to improve our ability to discriminate compliance using visual cues only. Psychometric plots show that visual information alone, under constrained maximum applied force and depth, can be used to judge softness of compliant objects, demonstrating the importance of making more use of visual information as well as optimizing the visio-haptic cross-modality present during basic surgical tasks such as palpation in LS or RALS.

While force control was found to be superior to position control during visual compliance discrimination, participants were able to discriminate compliance well under both configurations. In LS, RALS, and training simulators commercially available today, both visual and haptic feedback are used in tandem in order to provide the surgeon with the greatest amount of information and feedback necessary during any task. Hence, an optimal combination of visual and haptic information is sought.

The results from Chapters 4 and 5 suggest that visual feedback can be used to enhance performance in compliance discrimination tasks. As shown in the literature, pseudo-

haptics is a viable method of taking advantage of the visual feedback. In Chapter 6, the development of a haptic feedback system that separates visual from haptic information during indentation to a maximum force or depth is introduced. Such a system that uses pseudo-haptics to generate realistic sensations would serve to:

- Simulate the viscoelastic behaviour of tissue, a task yet to be successfully completed using pseudo-haptics. Chapter 6 aims to accomplish this task.
- Quantitatively determine the extent of the impact of visual dominance during indirect compliance discrimination tasks using a tool. This will be demonstrated in Chapter 7.

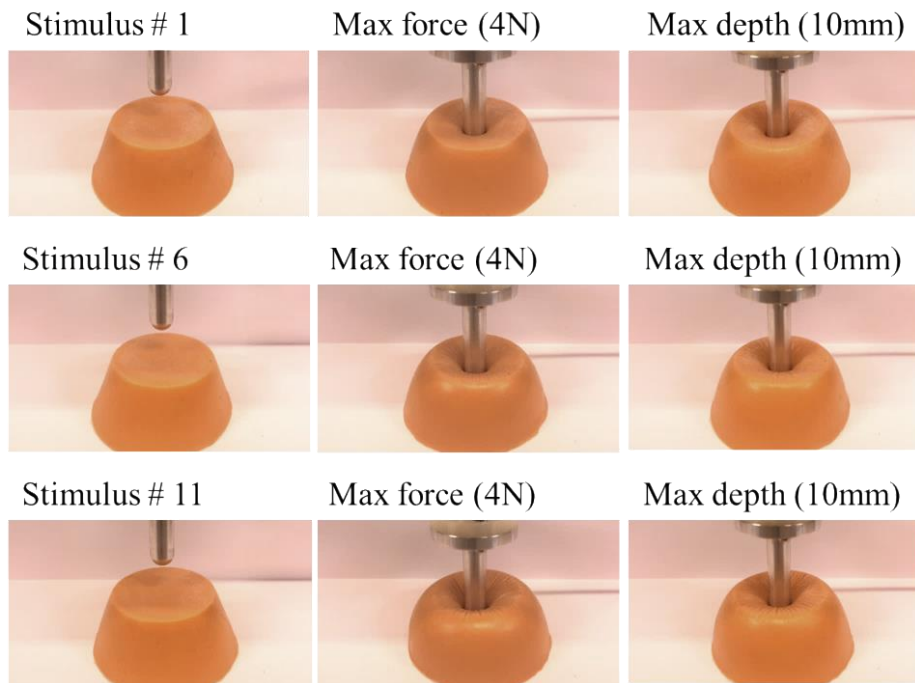


Figure 24. Visual variations at maximum indentation force and depth for samples 1, 6 (reference) and 11

6. Developing and Validating the Perceptual Fidelity of a Novel Robotic Pseudo-Haptic Feedback System

Abstract

This chapter describes the development of a novel robotic pseudo-haptic system that is capable of independently manipulating both visual and haptic feedback. The system's ability to accurately and precisely simulate the viscoelastic characteristics of compliant objects simulating human tissue is assessed through an experimental study. The aim of the experiment was to assess the pseudo-haptic system's ability to simulate viscoelastic behaviour of compliant materials. A 2AFC experiment was set up in which twelve participants remotely palpated sample pairs using a force feedback device. This device was used to manipulate a 7-DoF robot which in turn acted as the indenter. Visual access was restricted to a 2D computer monitor transmitting a live feed of the palpation process. Haptic feedback was generated using mathematical models of physical samples to determine the force to be displayed on the force feedback device. Participant responses were used to construct a psychometric function of compliance discrimination performance as well as calculate the Weber fraction of discriminating compliance using the pseudo-haptic system. With a 7.56% Weber's fraction, the pseudo-haptic feedback system was capable of simulating the viscoelasticity of compliant objects during indentation tasks. This emphasizes the need to further develop such systems for virtual reality surgical training. Future work will use this system in an attempt to determine the degree of contribution of vision during indirect palpation. Furthermore, the efficiency and usability of pseudo-haptics for haptic simulation within surgical training will be assessed.

6.1. Introduction

To set the context for this chapter, a brief review of compliance discrimination research that uses pseudo-haptic feedback is presented. Pseudo-haptics refers to the use of visual feedback in order to simulate haptic sensations. It has been used to simulate haptic properties such as the stiffness of a virtual spring [72], the texture of an image [73], the mass of a virtual object [33], and friction in a virtual passage [74]. Lecuyer et al. [62] used a passive isometric device (Spaceball™) along with visual feedback to provide a pseudo-haptic feedback effect. While isometric devices are known for not being able to return any forces, pseudo-haptics was used to create the illusion of a force by providing participants with on-screen virtual spring which behaved as normal springs would while they pressed on the isometric device. A 2AFC compliance discrimination task was set up between a virtual spring simulated using the isometric device and a real spring with equivalent compliance. Participants used their hand to press the real and virtual springs in similar fashion. A 13.4% JND which falls between the 8-22% previously found by Tan et al. [129] suggests consistent manual discrimination of compliance using a passive input device. However, using a force feedback device instead of an isometric one to perform compliance discrimination tasks between virtual and real stimuli has not yet been investigated.

Lecuyer et al. [72] attempted to identify the ‘boundary of illusion’ occurring during pseudo-haptic feedback. A force feedback device (PHANTOM™) was used to simulate the stiffness of two virtual springs. Within each pair of virtual springs presented, one had matching visual and haptic displacement behaviour while the other had either haptic or visual bias. While participants were able to discriminate compliance using the pseudo-haptic feedback system, their responses were often inconsistent. The authors demonstrated the capability of virtual visual feedback to distort perception of simulated haptic spring stiffness. However, it is still unknown if visual feedback in the form of real stimuli can distort the perception of simulated haptic stiffness. The significance of such an investigation is evident in RALS and RALS training where either real or simulated viscoelastic tissue is remotely manipulated using a haptic feedback system.

Stiffness discrimination has been assessed for virtual vs. virtual samples and virtual vs. real samples. In both cases, passive or active feedback devices were used to simulate simple springs represented by Hooke's law. To date, a pseudo-haptic feedback system simulating viscoelasticity of compliant objects has not yet been created. Moreover, none of the experiments in the literature utilized compliance discrimination using a tool. There is a need to simulate viscoelastic behaviour using pseudo-haptics [72]. Consequently, this chapter describes the development and validation of a robotic pseudo-haptic feedback system capable of simulating the viscoelasticity of compliant objects in order to assess people's ability to manually discriminate compliance using a tool via that system.

The aim was to assess the system's ability to accurately simulate the viscoelastic behaviour of compliant objects during indentation. This scenario simulates tissue palpation in RALS as well as VR training. Physical compliant objects were used as visual cues while haptic cues were provided through a commercial haptic feedback device. Tool-operated compliance discrimination tasks were performed by participants for a range of silicone samples. The success criteria for this experiment were as follows:

- Viscoelastic behaviour of physical compliant objects is simulated using a commercial haptic feedback device
- Visual cues are autonomously modified by the system via physical sample interchange
- Haptic cues are autonomously modified by the system via mathematical model unique to each physical sample available
- Synchronized visual and haptic cues during indentation are available to the participants
- The pseudo-haptic system is successfully designed and assembled
- Participants are able to accurately judge sample compliance using the visio-haptic setup, which is determined using psychophysical analyses (Psychometric function, Weber fraction)

6.2. Methods

Using the robotic system, participants took part in a 2AFC psychophysical experiment which utilizes the method of constant stimuli. The system design is described in section 6.2.1. The experimental design is described in Sections 6.2.4.

6.2.1. Pseudo-haptic system design

To simulate a pseudo-haptic effect, a haptic feedback system that can independently manipulate visual and haptic information transmitted to the subject was designed and assembled. For this experiment, the system requirements were as follows:

- Ability to independently manipulate the visual and haptic feedback provided
- Allow for haptic indentation using a haptic feedback device
- Display indirect visual cues during indentation that match the haptic cues felt through the haptic feedback device
- Actuated indenter setup to perform indentations at various speeds dictated by a haptic feedback device
- Haptic feedback device with a 100mm minimum vertical translation movement and 4N minimum force feedback for realistic indentation as per experiment requirements
- A circular tray rotated by a motor-actuated setup with a 2kg minimum allowable payload for stimuli interchanging.

While the author of this thesis designed the experimental setup and the system requirements, the technical development and programming of the system was developed externally through *Re-Solve Research Engineering Ltd.* A schematic of the pseudo-haptic system is shown in Figure 25. The system consisted of:

- Three 6-axis commercial robots (VS-068, Denso Robotics)
- An HD webcam (C920, Logitech)
- A 7 DoF haptic feedback device (Omega.7, Force Dimension)
- A Desktop computer that controls and links every component in the system together using a custom program via LabVIEW software (National Instruments)

The Omega.7 is a desktop 7 DoF (3 active translations, 3 active rotations, 1 active grasping) haptic interface used in aerospace and medical industries to control dexterous robots, as well as in haptics research. Its workspace, forces and resolution are shown in Table 13 below. The Omega.7 has been used extensively to simulate virtual environments in gaming, military, as well as robotic-assisted surgery [130], and hence is capable of accurately and precisely simulating the compliance of the samples used in this experiment.

Table 13. Omega.7 workspace, forces and resolution for all degrees of freedom

	Translation	Rotation	Grasping
Workspace	190 x 130 mm	235 x 140 x 200 deg	25 mm
Force	20.0 N	400 mN/m	±8.0 N
Resolution	0.0015 mm	0.013 deg	0.006 mm

With a maximum speed and payload of 11000mm/s and 7kg respectively, the 6-DoF Denso VS-068 robots used throughout this thesis are capable of fulfilling the requirements set by the remote indentation tasks. Robot specifications are shown in Table 14. The benefits of such robots include their high operation speed for agility and quick manoeuvrability and their high level of precision and accuracy allowing them to handle small and fragile materials with care.

Table 14. Denso VS-068 specifications

Item	Unit	Spec	
Overall arm length	mm	680	
Maximum reach	mm	710	
Maximum payload	kg	7	
Maximum speed	mm/sec	11,000	
Cycle time	sec	0.33	
Weight	kg	~ 49	
Maximum allowable inertia moment	Joints 4, 5	kgm ²	0.45
	Joint 6		0.1
Maximum allowable moment	Joints 4, 5	Nm	162
	Joint 6		6.86
Range of motion	Joint 1	Degrees	±170
	Joint 2		±135

	Joint 3		±153
	Joint 4		±270
	Joint 5		±120
	Joint 6		±360

Visual-haptic separation is achieved in this set-up by using mathematical models to simulate force feedback via a haptic feedback device, eliminating the need for force sensors attached to the indenter robot. The position of the haptic feedback device is mirrored by the robot indenter which in turn indents the sample. This indentation process is observed by the participants on a monitor via a webcam. An illustration of the robotic setup in contact with the physical samples during the process of indentation is shown in Figure 29. A flowchart illustrating the steps occurring within the robotic system during each sample indentation performed by the participants is shown in Figure 28. Haptic and visual feedback within the system were separated and controlled as described in Sections 6.3.3.1 and 6.3.3.2 respectively.

6.2.1.1. Force feedback:

The system provides force feedback through the Omega.7 haptic feedback device. A Voigt model for each physical sample was used to estimate their corresponding stiffness (E) and damping (η) coefficients, as described in Chapter 3. The obtained coefficients are tabulated in Section 3.2.3.2. These equations were then used to control the force feedback provided by the Omega.7 while participants indented the samples. In this set-up, participants move the tool connected to the end effector of the Omega.7. The position of the Omega.7 is sent to the robot indenter arm, which in turn mimics the position and speed of the Omega.7.

6.2.1.2. Visual feedback:

Visual feedback during indentation is provided through a 2D computer monitor. Physical samples located within the robotic setup away from the participant are interchanged by rotating a circular tray (Figure 26), allowing for a visual change in sample compliance. An HD webcam (C920, Logitech) was fixed facing the indenter at an angle mimicking indentation using direct visual access to the samples (Figure 30). The disc holding the samples was mounted onto another robot which rotates

based on which sample was to be indented. Eleven pre-set angular rotation values each corresponding to a sample were used to control the positions to which the robot moves. Since haptic and visual cues were separated from one another, participants used the Omega.7 to indent Voigt model representations of the physical samples while observing those physical samples on a computer monitor. The position of the indenter robot was governed by that of the Omega.7 end effector, which in turn was controlled by the participants.

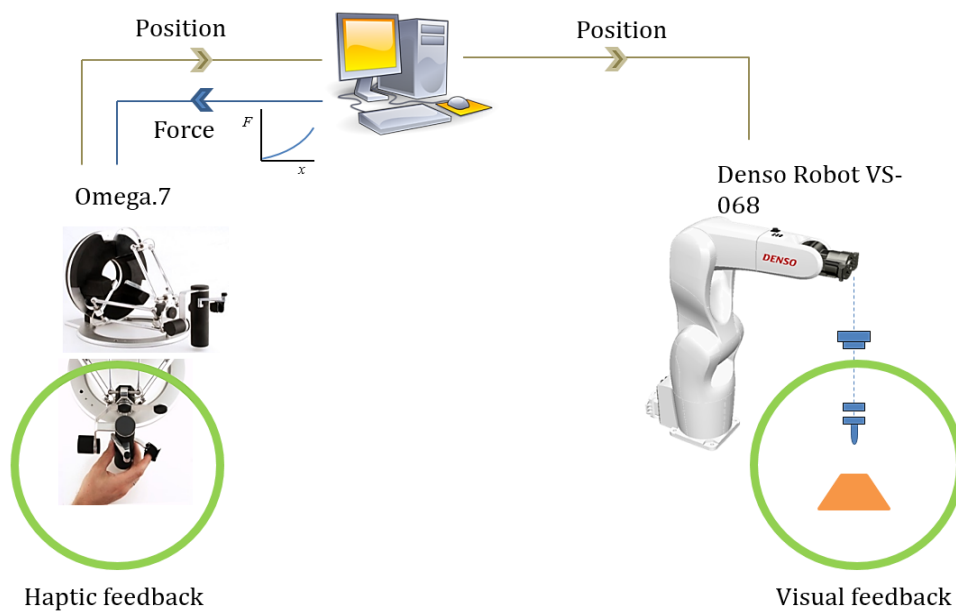


Figure 25. Pseudo-haptic feedback system design and set-up

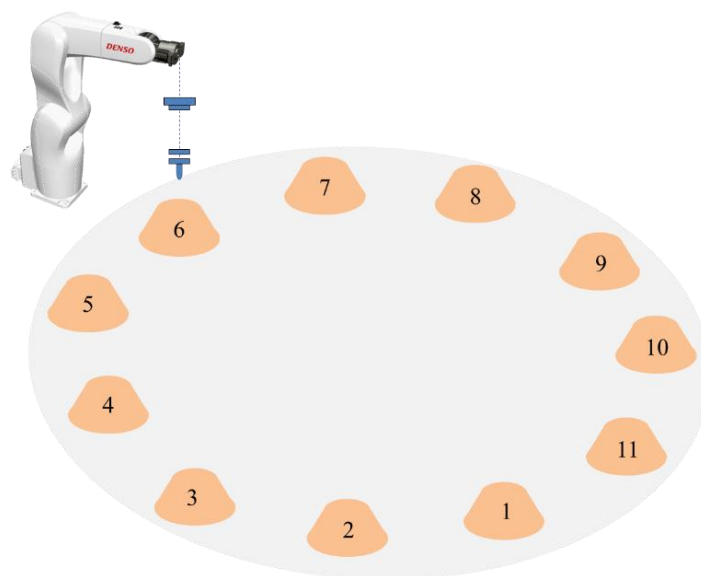


Figure 26. Schematic of indenter robot with the circular tray that holds all 11 samples

6.2.2. Participants

Twelve participants (nine male and three female) were recruited for this study. To avoid learning effects, one of the participants have taken part in any of the previous studies. All participants were students at the University of Leeds with ages ranging between 19 and 34. They were paid for taking part in this study. None of the participants had any eyesight impairment according to a completed questionnaire (Appendix A.1). The participants had no previous medical or surgical backgrounds and were naïve to the study beforehand. Ethical approval was obtained prior to commencing the experiment.

6.2.3. Stimuli

Silicone was used to fabricate the samples as described in Section 3.2.1. Eleven silicone mixture samples with unique stiffness and damping coefficients were obtained as described in Section 3.2.3.

6.2.4. Experimental design

A 2AFC experiment using the pseudo-haptic feedback system was set up. Twelve participants were instructed to determine the ‘softer’ sample within each presented pair. Participants were seated facing the 2D screen and the haptic feedback device (Figure 27). The entire robotic system in contact with the samples (Figure 29) was shielded from the participants so that the only source of visual information present during the experiment was through the screen in front of them. Participants were given a written document describing the experiment aim, procedure and protocol (Appendix A.4) which they were asked to read. The 2AFC experiment comprised 10 sample pairs, each repeated 10 times in random order. In total, each participant was presented with 100 sample pairs. Each pair consisted of the reference sample along with a test sample. The compliance of the reference sample is located at the centre of the available sample range. The positions of the test and reference sample as well as the order of each presented pair were randomly switched to prevent habitual errors and learning effects. To account for wear and tear of the reference sample, a new reference sample was fabricated for each participant. This allowed for an even indentation number for all samples, eliminating any property changes.

Each participant was presented one pair of samples at a time. Within each pair, samples were presented one after the other. Participants were asked to indent the samples in each pair with the tool attached to the Omega.7 using the schematic indentation guide displayed on the right hand side of the screen to maintain consistent indentation speed and depth. After indenting each pair, participants were asked to make a decision as to which of the two samples felt softer. If unsure about their decision, participants were allowed as many repeats of the sample pairs as necessary.

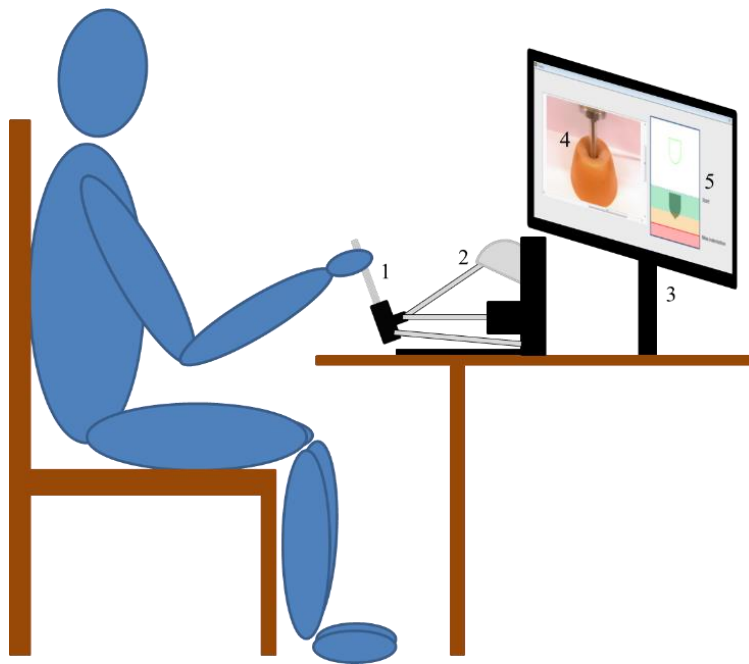


Figure 27. Experiment set-up: (1) indenter tool, (2) Omega.7 haptic feedback device, (3) computer monitor, (4) silicone sample observed during indentation, (5) speed & position indentation guide

Participants then lowered the tip until they reached the top of the green shaded region simulating the surface of the presented sample. Next, they were asked to indent the sample actively trying to follow the moving horizontal line. This line is an indication of the speed of palpation as well as the maximum depth necessary to register a valid palpation attempt. After performing 2-4 indents, participants were asked to shift their vision to the left hand side of the screen and observe the physical sample while continuing to indent at the same rate. Participants were then asked to use both visual and haptic information available to ‘have a feel’ for the softness of the sample. Participants were allowed to palpate as many times as necessary until they are ready to move on to the next sample of the pair. Once they are finished, they were asked to move the on-screen tip back to the initial position. At that point, the haptic feedback system automatically switches to the next sample while the screen blacks out to

prevent the participants from seeing the samples being changed in the robotic system. After the next sample was ready for palpation, the second sample in the pair appeared on the screen and the participant could now indent the sample as previously shown.

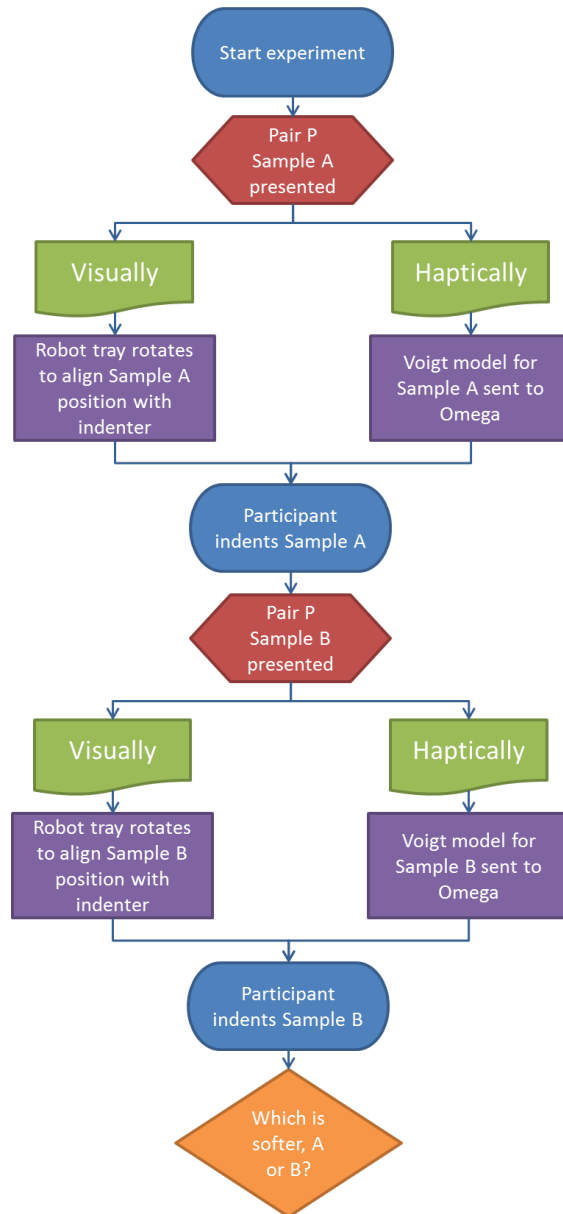


Figure 28. Flow chart describing the process occurring within the pseudo-haptic system during an indentation task. After indenting both samples in the pair, participants were asked to make a decision as to which sample of the two was ‘softer’. The participants responded verbally by stating the number corresponding to that sample. Each sample possesses a number above it during palpation (1 or 2). If unsure of their decision, participants were allowed up to three repeats per pair. After the pair was completed, the participants’ response

was recorded and the system automatically moved on to the next pair on the list. The entire experiment protocol is documented in Appendix B.

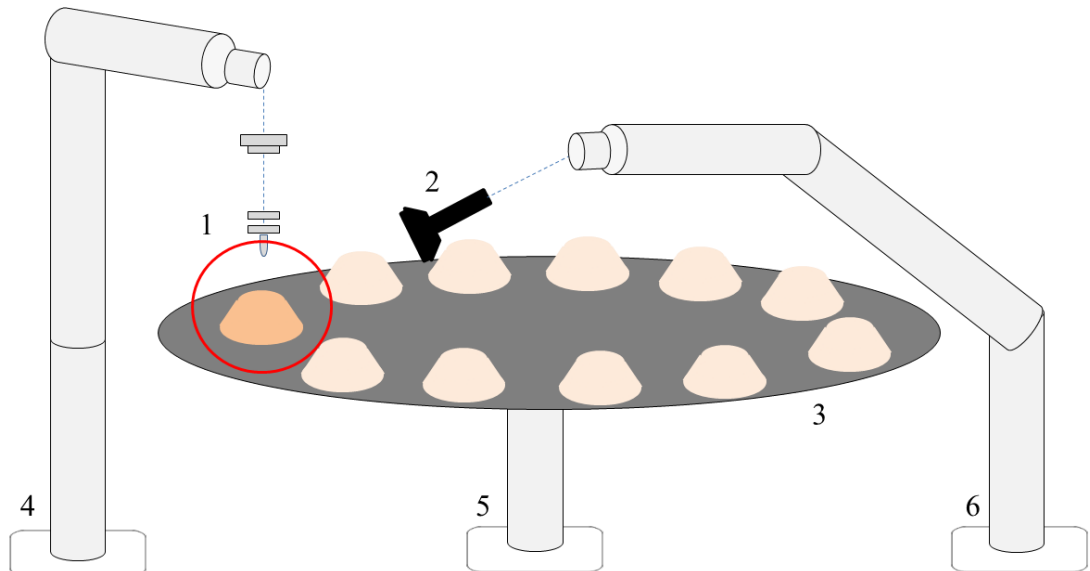


Figure 29. Robotic system set-up: (1) indenter position, (2) HD webcam, (3) Rotating tray, (4) robot used for linear sample indentations, (5) robot used to rotate tray to one of 11 set positions, (6) robot used to mount camera

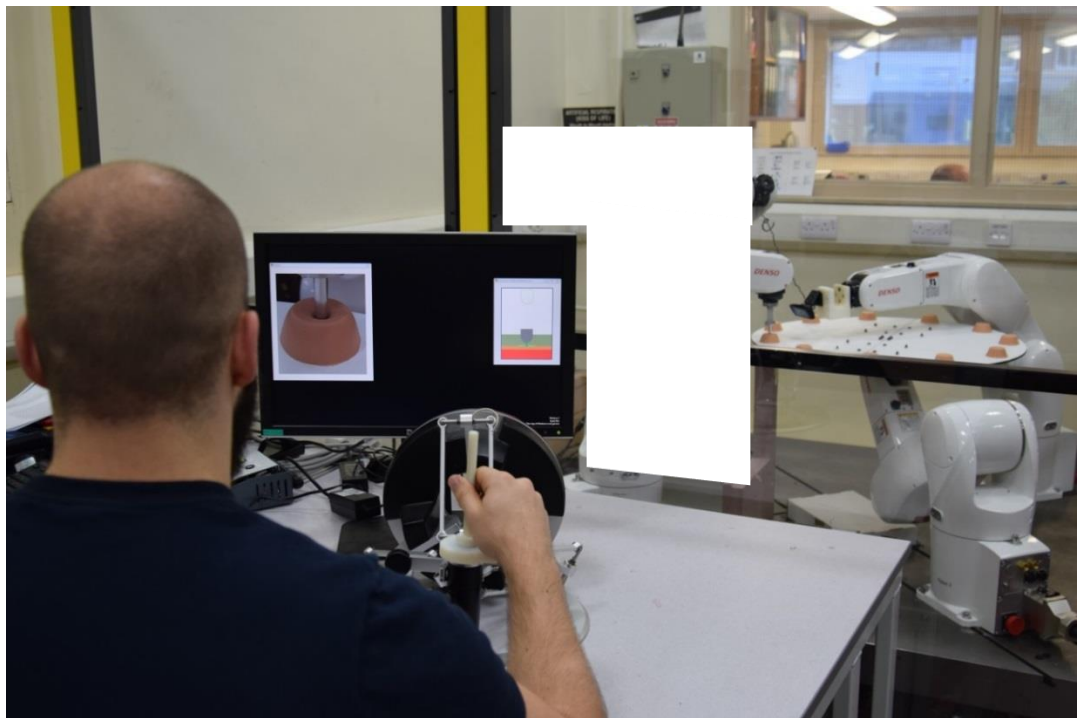


Figure 30. Participant performing a sample indentation

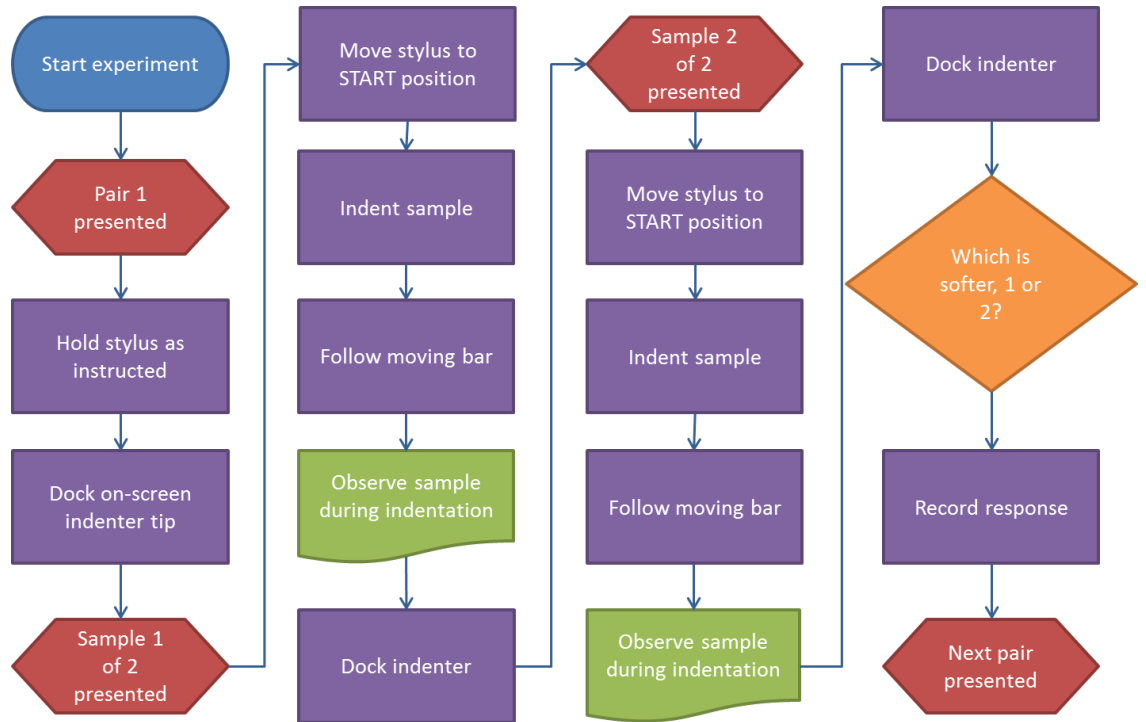


Figure 31. Flowchart describing the participant indentation procedure

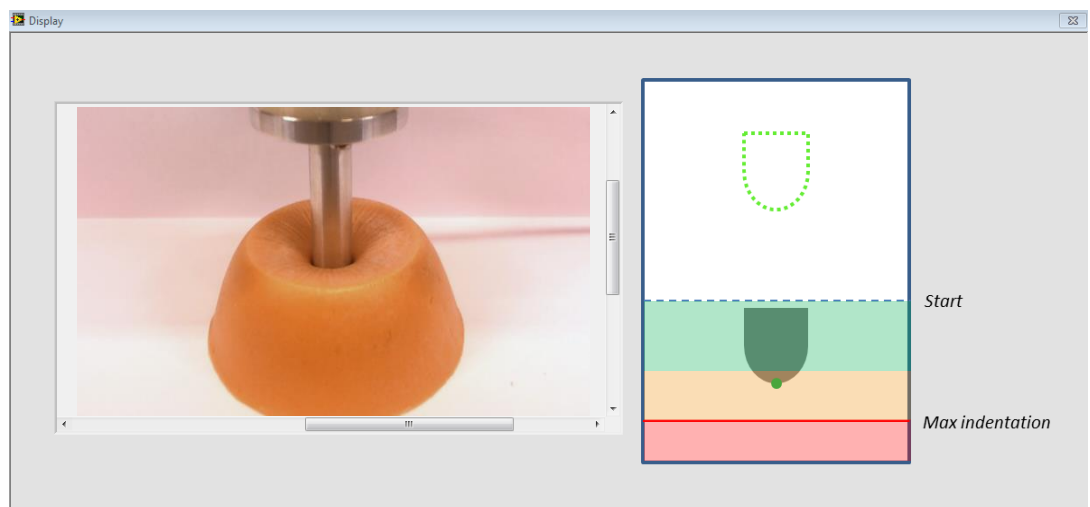


Figure 32. Participant's screen showing the physical sample on left and indentation illustration on right during the experiment

6.3. Experimental analysis

Using an iterative least squares method, the participants' responses were fitted to a parametric function [Equation (18)] referred to as the modified logistic function $P(x)$ using a mathematical modelling package (Mathworks, Matlab vR2011b). This model

which was found to be a good fit for psychometric functions in previous research [123]–[127].

$$P(x) = \gamma + (1 - \gamma) \cdot \left(\frac{1}{1 + \left(\frac{x}{\alpha}\right)^{-\beta}} \right) \quad (18)$$

Where γ is the probability of being correct by chance, β is the steepness of the function, and α is the stimulus intensity at the halfway point.

The values on the x-axis corresponded to the spring stiffness of each sample, while the y-axis corresponded to the number of times the reference sample was considered less compliant (stiffer) than the test stimulus represented as a percentage value. The responses for all participants were used to construct a psychometric function based on the modified logistic function. β was defined as the slope of the psychometric function at the halfway point. The slope of a psychometric function can be seen as a measure of performance. A steeper psychometric function resembling the form of a step function represents a higher slope, and consequently more accurate discriminability.

In order to analyse the psychometric function, the JND and PSE values were calculated. These thresholds are indications of the participants' sensitivity to changes in compliance. The JND is calculated by obtaining the difference between the stiffness corresponding to the psychometric function at the 84% ordinate and the PSE which is the stiffness corresponding to the psychometric function at the 50% ordinate [73], [81]. The Weber fraction (W) is then the JND divided by the PSE as follows:

$$W = \frac{P(x)_{84\%} - PSE}{PSE} \quad (19)$$

6.4. Results

All 12 participants completed the study successfully and without incident. The results were used to plot the psychometric function (Figure 33). Values for α and β are seen in Table 15.

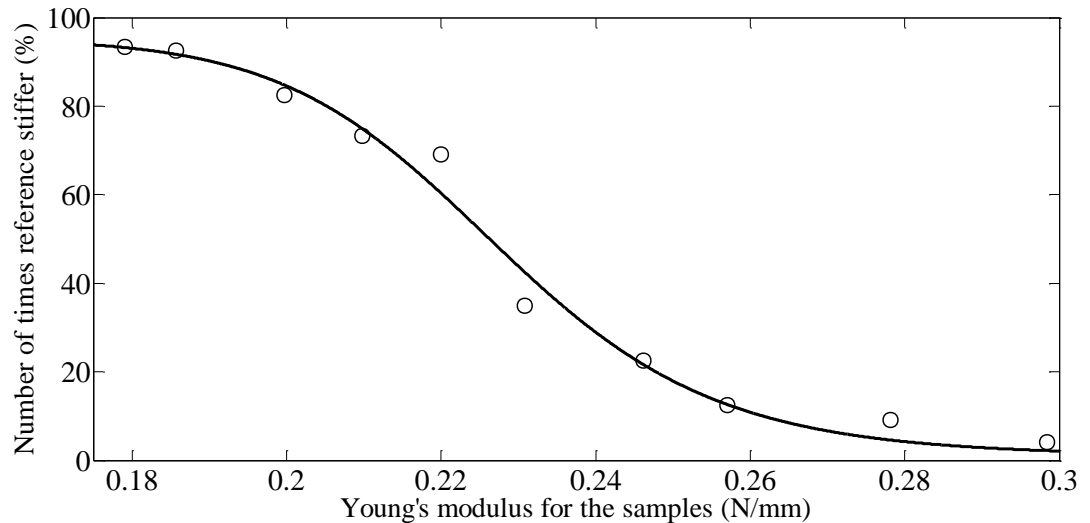


Figure 33. Psychometric function representing participants' performance during the experiment. The JND value is the difference in stiffness between those corresponding to the ratings at 84% and 50%

The psychometric function was then used to calculate the JND and Weber fraction. A 7.37% Weber fraction indicates a high sensitivity to differences in viscoelasticity of compliant silicone samples, meaning that participants were able to discriminate compliance of samples with relatively high accuracy.

Table 15. β values obtained by fitting participants' responses to P(x)

β (St. Dev.)	16.02 (2.023)
--------------------	---------------

Figure 34 shows the spread of Weber fractions across the participants. Since the average value (10.7%) is greater than the median (7.56%), the distribution appears to be right skewed. Removing the outlier (29.5%), however, has no significant effect on the median which turns out to be 7.45%. A Z-test confirmed that the difference between the median being 7.45% and 7.56%, $p = 0.0726$, is not statistically significant. With a 7.48% standard deviation from the mean, sensitivity to pseudo-haptic changes was varied between participants. Since the outlier was shown to have no significant effect on the average Weber fraction of the group, the Weber fractions for each participant (seen in Figure 34) ranged between 2.34% and 20.04% (4.79% SD).

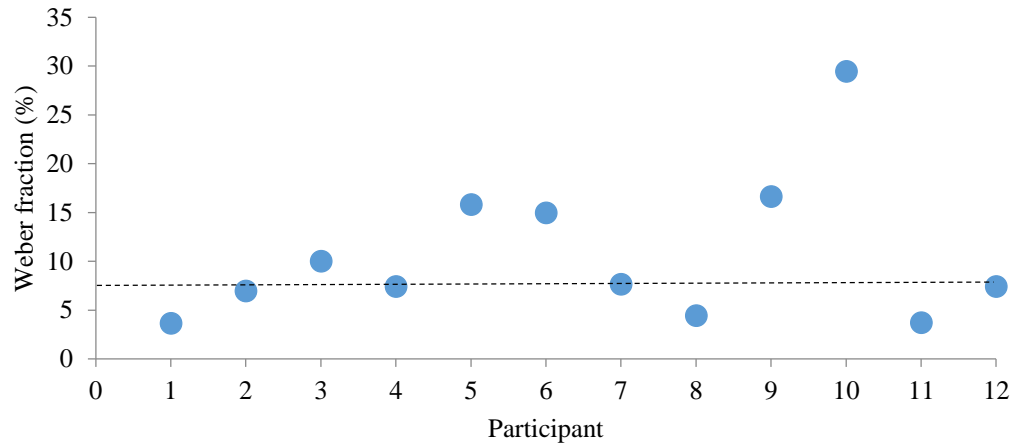


Figure 34. Weber fractions for all twelve participant

6.5. Discussion

Despite the separation between visual and haptic cues, participants were still able to judge the softness of sample pairs and provide good discrimination responses (7.37% Weber fraction). From the literature, Weber fractions obtained during compliance discrimination tasks using mechanical devices range between 7.7% and 37% depending on the method of application of pressure as well as the type and compliance of the stimulus [131]. None of these studies, however, used physical compliant samples to assess simulated compliance discriminability using a tool. Previous studies have primarily focused on compliance discrimination either using direct cutaneous contact or using some sort of mechanical device such as pulling plates together using the index finger and thumb. On the other hand, the experiment presented in this chapter focused on remote palpation using a haptic feedback device. The setup used simulates that of a RALS setting or a VR surgical training simulator. Hence, while it may be possible to compare Weber fractions of this study to previous compliance discrimination studies, a direct comparison is not applicable due to set-up variations.

Holding a tool connected to the Omega.7 similar to holding a pen during indentation proved to be a reliable compliance discrimination method during sample indentation. Participants were quick to associate the movement of the tool to that of the indenter attached onto the robot. It is worth noting that key components of the system design such as the visual-haptic separation via pseudo-haptics was not disclosed to the participants. Participants reported that the indentation tasks felt lifelike. None of the

participants showed any observable disconnection between the tool used for indentation and the indenter robot. Moreover, none of the participants reported any perceived sensory gaps or conflicts during indentation. In other words, participants were not aware that the compliance levels they were feeling through the haptic feedback device were in fact a result of model fits as opposed to instantaneous compliance measured in real-time during indentation of the physical samples using sensors.

During the experiments, participants were asked to begin palpation while focusing visually on the guide on the right hand side of the screen. After performing a few indentations at the desired pace, they were asked to redirect their sights to the left hand side of the screen where the physical sample was displayed using the webcam and continue indenting at the same pace. This process was designed in order to control the indentation speed and depth into the samples, which was shown to enhance compliance discriminability in Chapter 5. However, shortly after a few pairs, participants started focusing less on the guide and more on the physical sample displayed on the left. It was observed that participants started glancing at the guide from the corner of their eyes while maintaining focus on the sample being indented. This suggests that participants were quickly able to learn the required pace and position during indentations.

When comparing this novel pseudo-haptic system (11.8% Weber fraction, $\beta = 16.0$) to that simulating a LS setup which was explored in Chapter 4 (8.74% Weber fraction, $\beta = 27.8$), it can be observed that performance was superior in the latter. In the task simulating LS from Chapter 4, participants used a tool to actively indent physical samples while viewing the process through a 2D computer monitor using a webcam. Hence, participants had direct haptic access to the physical samples providing superior feedback during indentation. The similar Weber fraction values suggest that haptic feedback using a commercial haptic feedback device could provide sensations similar to those obtained when touching physical samples. Haptic feedback devices are used extensively in research as well as medical training. While virtual simulators have been shown to accelerate the learning of new and advanced tasks for surgeons [132], these simulators are usually commercially available as an entire all-in-one system. The cost of these systems is usually quite high. In this experiment, an inexpensive commercial

force feedback system was used to accurately simulate viscoelastic properties of compliant objects. Combined with pseudo-haptics, off-the-shelf haptic feedback system could be used in the future as an alternative to virtual medical simulators.

Although the two tasks presented similar performance, it can be observed that performance was superior when participants physically indented the samples themselves using a tool while observing the process through a 2D display via a webcam, such as in the case of LS ($\beta = 27.8 > \beta = 16.0$).

The effect of force and position on visual compliance discriminability using a tool was investigated in Chapter 5. The results showed that when the maximum force or depth during indentation was controlled, participants are able to accurately judge the compliance of physical samples using indirect visual cues only. With 5.14% and 4.11% Weber fractions for the fixed depth and fixed force tasks respectively, it may be inferred that visual information can substitute for unavailable haptic feedback. In the experiment conducted in this chapter, visual cues were coupled with indirect haptic cues using a haptic feedback device. What is interesting is that the same visual conditions were present during this experiment as well as the two conducted in Chapter 5. One would assume that the added sensory feedback - haptic feedback - would enhance compliance discrimination performance. On the contrary, the addition of force feedback appeared to have weakened the participants' performance. While the visual setup was similar in these two experiments, the indentation rate was different.

In Chapter 5, participants simply watched the samples being indented by a rig at constant speed. Participants had no control over the indenter observed on-screen. In the experiment conducted in this chapter, however, participants had complete control over the position and rate of the indenter via the haptic feedback device. While providing an added source of sensory information to participants, this may have led to a reduction in the participants' performance. The manual control of the indenter along with the on-screen indentation guide may have reduced the participants' ability to focus on visual cue changes that perhaps were obvious when less sensory information was provided. Experiments in Chapter 3 showed that a cross-modal integration exists between vision and direct touch either using a tool or the finger. However, the findings in Chapters 5 suggest that visual cues could be sufficient during

compliance discrimination tasks. Herein lies the necessity to investigate the scope of visual dominance during compliance discrimination of objects using the pseudo-haptic feedback system introduced in this chapter.

7. Identifying the Visual 'Boundary of Illusion' Using a Pseudo-Haptic Feedback System

Abstract

In this chapter, the pseudo-haptic system developed in Chapter 6 was used to quantitatively determine the extent to which visual information could generate sensations of compliance. The aim was to evaluate the contribution of visual cues during a haptic feedback surgical task such as palpation. Thirty-two participants took part in a psychophysical magnitude estimation experiment in which they were asked to subjectively rate the magnitude of softness for several samples based on a reference sample having a fixed unit-less rating. Change in visual compliance of the samples was controlled by switching physical samples shown to participants during indentation. For all samples, haptic compliance corresponded to the reference sample. Any variations in haptic sensations were a result of pseudo-haptic illusions. Participants' ratings were collated and fitted to Steven's power function. A 0.18 power exponent suggests that the system was successful in generating viscoelastic properties through variations in visual information only. The Weber fraction suggests that in order to perceive a change in haptic compliance using the pseudo-haptic system, a 19.6% visual change from the reference compliance is necessary. These findings could prove beneficial in research and educational facilities where advanced force feedback devices are limited or inaccessible. Pseudo-haptics could be used to simulate virtual tissue for training purposes without the need for force feedback.

7.1. Introduction

Current surgical training systems use a combination of haptic and visual feedback to provide medical students and novice surgeons with a realistic experience similar to that of a real operating theatre without the worry of causing any harm. While effective, these systems are not accessible to all hospitals and teaching facilities due to their high cost. Off-the-shelf haptic feedback devices can be used to design and assemble similar surgical training systems. However, this would require expertise in software and hardware design and programming. While these devices are relatively inexpensive and so are more accessible, the accuracy and force output of these devices are usually limited. If pseudo-haptics is proven successful at simulating haptic sensations during manipulation of simulated tissue, it may be possible to improve the performance of inexpensive haptic feedback devices allowing them to be used in tasks that are previously only done on advanced VR surgical training systems.

While researchers have shown the potential of pseudo-haptics in producing several haptic sensations [72], [76], [80], [133]–[136], the extent of that potential, specifically within surgical technologies, is yet to be explored. In this chapter, the aim was to determine the extent to which pseudo-haptics realistically simulates haptic sensations through visual augmentation using a psychophysical magnitude estimation experiment. By independently controlling the visual and haptic information presented to participants, it becomes possible to identify the human visual boundaries, or limitations, of illusion. Such information can be applied onto laparoscopic simulators and haptic feedback devices to simulate greater force ranges, reduce errors, and enhance accuracy.

7.2. Methods

A magnitude estimation experiment was designed to quantitatively determine the contribution of visual feedback during haptic discrimination of compliance using a robotic pseudo-haptic system. Participants rated the softness of stimuli based on that of a reference stimulus with known softness rating.

7.2.1. Participants

Thirty-two participants (16 male and 16 female) took part in this study. None of them had any known hand or eyesight impairments according to a completed questionnaire (Appendix A.1). Participants were undergraduate students, postgraduate students and staff at the University of Leeds with ages ranging between 18 and 37. To avoid learning effects, one of the participants have taken part in any of the previous studies. Participants were naïve to the aims of the experiment, without any medical background. Ethical approval was obtained before commencing the experiment.

7.2.2. Stimuli

Similarly to previous experiments, 11 silicone-mixture samples were used in this study. Sample fabrication, compliance testing, and viscoelastic modelling is described in 3.2.

7.2.3. Experimental design

A novel pseudo-haptic system capable of simulating viscoelasticity was designed as described in Chapter 6. The system employs 7-DoF Denso robots controlled via Omega.7 haptic feedback devices using LabVIEW software. The advantage of this system is in its ability to independently manipulate the visual and haptic cues available to participants. Instead of attaching a force sensor to the robot indenter tip and relay that force to the end effector haptic feedback device (Omega.7) in real time, this system utilizes pre-set mathematical models which have been shown to accurately represent the viscoelastic behaviour of the samples during an indentation process. Each sample is represented by a Voigt model with its own unique spring stiffness constant and dashpot damping coefficient. Model fitting was described in Section 3.2.3.2.

Throughout this experiment, the pseudo-haptic system was used to create a visual-haptic sensory mismatch was present during sample indentation. For the reference sample, haptic feedback obtained through the Omega.7 during indentation matched the visual feedback observed on the screen, meaning that the stiffness and damping coefficients used to simulate viscoelastic behaviour by the Omega.7 matched the

viscoelasticity of the physical sample observed during indentation. Viscoelastic properties of the test samples, however, were inconsistent with the physical samples presented during indentation. Visually, test samples were selected from a range of 10 samples with different levels of viscoelasticity. On the other hand, haptic viscoelasticity relayed through the Omega.7 feedback device simulated viscoelastic behaviour of the reference sample for all the test samples. The mechanical properties of the reference sample were obtained in Chapter 3 by fitting the stress-strain sample indentation data to a Voigt mathematical model, which was used to extract the spring stiffness and damping coefficients. This visual-haptic discrepancy is the basis of the “boundary of illusion”.

Each participant took part in a magnitude estimation experiment in which they were asked to assign numeric values to the softness of a test sample based on a reference sample with pre-set fixed softness rating. Within each presented pair, participants used the end effector stylus tool to move the robot arm which in turn indented the samples. Participants had indirect visual access to the indentation process through a computer screen which relayed a live feed from a HD webcam mounted near the indenter robot. Participants were asked to first indent the reference sample which was assigned a unit-less subjective softness value of 100, while observing the indentation process on the screen in front of them. They were then asked to perform the same indentation process on the test sample. After participants were finished indenting both samples, they were asked to assign a softness rating value to the test sample, based on that for the reference sample. This process is illustrated in Figure 35.

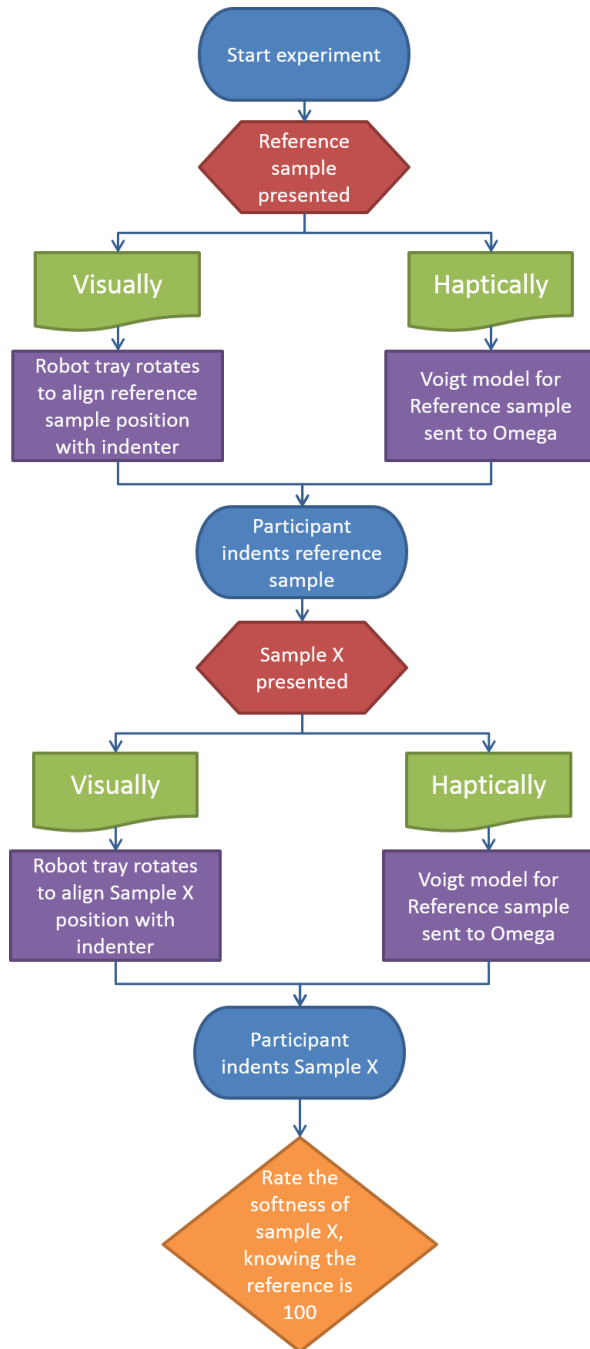


Figure 35. Flow chart describing the process occurring within the pseudo-haptic system during an indentation task

7.2.4. Experimental Procedure

Sample indentation is similar to that described in Section 6.2.4. However, the experimental design is numeric estimation of the magnitude of softness instead of a forced choice comparison. Instead of selecting the sample that felt softest in each pair, participants were required to associate a numerical value to the softness of the test sample based on that of the reference sample. The latter was presented before each

test sample to allow participants to perform direct comparisons and hence provide precise ratings for test sample repeats. For basic training purposes, participants undertook two magnitude estimation trials prior to the experiment, each consisting of a reference sample followed by a random test sample. The results from these trials were not recorded. The experiment protocol is illustrated in Figure 37.

Seating and instructions

Participants were seated in front of a screen and a haptic feedback device. Participants were given a document describing the experiment setup and procedure which they were asked to read (Appendix A.5). They were presented with the reference sample on the screen in front of them (Figure 36). Within each pair, the reference sample was always presented before each test sample so that participants could always compare the reference to the following test sample and provide a softness rating for that sample.

Reference sample indentation

Participants were asked to hold the stylus with their dominant hand as they would hold a pen. Moving the stylus up and down moves an on-screen green hemispherical shape located on the right hand side of the screen (Figure 36). This shape represented the indenter tip attached to the robotic system and is an illustration of the position and speed of the indenter tip. On the right hand side of the screen, an interactive diagram was created to allow the participant when to start palpating, where to start from, how deep to palpate sample, and at what rate. On the left hand side of the screen, the physical sample is displayed using an HD webcam attached to a robotic arm facing the indenter tip. Moving the stylus with their hand, participants moved the on-screen tip to the initial position at the top of the illustration shown as the dotted green fixed hemispherical dock. Participants lowered the tip from the dock until they reached the ‘start’ position at the top of the green shaded region simulating the surface of the presented sample. Participants were told that the reference sample they were about to indent is given a softness rating value of 100. They were asked to indent the reference sample actively trying to follow the moving horizontal line. This line was an indication of the speed of palpation as well as the maximum depth necessary to register a valid palpation attempt. While continuing to indent the reference sample, participants were asked to shift their vision to the left hand side of the screen and

observe the physical stimulus being indented. Participants were asked to use both visual and haptic information available to ‘have a feel’ for the softness of the sample and try to associate the softness of this sample to the value of 100 given earlier. Participants were allowed to palpate as many times as needed. They were asked to move the on-screen tip back to the initial position.

Test sample indentation

At that point, the haptic feedback system automatically switches to the first test sample within that pair while the screen blacks out for two seconds to prevent the participants from seeing the samples being changed in the robotic system. After the test sample was ready for palpation, a test sample in the pair appeared on the screen and the participant could indent the sample as previously demonstrated.

Test sample rating

After indenting the test sample, participants were asked to assign a softness rating value to this test sample based on that assigned to the reference sample. For instance, if they felt the test sample was twice as soft as the reference sample, then they would say 200. If they felt the test sample was half as soft as the reference, they would say 50. There was no upper or lower limit on ratings and there was no time limit. The participants responded verbally by stating the softness value they assigned to each presented test sample. If unsure of what rating to provide, participants could ask for the reference and test samples to be presented again. After the pair was completed, the participants’ rating was recorded and the system automatically moved on to the next pair on the list.

General information

Each pair started with the same reference sample followed by a test sample. Each participant was presented with 10 pairs in random order repeated 10 times each in random order as well. Pairs consisted of a reference sample with defined viscoelastic stiffness and damping as well as a test sample which changes randomly from a pair to the next. In total, 10 test samples with different levels of compliance were used in this experiment. The order within each pair was randomized to reduce learning effects. The entire experiment protocol is documented in Appendix B.

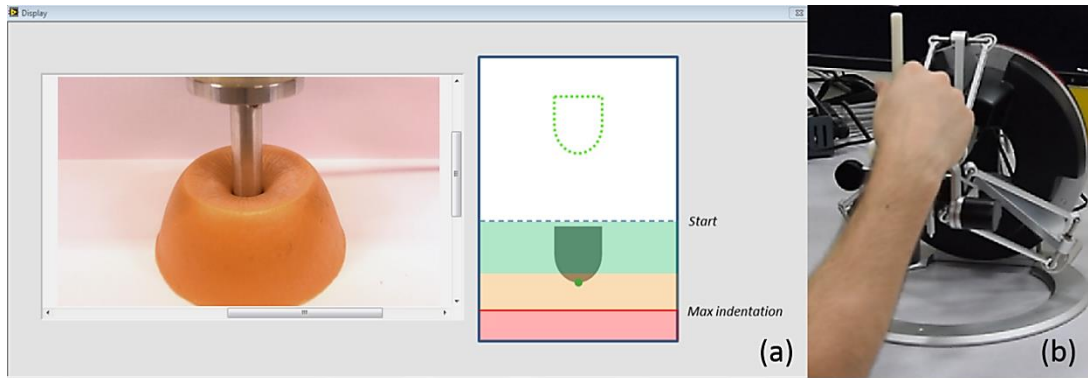


Figure 36. (a) Participant's screen showing the physical sample on left and indentation illustration on right during the experiment, (b) participant indenting stimuli using the haptic feedback device

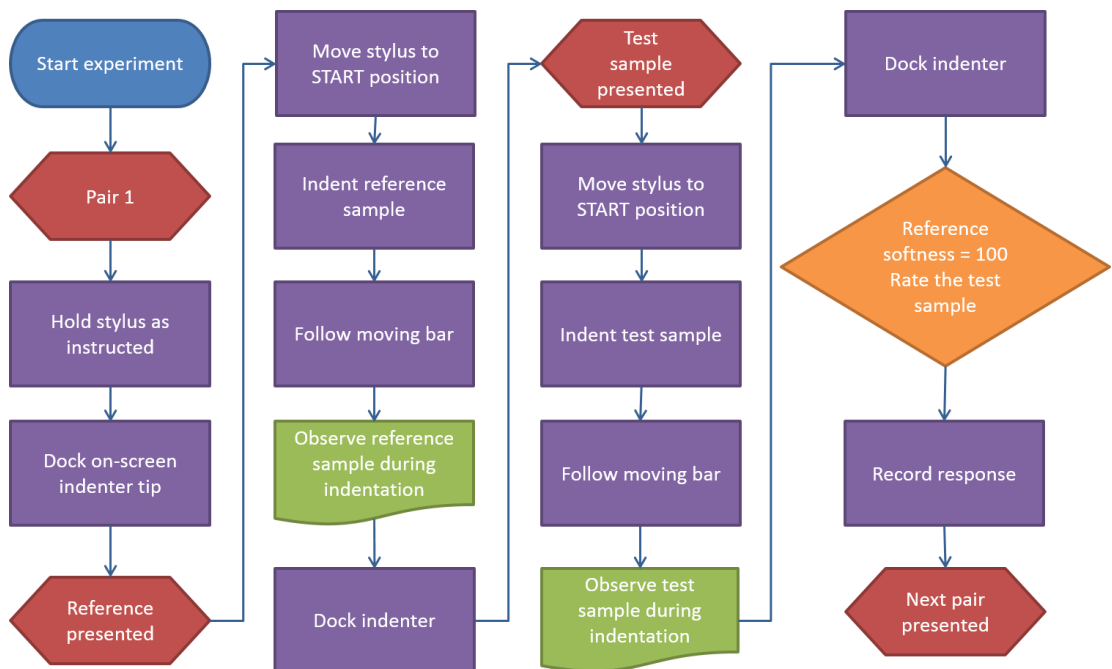


Figure 37. Flowchart describing the participant indentation procedure

7.3. Experimental Analysis

Participants' ratings were collated and fitted to Steven's power law. Described in Chapter 2, the power law is a psychophysical relationship between the physical magnitude of a stimulus and its perceived intensity [81]. Because it describes a broader range of sensations, the power law often replaces Weber's law in psychophysical analyses [81]. Steven's power law is governed by Equation (20) as follows:

$$\Psi = k \Phi^a \quad (20)$$

Where Ψ is the sensation magnitude, Φ is the stimulus intensity, k is a constant which determines the scale unit, and a is the power exponent which varies depending on the stimulus sensory type.

Using the participants' ratings to calculate Ψ values, and substituting the stiffness values for Φ values, the power exponent (a) can then be estimated over the range of samples. As the power exponent increases, the impact of visual changes in sample viscoelasticity on perceived haptic viscoelasticity increases. In other words, as the power exponent increases, the pseudo-haptic effect increases. To the best of the author's knowledge, this is the first instance in which a power exponent describing the relationship between the viscoelasticity of compliant objects and their perceived softness using a pseudo-haptic feedback system was extracted.

Table 16 shows the compliance of each physical sample, along with the theoretical ratings, the participants' ratings, and the standard deviations corresponding to the participants' ratings. The average participant ratings were obtained by calculating the median of all participant ratings for each test sample. Using the stiffness of the samples, theoretical ratings based on the reference rating of 100 were calculated (Table 16). These ratings express the compliance of the samples in the same unit as the participants' ratings. The theoretical values (visual compliance) were compared to the participants' ratings (perceived haptic compliance) to obtain the visual 'boundaries of illusion'. Finally, participants' responses were collected and used to calculate the power exponent corresponding to Steven's power law.

7.4. Results

The objective of pseudo-haptics is to simulate haptic sensations using either visual information only or a combination of visual and haptic information. While the pseudo-haptic system used in this chapter does provide the user with some haptic feedback, it is necessary to bear in mind that the haptic feedback provided always corresponded to the viscoelastic behaviour of the same sample; the reference sample, regardless of which sample is observed visually on the screen during indentation. Table 17 shows the variation in visual compliance as well as the variation in perceived haptic

compliance from the reference sample. The perceived haptic compliance based on a range of visual compliance levels is observed in Figure 39. Fitting both sets of data to a linear trend line, it is possible to estimate the slope or rate of change of each.

Table 16. Stiffness, theoretical softness rating and mean participant rating for each sample

Sample	1	2	3	4	5	6	7	8	9	10	11
Stiffness (N/mm²)	0.298	0.278	0.257	0.246	0.235	0.23	0.22	0.209	0.199	0.1857	0.179
Compliance (mm/N)	3.35	3.59	3.89	4.06	4.24	4.33	4.55	4.77	5.01	5.39	5.58
Theoretical ratings	77.3	82.9	89.8	93.7	97.9	100	105	110	116	124	129
Participant ratings	98.01	100.3	100.5	99.8	101.0	100	106.4	103.7	104.9	106.6	108.1
Standard deviation	14.39	15.23	13.48	14.14	15.11	-	16.79	15.34	14.53	15.14	16.77

Table 17. Visual stiffness and perceived haptic stiffness for each test sample compared to the reference sample

Sample	1	2	3	4	5	6(ref)	7	8	9	10	11
Theoretical compliance (%)	-22.7	-17	-10.2	-6.7	-6.3	0	4.9	10	15.6	24.3	28.9
Perceived compliance (%)	-2	0.3	0.5	-0.2	1.0	0	6.4	3.7	4.9	6.6	8.1

Throughout the experiment, physical samples were interchanged in order to simulate several visual compliance levels. Hence, the data describing the change in visual compliance matched that of the physical sample compliance with a one to one ratio. However, the perceived haptic compliance seen in Figure 39 represents collated participants' responses corresponding to visually induced changes in haptic sensation. An estimate of the slope of the trend line fitted to the collated data suggests that in order to perceive a change in haptic compliance using the pseudo-haptic system, a 19.6% visual change from the reference compliance is necessary. This value

represents the estimated Weber fraction for compliance discrimination using a pseudo-haptic feedback system. Figure 38 shows the distribution of the Weber fractions as well as the Stevens power exponents calculated for each participant based on their unique responses.

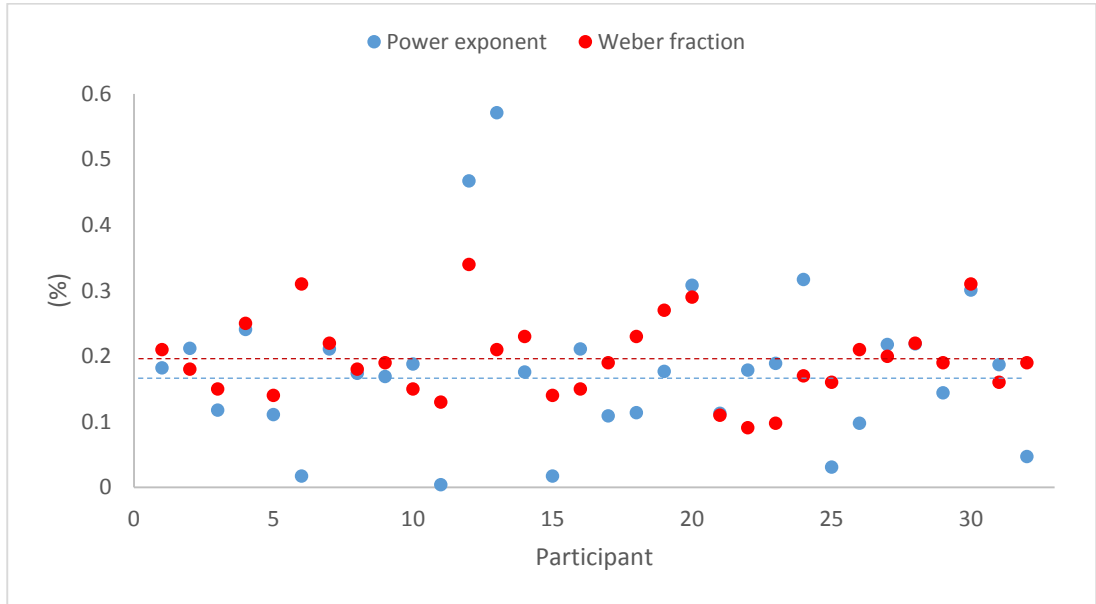


Figure 38. Distribution of Weber fractions and Steven’s power constants across all the participants, with the dotted lines representing the group means

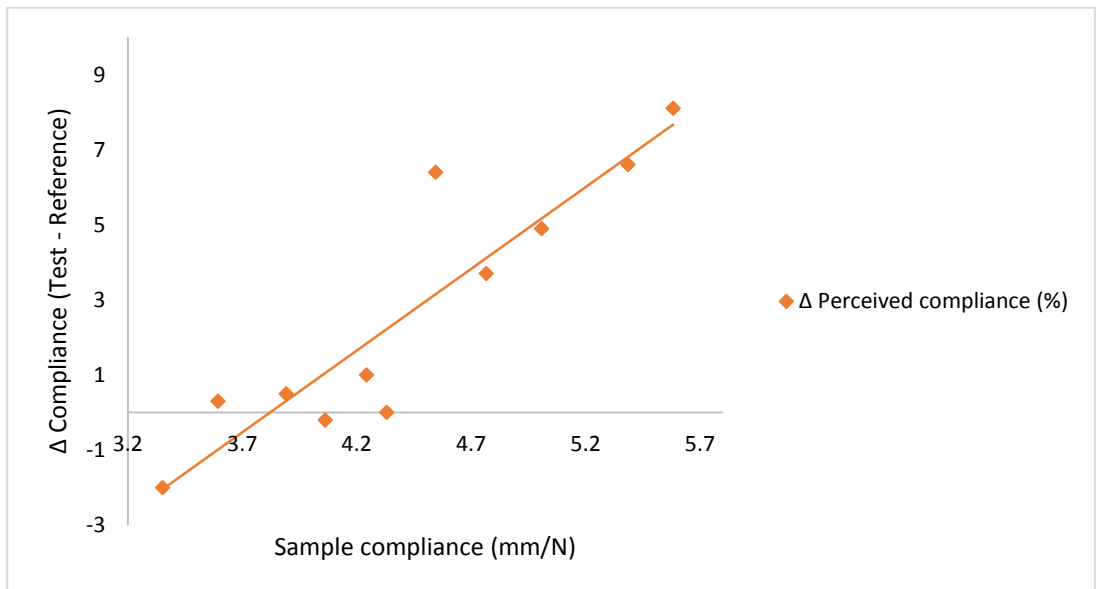


Figure 39. Visual difference and perceived haptic difference in compliance between reference and test samples
 Sample compliance and participants’ softness ratings were used to calculate Steven’s power exponent. Fitting the collated ratings to Steven’s power law function, k and a constants are estimated. This function [Equation (21)] is plotted in Figure 40.

$$\Psi = 78.2 \Phi^{0.18}$$

(21)

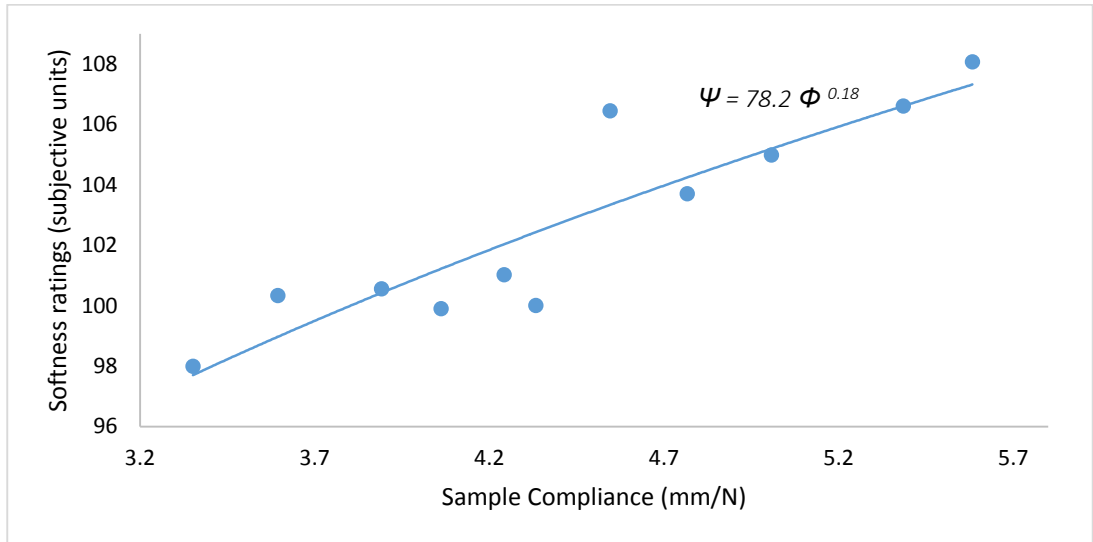


Figure 40. Steven’s power function fitted to the participants’ softness ratings

A 0.18 power exponent obtained through compliance discrimination using the pseudo-haptic system which is less than 1 implies that this is a negatively accelerated or compressive function. Nevertheless, a positive power exponent value suggests that the simulation of haptic sensations via visual alterations is possible.

7.5. Discussion

Stevens [88] conducted experiments on a range of stimulus conditions documenting the power exponent for continua covering the most common sensory fields. This list of representative exponents is tabulated in Section 2.4.2.3. These exponents are still used today to relate stimulus intensity to sensation magnitude for numerous continua. Figure 41 illustrates the power law function for the experiment conducted in this chapter, along with those obtained for similar continua [88], plotted on a log-log scale. For viscosity, stirring silicone fluids resulted in a power exponent of 0.42. Silicone fluids are still in a purely viscous state and hence do not possess any elastic properties. For tactual hardness, squeezing rubber resulted in a power exponent of 0.82. The hardness of an object is its resistance to permanent change when a compressive force is applied onto it. It is dependent upon several properties including compliance and viscoelasticity. These two stimulus conditions were used for comparison analysis as

they most closely reflect the mechanical properties of the continuum used in the pseudo-haptic system.

Due to the nature of the power function, using a log-log scale to plot the participants' ratings as a function of compliance results in straight lines where the slope of each function corresponds to the exponent of the power function. A greater slope indicates that the sensation magnitude is more sensitive to changes in stimulus intensity, and vice versa. From Figure 41 it is clear that sensitivity to changes in compliance is lowest when using the pseudo-haptic feedback system. However, changes in compliance in the pseudo-haptic system were only visual changes. The power exponents for squeezing rubber and stirring viscous fluids were obtained by direct experimentation without any pseudo-haptic effect.

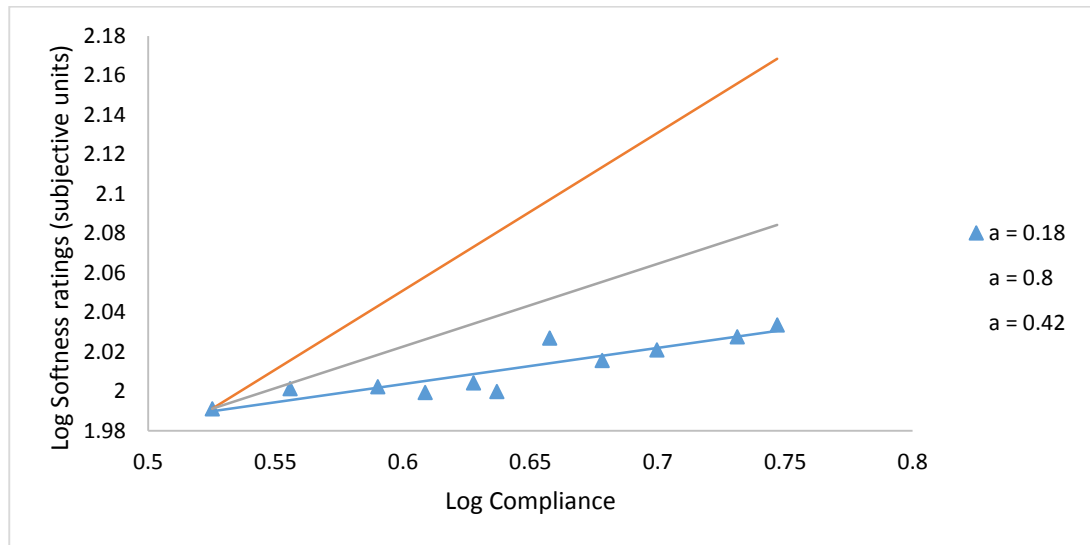


Figure 41. Softness ratings vs compliance of the samples for $a = 0.18$ (obtained from the results), 0.42 and 0.8 (retrieved from [88]), plotted in log-log scale

Figure 42 predicts participants' sensitivity to changes in stimulus intensity. Using the power exponents, the power functions for 'viscosity', 'tactual hardness' and 'viscoelasticity using pseudo-haptics' were plotted. A zero power exponent implies that the function becomes a straight horizontal line governed by the value of the constant, k . This means that no change in sensation occurred as stimulus intensity was varied. Since the magnitude estimation experiment conducted in this chapter applied the same haptic stimulus intensity for all visual samples, failure of pseudo-haptics to simulate any sensations would have resulted in a power exponent of zero. However,

with a power exponent of 0.18, the system has shown the significance of utilizing pseudo-haptic feedback for simulation of viscoelastic behaviour of compliant objects.

Unlike previously obtained exponents [88], the relationship reported here predicts haptic softness magnitude based on variations in visual cues only. Using the obtained constant k and a , it is possible to predict the softness sensation magnitude of any compliance intensity. Throughout the thesis, a finite number of physical samples was used. This power function can be used to predict performance at larger and smaller compliance levels that are otherwise troublesome to fabricate. Moreover, the smallest increment change in compliance between samples was limited by sample fabrication methods. With this equation, it becomes possible to predict performance for samples with compliance levels that fall between the physical ones fabricated.

While the results show that pseudo-haptics can potentially be a viable substitute to haptic feedback simulation, some research questions remained unanswered. In Table 17, when presented with a test stimulus that was visually less compliant than the reference sample, participants struggled to notice any haptic change. The table shows that participants were more sensitive to visual changes as the compliance of the test sample increased implying that the sensory illusion was magnified as the visual compliance was increased. In 2001, Lecuyer et al. [72] conducted an experiment exploring what they coined “the boundary of illusion”: the point after which humans can no longer be tricked into feeling a haptic sensation through modification, distortion or augmentation of visual information. Their results showed that pseudo-haptics was successful for generation of haptic sensations using different visual feedbacks, hinting at a need to study the simulation of properties such as viscoelasticity in the future. While their work implemented pseudo-haptics for generation of virtual spring stiffness, the work conducted in this chapter was successful at generating viscoelastic properties (i.e. spring and damper systems).

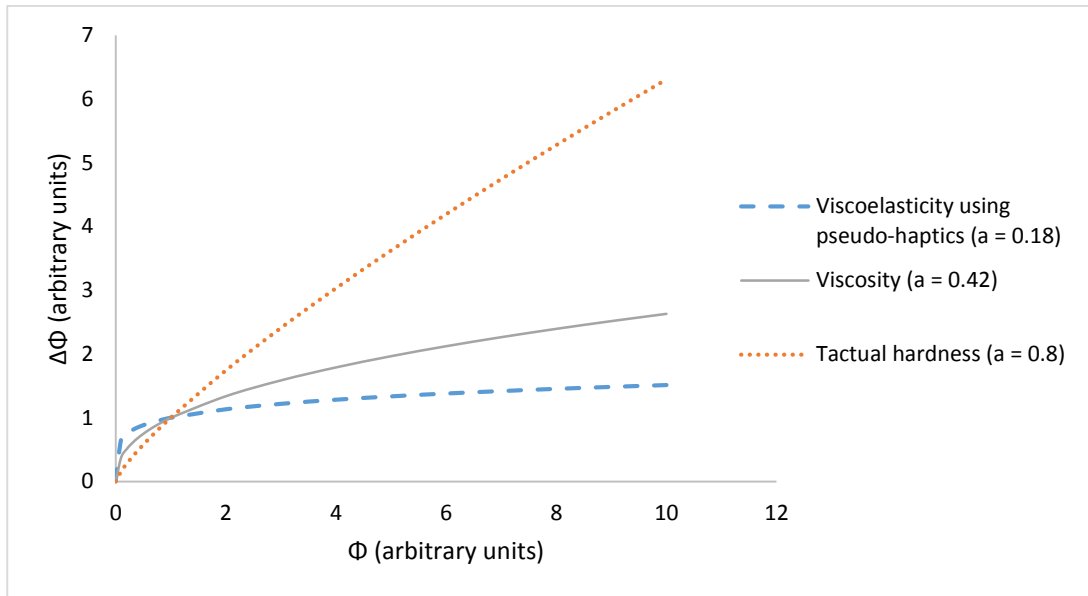


Figure 42. Steven's power law plotted for the power function obtained in this chapter, as well as for viscosity and tactual hardness obtained from the literature [88]

8. Conclusions

8.1. Summary

The research conducted throughout this thesis focused on determining compliance discrimination under different visual and haptic conditions. The results obtained are summarised in Table 18 in the form of the resultant Weber fractions and β values for ease of comparison. The standard errors for the Weber fractions are shown in Appendix D. This section summarises the key experimental studies conducted during the research and the significance of their outcomes.

Table 18. Weber fractions obtained in each psychophysical experiment

Finger pad only	Direct vision + tool	Fixed force + indirect vision	Fixed depth + indirect vision	Novel robotic system	Indirect vision + tool	Tool touch only	Indirect vision only	Pseudo-haptics
1.73	3.48	4.11	5.14	7.37	8.74	10.3	11.9	19.6

Chapter 4 described the first series of experiments in which the effects of various types of visual cues on the ability to discriminate compliance were assessed. This experiment allowed for a comparison of participants' performances across a range of surgical set-ups. The results suggested that participants performed best when using their finger to discriminate the softness of the samples, i.e. the baseline task, which is in line with previous literature [10], [17], [18]. For the remaining four tasks, participants performed best in the task utilizing direct visual access and touch using a tool followed by that utilizing indirect 2D visual access coupled with touch through a tool. The latter presented better compliance discriminability than the tool-touch-only and 2D-vision-only tasks, suggesting a cross-modal integration between vision and touch.

The first experiment described in Chapter 4 further emphasized the significance of visual information and how different variations of it lead to different levels of

performance during compliance discrimination. Participants performed similarly in both tool-touch-only and 2D-vision-only. In the 2D-vision-only task, participants watched video recordings of the samples being indented by someone else. While participants were able to discriminate softness visually in this task, their decision-making process was unclear. In other words, it could not be determined for certain which cues participants were using during discrimination between sample pairs. Each clip consisted of the sample pairs being indented using a tool without any measured fixed indentation rate or maximum depth or force applied. A post-experiment survey revealed that various strategies were implemented during indentation. Some participants focused on the speed of recovery of the surface of the sample after indentation, or on the extent of the bulging of the sides. Others focused on the depth the tool travelled into the sample, or even the discoloration of the indenter's fingers during application of high forces. Hence, it was necessary to isolate visual cues in order to determine the main source(s) of visual information used when judging compliance.

To further investigate the findings from Chapter 4 regarding visual dominance, the experiment in Chapter 5 examined the effect of the maximum indentation force and depth on people's ability to accurately discriminate compliance using indirect visual information only. Participants observed video recordings of a computer-actuated tip indent the sample pairs to one of two conditions: maximum depth of 10 mm into the sample or a maximum force of 4N applied by the indenter. Psychometric plots were constructed from the results suggesting that participants were able to discriminate compliance to a high level of accuracy (5.14% and 4.11% Weber's fractions for the fixed-depth and fixed-force tasks respectively), which not only showcases the dominance of visual feedback during compliance discrimination tasks but also sheds light on how controlling force and position can influence and enhance the ability to accurately discriminate compliance. Provided force or position cues were controlled, visual feedback could be sufficient to determine the compliance of objects. The results also suggested that participants were better able to discriminate compliance when the samples were being indented up to a set force than to a set depth.

While Chapter 5 showed the significance of controlling force and position cues during indirect visual compliance discrimination, the extent of visual dominance was yet to

be determined. Visual feedback has been shown to dominate and often substitute for absent or distorted haptic feedback [52], [56], [58], [93]. Researchers have been able to successfully generate haptic sensations by manipulating visual cues [71], [72], [74], [80], [134], [136]–[138]. This relatively new concept referred to as pseudo-haptics has not yet been used to simulate viscoelastic properties of compliant objects. A haptic feedback system that uses pseudo-haptics would be useful not only to determine the extent of the contribution of visual feedback in haptic compliance discrimination tasks, but can also be used to augment, modify or generate haptic sensations.

A haptic feedback system with the ability to independently manipulate visual information as well as haptic information was designed and set up in Chapter 6. Visual feedback consisted of physical silicone samples interchanged using 7 DoF robots. Haptic feedback was obtained using a commercial force feedback device. This device controlled the motion of a robot which in turn indented the samples. Viscoelastic properties of compliant samples were simulated using mathematical model fits. Before introducing pseudo-haptic feedback in a surgical application, it was necessary to validate the system's ability to accurately simulate the viscoelastic behaviour of compliant objects which simulate tissue. Participant responses from a 2AFC compliance discrimination experiment were used to extract a psychometric function from which the Weber's fraction were obtained. A Weber fraction of 7.36% indicated that participants were able to accurately and precisely judge the softness of the samples using the novel pseudo-haptic feedback system, thus validating the system's ability to accurately simulate viscoelasticity.

Following the validation of the system's ability to allow for accurate simulation of viscoelasticity, the concept of pseudo-haptics was employed in order to quantitatively determine the extent of the visual impact on haptic discrimination of compliance in Chapter 7. Participant ratings from a magnitude estimation experiment were collated and fitted to Steven's power function. A 0.18 power exponent suggests that method of pseudo-haptics, as implemented on our novel system, was successful in generating viscoelastic properties. Results also show that in order to perceive a change in haptic compliance using the pseudo-haptic system, a 19.6% visual change from the reference compliance is necessary.

As a final note, the main objective of pseudo-haptics has been to simulate haptic sensations without the use of a haptic interface [71]. It is a simple method of generating sensations when expensive haptic systems are not accessible. Pseudo-haptics has mainly been used to simulate haptic sensations using passive systems. The work conducted in this thesis, however, explores a new concept, the introduction of pseudo-haptics into an active haptic interface in order to determine the contribution of visual feedback during compliance discrimination as well as assess its potential in simulating more complicated tasks such as virtual tissue palpation in VR training and RALS.

8.2. Assessment of research objectives

In chapter two, seven research objectives were identified, necessary to achieve the aims of this research. This section assesses those objectives and the contributions they make to the literature.

1. *Create an array of samples mimicking real tissue softness, with similar stress-strain behaviour to a known soft tissue organ such as the liver.* Plastil gels and a plasticizer were used to create 11 compliant stimuli which mimic the behaviour of soft tissue during indentation. Stress-strain data was obtained for each sample using three different indentation rigs. The stimuli displayed viscoelastic behaviour similar to that of tissue.
2. *Select and implement a suitable mathematical model linking physical compliance of the samples to viscoelastic parameters such as stiffness and viscosity coefficients.* The Maxwell and Voigt models were used to estimate stiffness and damping coefficients for each sample. These coefficients are a representation of the viscoelastic properties of the samples.
3. *Determine the effect of the type of visual cues available during modes of surgery on the ability to discriminate compliance of soft sample.* A 2AFC experiment was set up investigating the effect of varying visual cues on the ability to discriminate softness of compliant objects. The results showed that visual information was shown to dominate over haptic information during

compliance discrimination. While cutaneous information was shown to be the most reliable source of information, haptic feedback using a tool could be effective if coupled with optimised visual feedback.

4. *Assess the effect of indentation force and displacement on the ability to visually discriminate compliance.* A 2AFC experiment was set up investigating the effect of indentation depth and force on the ability to visually discriminate softness of compliant objects. Results show that implementing force and position constraints could lead to enhanced compliance discriminability.
5. *Develop a pseudo-haptic feedback robotic system capable of independently manipulating visual and haptic feedback.* A novel pseudo-haptic feedback system was designed and assembled in order to determine the extent of impact of visual feedback on compliance discrimination. A haptic feedback device remotely controls the movement of a robotic system. The novelty of this system lies in its ability to independently manipulate visual and haptic cues.
6. *Validate the pseudo-haptic system's ability to simulate viscoelastic behaviour of compliant objects.* A 2AFC experiment was successful at validating the system's ability to accurately simulate viscoelastic properties. Participants were able to judge the softness of the physical compliant objects using the system. The system can be used to accurately mimic the visual and haptic behaviour of compliant objects. The novelty here is that the system is able to simulate the viscoelastic behaviour of physical stimuli using unique mathematical models that control the behaviour of a haptic feedback device.
7. *Determine the extent to which visual feedback augmentation can generate realistic sensations of haptic compliance.* The pseudo-haptic system was used to set up a magnitude estimation experiment. A 19.6% Weber fraction marks the boundary of visual illusion during haptic compliance discrimination. This is the first instance in which a pseudo-haptic system has been used to successfully generate haptic viscoelastic sensations.

8.3. General Discussion

Considering this piece of research as a whole, a number of discussion points were identified which identify key themes of the work and how they relate to the wider research literature. These are detailed in the following sections:

The effect of visual-haptic integration on compliance discrimination

Chapter 4 suggests that visual and haptic feedback are optimally integrated when attempting to judge mechanical properties such as the softness of compliant stimuli, which is in line with previous literature [58], [69], [139]. Furthermore, while the cutaneous feedback remains the most reliable source of information [7], [8], [131], tool-operated haptic feedback, when coupled with indirect visual feedback (MIS setup), has been shown to provide sufficient information for compliance discrimination. With extensive literature highlighting the weaknesses associated with using a tool [2], [8], [15], [19], [45], [50], the results from Chapters 4 and 5 suggest that when combined with controlled visual feedback, tool-operated haptic feedback can be a reliable source of information during compliance discrimination.

The dominance of visual feedback

In line with previous literature [52], the experiments conducted in Chapters 4 and 5 highlight the impact and dominance of visual feedback during compliance discrimination. A Kruskal-Willis one-way analysis of variance by ranks test followed by a Dunn's multiple comparison test with correction to adjust for inflations of type 1 error were performed. The results for Dunn's test comparing all experiments is documented in Appendix C. No significant difference in performance between the indirect vision only and the indirect vision with tool touch was detected, suggesting that the addition of haptic feedback might not necessarily result in improved compliance discrimination performance. In the future, controlling visual cues such as force and depth during indentation can potentially substitute for weakened, distorted, or absent haptic feedback.

Using pseudo-haptics to generate viscoelastic sensations

Previous researchers have assessed the potential of pseudo-haptics for the generation and augmentation of haptic sensations such as stiffness [72], [78], [134], [135]. None have done so, however, for the compliance of tissue during palpation. Lecuyer et al. [72] described a need to simulate more complex properties such as viscoelasticity using pseudo-haptics. A novel robotic pseudo-haptic feedback system developed in Chapter 6 simulated the viscoelastic behaviour of compliant objects. A 19.6% Weber fraction as well as a positive power exponent (0.18) obtained by fitting participants' responses to Steven's power law suggest that haptic viscoelastic sensations were successfully generated through visual augmentations. This highlights the potential for using pseudo-haptics within a surgical context such as in future VR medical training simulators.

Pseudo-haptics in active haptic feedback systems

Unlike 'active' haptic feedback, pseudo-haptic feedback does not necessarily require the use of a haptic interface in order to simulate haptic sensations [71]. Furthermore, using pseudo-haptics allows for a dynamic modification of the properties of the manipulated object in the virtual environment [71].

While passive systems such as a computer mouse or a joystick have been used in the literature to simulate haptic sensations [78], [80], [134], [138], the results from Chapter 7 show the potential for integrating pseudo-haptics into active haptic feedback systems. In many cases, haptic feedback devices with greater force ranges or resolution are required, either for research or training purposes. The options in this case would be either to purchase a new haptic device with specifications that meet the desired purpose, or modify an existing one. Pseudo-haptics can be incorporated into standard off-the-shelf haptic feedback devices in order to enhance force ranges or reduce error without adding any added hardware costs. Alternatively, these relatively inexpensive haptic feedback devices are difficult to modify mechanically or electronically as they have fixed specifications, workspaces, and force outputs (see Table 1) and are not suitable for customisation.

Pseudo-haptics in RALS and VR training

The da Vinci surgical robot offers no force feedback [140]. As explained in Section 1.1.3, the value of force feedback in RALS remains uncertain. Visual feedback is primarily used to judge mechanical properties of tissue during procedures performed using the da Vinci as tissue stiffness acquisition remains an issue [78]. Pseudo-haptics can potentially be incorporated into the da Vinci to generate sensations of resistance without the need for adding any new force sensors or complicated equipment. This can be accomplished by modifying the position ratio between the instruments controlled by the surgeon at the console and the robotic instruments at the robotic tower, hence creating a sensory illusion.

The benefits of using haptic feedback systems in VR surgical training has been recognized in the literature [141]–[144]. Pseudo-haptics can be introduced in RALS training systems such as the da Vinci Skills Simulator. Since these systems operate in a virtual environment, the mechanical properties of simulated tissue are known and simulated using mathematical models. Visual augmentations can be introduced onto certain areas to simulate a broader range of properties without the need to modify the haptic feedback relayed to the surgeon.

The pseudo-haptic feedback system designed and used in Chapters 6 and 7 could also be used with the force feedback mode turned off. Further psychophysical experiments would be necessary to investigate the extent at which pseudo-haptic generation of viscoelastic properties is possible. If proven successful, the ability to simulate compliance of tissue-like objects without the need for force feedback devices would then be possible. Such a system relying solely on visual feedback to produce sensations of softness would be useful for underprivileged education systems where advanced medical equipment as well as VR simulation via high-end force feedback systems is not yet accessible. Surgical training should not be limited to hospitals and residency programs. On the contrary, surgical simulation needs to be integrated into medical undergraduate programs so that the process of learning starts at a the university level, before reaching residency programmes and operating theatres [145].

Reducing excessive forces in LS

Described in Section 2.3.5.1, surgeons in LS use excessive forces in order to prevent tissue from slipping [67]. Haptic information transmitted from the grasper jaws to the surgeon's hand has been shown to be distorted [68]. The pseudo-haptic system developed in Chapter 6 can be used to investigate the effect of transmitted force errors on a surgeon's ability to discriminate compliance of tissue during laparoscopic procedures. By maintaining the same visual information while augmenting the haptic one (simulating disturbed or limited transmitted forces), it would be possible to quantify the extent of the effect of transmitted force disruptions on compliance discrimination.

General applications of pseudo-haptics

Outside the scope of surgical technologies, pseudo-haptics can be used to generate stimuli such as loudness, brightness, and heaviness. Moreover, by combining compliance analysis conducted in this thesis with human and object mapping into avatars as discussed by [23], pseudo-haptics could be used to simulate physical interactive activities, which can be useful in training as well as rehabilitation. Virtual activities such as press-ups, pull-ups, and contact sports could possibly be simulated. Such a system could also be used in gaming, where force, vibration as well as numerous other haptic sensations can be simulated without the need for sophisticated feedback systems.

8.4. Future work

Following the completion of this work, several areas have been determined to be areas for future work.

Hand-instrument ratio using the da Vinci

The latest da Vinci Xi robot allows surgeons to operate through a few small incisions, with the capabilities of traditional open surgery. A three-dimensional HD visual feedback system allows for a clear magnified view of the operating region. The system translates the surgeon's hand movements into smaller more precise ones of miniscule instruments inside the patient's body [140]. To the best of the author's knowledge,

this position ratio between hand movement and robotic instrument movement is not yet investigated. The pseudo-haptic feedback system designed in this thesis can be modified to function similar to the da Vinci robot. Control systems can be implemented to provide more precise movement of the robotic arms when controlled by the Omega.7 haptic devices. By varying the position ratio between the haptic device arm and the robot arm, it would be possible to study the effect of varying hand-instrument ratios on a surgeon's ability to perform delicate tasks with a high level of precision. Results from such a study might be used to modify the hand-instrument ratios currently implemented in order to enhance the surgeon's performance.

Full-factorial pseudo-haptics investigation

Although the magnitude estimation experiment described in Chapter 7 yielded promising results regarding the effectiveness and potential of pseudo-haptics, the extent of this potential is far from fully uncovered. A full factorial magnitude estimation experiment which assesses compliance discrimination performance for a range of compliance levels is necessary. Table 19 describes an example of such an experiment. While pseudo-haptics is focused on simulating haptic sensations using visual augmentations, it may be more advantageous to incorporate some level of force feedback to enhance the sensory experience during compliance discrimination. A full factorial experiment would provide insight into the minimum and maximum necessary haptic feedback necessary for a pseudo-haptic sensory experience to be perceived 'real'.

Table 19. Example of a full factorial pseudo-haptic experiment design

		Visual Δ compliance from reference (%)						
		-30	-20	-10	0	10	20	30
Haptic Δ compliance from reference (%)	-30							
	-20							
	-10							
	0							
	10							
	20							
	30							

Pseudo-haptics in more complex tasks

Perreault and Cao [42] investigated the effect of vision on compliance discrimination using a laparoscopic tool. Their results suggested that although vision may compensate for missing or distorted haptic information, it may not be sufficient in tasks more complex than probing. The experiments conducted throughout this thesis have illustrated the power and dominance of visual information during compliance discrimination tasks using a tool. However, more complex tasks were not attempted with the pseudo-haptic robotic system described in Chapter 6. In the future, the impact of visual information could be investigated for more complex surgical procedures and tasks such suturing and needle insertion could be introduced. The possibility of using pseudo-haptics to simulate realistic sensations during such complex tasks would be advantageous in places where expensive VR training systems capable of simulating such tasks are unavailable.

Enhancing force range and accuracy of haptic feedback devices

State-of-the-art force feedback devices can be expensive [146]. As stated earlier, pseudo-haptics can act to augment as well as generate haptic sensations through alteration of visual cues. When active haptic feedback devices are not available, pseudo-haptics can be used to generate sensations without the need for any force feedback whatsoever. This has been proven successful in previous literature [71], [73], [80], [134], [136]–[138]. Alternatively, pseudo-haptics can be incorporated into off-the-shelf haptic feedback devices to simulate larger force fields and enhance accuracy which can be useful for basic surgical tasks in undergraduate medical training classes.

References

- [1] J. Chen, “Human haptic interaction with soft objects: discriminability, force control, and contact visualization,” DTIC Document, 1998.
- [2] O. Aziz, V. Constantinides, P. P. Tekkis, T. Athanasiou, S. Purkayastha, P. Paraskeva, A. W. Darzi, and A. G. Heriot, “Laparoscopic versus open surgery for rectal cancer: a meta-analysis,” *Ann. Surg. Oncol.*, vol. 13, no. 3, pp. 413–424, 2006.
- [3] A. G. Gallagher, E. M. Ritter, H. Champion, G. Higgins, M. P. Fried, G. Moses, C. D. Smith, and R. M. Satava, “Virtual reality simulation for the operating room: proficiency-based training as a paradigm shift in surgical skills training,” *Ann. Surg.*, vol. 241, no. 2, p. 364, 2005.
- [4] A. Zanghì, “Liver biliopancreatic workshop surgery,” *Eur. Rev. Med. Pharmacol. Sci.*, vol. 18, no. 2 Suppl, pp. 1–1, 2014.
- [5] S. Schostek, M. O. Schurr, and G. F. Buess, “Review on aspects of artificial tactile feedback in laparoscopic surgery,” *Med. Eng. Phys.*, vol. 31, no. 8, pp. 887–898, 2009.
- [6] R. Morison and C. F. M. Saint, *An Introduction to Surgery*. Wright, 1935.
- [7] E. Fakhoury, P. Culmer, and B. Henson, “The Effect of Vision on Discrimination of Compliance Using a Tool,” *Int. J. Hum.-Comput. Interact.*, vol. 30, no. 11, pp. 882–890, 2014.
- [8] M. V. Ottermo, M. Øvstedal, T. Langø, Ø. Stavadahl, Y. Yavuz, T. A. Johansen, and R. M\aarvik, “The role of tactile feedback in laparoscopic surgery,” *Surg. Laparosc. Endosc. Percutan. Tech.*, vol. 16, no. 6, pp. 390–400, 2006.
- [9] R. Veldkamp, E. Kuhry, W. C. Hop, J. Jeekel, G. Kazemier, H. J. Bonjer, E. Haglind, L. Pahlman, M. A. Cuesta, S. Msika, and others, “Laparoscopic surgery versus open surgery for colon cancer: short-term outcomes of a randomised trial,” *Lancet Oncol*, vol. 6, no. 7, pp. 477–484, 2005.
- [10] N. Langrana, G. Burdea, J. Ladeji, and M. Dinsmore, “Human performance using virtual reality tumor palpation simulation,” *Comput. Graph.*, vol. 21, no. 4, pp. 451–458, 1997.

-
- [11] H. Xin, J. S. Zelek, and H. Carnahan, "Laparoscopic surgery, perceptual limitations and force: A review," in *First Canadian Student Conference on Biomedical Computing, Kingston, Ontario, Canada*, 2006, vol. 144.
- [12] J. S. Park, G.-S. Choi, K. H. Lim, Y. S. Jang, and S. H. Jun, "S052: a comparison of robot-assisted, laparoscopic, and open surgery in the treatment of rectal cancer," *Surg. Endosc.*, vol. 25, no. 1, pp. 240–248, 2011.
- [13] R. S. Poston, R. Tran, M. Collins, M. Reynolds, I. Connerney, B. Reicher, D. Zimrin, B. P. Griffith, and S. T. Bartlett, "Comparison of economic and patient outcomes with minimally invasive versus traditional off-pump coronary artery bypass grafting techniques," *Ann. Surg.*, vol. 248, no. 4, p. 638, 2008.
- [14] B. Wallace, "The da Vinci® Surgical System: Validated Reprocessing Methods and Regulatory Compliance," *THE POUCHMAKER*, p. 8.
- [15] P. Culmer, J. Barrie, R. Hewson, M. Levesley, M. Mon-Williams, D. Jayne, and A. Neville, "Reviewing the technological challenges associated with the development of a laparoscopic palpation device," *Int. J. Med. Robot.*, vol. 8, no. 2, pp. 146–159, 2012.
- [16] R. Brydges, H. Carnahan, and A. Dubrowski, "Surface exploration using laparoscopic surgical instruments: The perception of surface roughness," *Ergonomics*, vol. 48, no. 7, pp. 874–894, 2005.
- [17] D. R. Fletcher, M. S. Hobbs, P. Tan, L. J. Valinsky, R. L. Hockey, T. J. Pikora, M. W. Knuiman, H. J. Sheiner, and A. Edis, "Complications of cholecystectomy: risks of the laparoscopic approach and protective effects of operative cholangiography: a population-based study," *Ann. Surg.*, vol. 229, no. 4, pp. 449–457, 1999.
- [18] A. Kazi, "Operator performance in surgical telemanipulation," *Presence Teleoperators Virtual Environ.*, vol. 10, no. 5, pp. 495–510, 2001.
- [19] O. S. Bholat, R. S. Haluck, W. B. Murray, P. J. Gorman, and T. M. Krummel, "Tactile feedback is present during minimally invasive surgery," *J. Am. Coll. Surg.*, vol. 189, no. 4, pp. 349–355, 1999.
- [20] T. R. Coles, D. Meglan, and N. W. John, "The role of haptics in medical training simulators: a survey of the state of the art," *Haptics IEEE Trans. On*, vol. 4, no. 1, pp. 51–66, 2011.

-
- [21] O. Gerovichev, P. Marayong, and A. Okamura, "The effect of visual and haptic feedback on manual and teleoperated needle insertion," *Med. Image Comput. Comput.-Assist. Interv. 2002*, pp. 147–154, 2002.
- [22] M. Tavakoli, R. V. Patel, and M. Moallem, "Haptic feedback and sensory substitution during telemanipulated suturing," in *Eurohaptics Conference, 2005 and Symposium on Haptic Interfaces for Virtual Environment and Teleoperator Systems, 2005. World Haptics 2005. First Joint*, 2005, pp. 543–544.
- [23] L. S. Leddy, T. S. Lendvay, and R. M. Satava, "Robotic surgery: applications and cost effectiveness," *Open Access Surg.*, vol. 3, pp. 99–107, 2010.
- [24] A. R. Lanfranco, A. E. Castellanos, J. P. Desai, and W. C. Meyers, "Robotic surgery: a current perspective," *Ann. Surg.*, vol. 239, no. 1, p. 14, 2004.
- [25] G. H. Ballantyne and F. Moll, "The da Vinci telerobotic surgical system: the virtual operative field and telepresence surgery.," *Surg. Clin. North Am.*, vol. 83, no. 6, p. 1293, 2003.
- [26] F. Corcione, C. Esposito, D. Cuccurullo, A. Settembre, N. Miranda, F. Amato, F. Pirozzi, and P. Caiazzo, "Advantages and limits of robot-assisted laparoscopic surgery: preliminary experience," *Surg. Endosc. Interv. Tech.*, vol. 19, no. 1, pp. 117–119, 2005.
- [27] J. C. Byrn, S. Schluender, C. M. Divino, J. Conrad, B. Gurland, E. Shlasko, and A. Szold, "Three-dimensional imaging improves surgical performance for both novice and experienced operators using the da Vinci Robot System," *Am. J. Surg.*, vol. 193, no. 4, pp. 519–522, 2007.
- [28] J. C. Gwilliam, M. Mahvash, B. Vagvolgyi, A. Vacharat, D. D. Yuh, and A. M. Okamura, "Effects of haptic and graphical force feedback on teleoperated palpation," in *Robotics and Automation, 2009. ICRA '09. IEEE International Conference on*, 2009, pp. 677–682.
- [29] A. J. Vickers, C. J. Savage, M. Hruza, I. Tuerk, P. Koenig, L. Martínez-Piñeiro, G. Janetschek, and B. Guillonneau, "The surgical learning curve for laparoscopic radical prostatectomy: a retrospective cohort study," *Lancet Oncol.*, vol. 10, no. 5, pp. 475–480, 2009.

-
- [30] A. Liu, F. Tendick, K. Cleary, and C. Kaufmann, "A survey of surgical simulation: applications, technology, and education," *Presence Teleoperators Virtual Environ.*, vol. 12, no. 6, pp. 599–614, 2003.
- [31] I. NISKY, F. HUANG, A. MILSTEIN, C. M. PUGH, F. A. MUSSA-IVALDI, and A. KARNIEL, "Perception of Stiffness in Laparoscopy—the Fulcrum Effect," *Stud. Health Technol. Inform.*, vol. 173, pp. 313–319, 2012.
- [32] D. Morris, H. Tan, F. Barbagli, T. Chang, and K. Salisbury, "Haptic feedback enhances force skill learning," in *EuroHaptics Conference, 2007 and Symposium on Haptic Interfaces for Virtual Environment and Teleoperator Systems. World Haptics 2007. Second Joint*, 2007, pp. 21–26.
- [33] L. Dominjon, A. Lécuyer, J.-M. Burkhardt, P. Richard, and S. Richir, "Influence of control/display ratio on the perception of mass of manipulated objects in virtual environments," in *Virtual Reality, 2005. Proceedings. VR 2005. IEEE*, 2005, pp. 19–25.
- [34] S. Allin, Y. Matsuoka, and R. Klatzky, "Measuring just noticeable differences for haptic force feedback: implications for rehabilitation," in *Haptic Interfaces for Virtual Environment and Teleoperator Systems, 2002. HAPTICS 2002. Proceedings. 10th Symposium on*, 2002, pp. 299–302.
- [35] C. R. Wagner, R. D. Howe, and N. Stylopoulos, "The role of force feedback in surgery: analysis of blunt dissection," in *Haptic Interfaces for Virtual Environment and Teleoperator Systems, International Symposium on*, 2002, pp. 73–73.
- [36] C. R. Wagner and R. D. Howe, "Mechanisms of performance enhancement with force feedback," in *Eurohaptics Conference, 2005 and Symposium on Haptic Interfaces for Virtual Environment and Teleoperator Systems, 2005. World Haptics 2005. First Joint*, 2005, pp. 21–29.
- [37] A. Gawande, "Two hundred years of surgery," *N. Engl. J. Med.*, vol. 366, no. 18, pp. 1716–1723, 2012.
- [38] R. H. Meade, *An introduction to the history of general surgery*. Saunders, 1968.
- [39] R. Sekuler and R. Blake, *Perception*. McGraw-Hill, 1994.
- [40] S. M. Kosslyn and A. L. Sussman, "Roles of imagery in perception: Or, there is no such thing as immaculate perception," 1995.
- [41] E. Goldstein, *Sensation and perception*. Cengage Learning, 2013.

-
- [42] J. O. Perreault and C. G. Cao, "Effects of vision and friction on haptic perception," *Hum. Factors J. Hum. Factors Ergon. Soc.*, vol. 48, no. 3, pp. 574–586, 2006.
- [43] R. M. Friedman, K. D. Hester, B. G. Green, and R. H. LaMotte, "Magnitude estimation of softness," *Exp. Brain Res.*, vol. 191, no. 2, pp. 133–142, 2008.
- [44] E. E. Konofagou, J. Ophir, F. Kallel, and T. Varghese, "Elastographic dynamic range expansion using variable applied strains," *Ultrason. Imaging*, vol. 19, no. 2, pp. 145–166, 1997.
- [45] O. S. Bholat, R. S. Haluck, R. H. Kutz, P. J. Gorman, and T. M. Krummel, "Defining the role of haptic feedback in minimally invasive surgery," *Stud. Health Technol. Inform.*, pp. 62–66, 1999.
- [46] D. S. Tan, R. Pausch, J. K. Stefanucci, and D. R. Proffitt, "Kinesthetic cues aid spatial memory," in *CHI'02 extended abstracts on Human factors in computing systems*, 2002, pp. 806–807.
- [47] M. A. Srinivasan and R. H. LaMotte, "Tactual discrimination of softness," *J. Neurophysiol.*, vol. 73, no. 1, pp. 88–101, 1995.
- [48] W. M. Bergmann Tiest and A. Kappers, "Cues for haptic perception of compliance," *Haptics IEEE Trans. On*, vol. 2, no. 4, pp. 189–199, 2009.
- [49] K. T. Den Boer, J. L. Herder, W. Sjoerdsma, D. W. Meijer, D. J. Gouma, and H. G. Stassen, "Sensitivity of laparoscopic dissectors," *Surg. Endosc.*, vol. 13, no. 9, pp. 869–873, 1999.
- [50] R. H. LaMotte, "Softness discrimination with a tool," *J. Neurophysiol.*, vol. 83, no. 4, pp. 1777–1786, 2000.
- [51] J. J. Gibson, *The Ecological Approach to Visual Perception: Classic Edition*. Psychology Press, 2014.
- [52] M. A. Srinivasan, G. L. Beauregard, and D. L. Brock, "The impact of visual information on the haptic perception of stiffness in virtual environments," in *ASME Winter Annual Meeting*, 1996, vol. 165.
- [53] K. Drewing, A. Ramisch, and F. Bayer, "Haptic, visual and visuo-haptic softness judgments for objects with deformable surfaces," in *EuroHaptics conference, 2009 and Symposium on Haptic Interfaces for Virtual Environment and Teleoperator Systems. World Haptics 2009. Third Joint*, 2009, pp. 640–645.

-
- [54] M. Kuschel, M. Buss, F. Freyberger, B. Farber, and R. L. Klatzky, "Visual-haptic perception of compliance: fusion of visual and haptic information," in *Haptic interfaces for virtual environment and teleoperator systems, 2008. haptics 2008. symposium on*, 2008, pp. 79–86.
- [55] R. M. Johnson, P. C. Burton, and T. Ro, "Visually induced feelings of touch," *Brain Res.*, vol. 1073, pp. 398–406, 2006.
- [56] I. Rock and J. Victor, "Vision and touch: An experimentally created conflict between the two senses.," *Science*, 1964.
- [57] A. T. Woods and F. N. Newell, "Visual, haptic and cross-modal recognition of objects and scenes," *J. Physiol.-Paris*, vol. 98, no. 1, pp. 147–159, 2004.
- [58] M. O. Ernst and M. S. Banks, "Humans integrate visual and haptic information in a statistically optimal fashion," *Nature*, vol. 415, no. 6870, pp. 429–433, 2002.
- [59] F. Biocca, J. Kim, and Y. Choi, "Visual touch in virtual environments: An exploratory study of presence, multimodal interfaces, and cross-modal sensory illusions," *Presence*, vol. 10, no. 3, pp. 247–265, 2001.
- [60] W.-C. Wu, C. Basdogan, and M. A. Srinivasan, "Visual, haptic, and bimodal perception of size and stiffness in virtual environments," *ASME DYN SYST CONTROL DIV PUBL DSC*, vol. 67, pp. 19–26, 1999.
- [61] J. F. Norman, H. F. Norman, A. M. Clayton, J. Lianekhammy, and G. Zielke, "The visual and haptic perception of natural object shape," *Atten. Percept. Psychophys.*, vol. 66, no. 2, pp. 342–351, 2004.
- [62] A. Lecuyer, S. Coquillart, A. Kheddar, P. Richard, and P. Coiffet, "Pseudo-haptic feedback: Can isometric input devices simulate force feedback?," in *Virtual Reality, 2000. Proceedings. IEEE*, 2000, pp. 83–90.
- [63] D. Couroussé, G. Jansson, J.-L. Florens, and A. Luciani, "Visual and Haptic perception of object elasticity in a virtual squeezing event," *EuroHaptics 2006*, 2006.
- [64] G. Tholey, J. P. Desai, and A. E. Castellanos, "Force feedback plays a significant role in minimally invasive surgery: results and analysis," *Ann. Surg.*, vol. 241, no. 1, p. 102, 2005.

-
- [65] E. P. Westebring–Van Der Putten, R. H. M. Goossens, J. J. Jakimowicz, and J. Dankelman, “Haptics in minimally invasive surgery—a review,” *Minim. Invasive Ther. Allied Technol.*, vol. 17, no. 1, pp. 3–16, 2008.
- [66] T. Akinbiyi, “Intelligent Instruments and Visual Force Feedback in Laparoscopic Minimally Invasive Surgery,” *Masters Thesis Johns Hopkins Univ. Baltim. Md.*, 2005.
- [67] E. P. Westebring-van der Putten, J. J. van den Dobbelen, R. H. Goossens, J. J. Jakimowicz, and J. Dankelman, “Effect of laparoscopic grasper force transmission ratio on grasp control,” *Surg. Endosc.*, vol. 23, no. 4, pp. 818–824, 2009.
- [68] W. Sjoerdsma, J. L. Herder, M. J. Horward, A. Jansen, J. J. G. Bannenberg, and C. A. Grimbergen, “Force transmission of laparoscopic grasping instruments,” *Minim. Invasive Ther. Allied Technol.*, vol. 6, no. 4, pp. 274–278, 1997.
- [69] J.-P. Bresciani, F. Dammeier, and M. O. Ernst, “Vision and touch are automatically integrated for the perception of sequences of events,” *J. Vis.*, vol. 6, no. 5, 2006.
- [70] A. Lécuyer, S. Cuquillart, and P. Coiffet, “Simulating haptic information with haptic illusions in virtual environments,” DTIC Document, 2001.
- [71] A. Lécuyer, “Simulating haptic feedback using vision: A survey of research and applications of pseudo-haptic feedback,” *Presence Teleoperators Virtual Environ.*, vol. 18, no. 1, pp. 39–53, 2009.
- [72] A. Lécuyer, J.-M. Burkhardt, S. Coquillart, and P. Coiffet, “‘Boundary of illusion’: an experiment of sensory integration with a pseudo-haptic system,” in *Virtual Reality, 2001. Proceedings. IEEE*, 2001, pp. 115–122.
- [73] F. Argelaguet, D. A. G. Jáuregui, M. Marchal, and A. Lécuyer, “A novel approach for pseudo-haptic textures based on curvature information,” in *Haptics: Perception, Devices, Mobility, and Communication*, Springer, 2012, pp. 1–12.
- [74] A. Lécuyer, J.-M. Burkhardt, and L. Etienne, “Feeling bumps and holes without a haptic interface: the perception of pseudo-haptic textures,” in *Proceedings of the SIGCHI conference on Human factors in computing systems*, 2004, pp. 239–246.

-
- [75] P. Kadleček, P. Kmoch, and J. Křivánek, “Haptic rendering for under-actuated 6/3-DOF haptic devices,” in *Haptics: Neuroscience, Devices, Modeling, and Applications*, Springer, 2014, pp. 63–71.
- [76] Y. Ban, T. Kajinami, T. Narumi, T. Tanikawa, and M. Hirose, “Modifying an identified curved surface shape using pseudo-haptic effect,” in *Haptics Symposium (HAPTICS), 2012 IEEE*, 2012, pp. 211–216.
- [77] M. Li, J. Konstantinova, E. L. Secco, A. Jiang, H. Liu, T. Nanayakkara, L. D. Seneviratne, P. Dasgupta, K. Althoefer, and H. A. Wurdemann, “Using visual cues to enhance haptic feedback for palpation on virtual model of soft tissue,” *Med. Biol. Eng. Comput.*, pp. 1–10, 2015.
- [78] M. Li, H. Liu, J. Li, L. D. Seneviratne, and K. Althoefer, “Tissue stiffness simulation and abnormality localization using pseudo-haptic feedback,” in *Robotics and Automation (ICRA), 2012 IEEE International Conference on*, 2012, pp. 5359–5364.
- [79] L. Bibin, A. Lécuyer, J.-M. Burkhardt, A. Delbos, and M. Bonnet, “SAILOR: a 3-D medical simulator of loco-regional anaesthesia based on desktop virtual reality and pseudo-haptic feedback,” in *Proceedings of the 2008 ACM symposium on Virtual reality software and technology*, 2008, pp. 97–100.
- [80] F. Argelaguet, D. A. G. Jáuregui, M. Marchal, and A. Lécuyer, “Elastic images: Perceiving local elasticity of images through a novel pseudo-haptic deformation effect,” *ACM Trans. Appl. Percept. TAP*, vol. 10, no. 3, p. 17, 2013.
- [81] G. A. Gescheider, *Psychophysics: the fundamentals*. Psychology Press, 2013.
- [82] F. A. A. Kingdom and N. Prins, *Psychophysics: a practical introduction*. Academic Press London, 2010.
- [83] Gös. Ekman, “Weber’s law and related functions,” *J. Psychol.*, vol. 47, no. 2, pp. 343–352, 1959.
- [84] H. Z. Tan, N. I. Durlach, G. L. Beauregard, and M. A. Srinivasan, “Manual discrimination of compliance using active pinch grasp: The roles of force and work cues,” *Percept. Psychophys.*, vol. 57, no. 4, pp. 495–510, 1995.
- [85] N. Dhruv and F. Tendick, “Frequency dependence of compliance contrast detection,” *Proceedings ASME Dyn. Syst. Control Div.*, 2000.

-
- [86] L. Nicholson, R. Adams, and C. Maher, "Reliability of a discrimination measure for judgements of non-biological stiffness," *Man. Ther.*, vol. 2, no. 3, pp. 150–156, 1997.
- [87] M. Jogan and A. A. Stocker, "A new two-alternative forced choice method for the unbiased characterization of perceptual bias and discriminability," *J. Vis.*, vol. 14, no. 3, p. 20, 2014.
- [88] S. S. Stevens, *Psychophysics: Introduction to its perceptual, neural, and social prospects*. Transaction Publishers, 1975.
- [89] G. L. Poling, J. M. Weisenberger, and T. Kerwin, "The role of multisensory feedback in haptic surface perception," in *Haptic Interfaces for Virtual Environment and Teleoperator Systems, 2003. HAPTICS 2003. Proceedings. 11th Symposium on*, 2003, pp. 187–194.
- [90] J. Eck, A. L. Kaas, and R. Goebel, "The effect of sensory modality and previous experience on perceived roughness," in *World Haptics Conference (WHC), 2011 IEEE*, 2011, pp. 209–214.
- [91] S. Ballesteros, "Implicit and explicit memory effects in haptic perception," *Hum. Haptic Percept. Basics Appl.*, pp. 183–198, 2008.
- [92] H. Mitterer, J. M. Horschig, J. Müsseler, and A. Majid, "The influence of memory on perception: It's not what things look like, it's what you call them.," *J. Exp. Psychol. Learn. Mem. Cogn.*, vol. 35, no. 6, p. 1557, 2009.
- [93] M. Kuschel, M. Di Luca, M. Buss, and R. L. Klatzky, "Combination and integration in the perception of visual-haptic compliance information," *Haptics IEEE Trans. On*, vol. 3, no. 4, pp. 234–244, 2010.
- [94] M. Rosen and J. Ponsky, "Minimally invasive surgery.," *Endoscopy*, vol. 33, no. 4, pp. 358–366, 2001.
- [95] S. Najarian, M. Fallahnezhad, and E. Afshari, "Advances in medical robotic systems with specific applications in surgery-a review," *J. Med. Eng. Technol.*, vol. 35, no. 1, pp. 19–33, 2011.
- [96] J. Binder and W. Kramer, "Robotically-assisted laparoscopic radical prostatectomy," *BJU Int.*, vol. 87, no. 4, pp. 408–410, 2001.
- [97] H. Delingette, "Toward realistic soft-tissue modeling in medical simulation," *Proc. IEEE*, vol. 86, no. 3, pp. 512–523, 1998.

-
- [98] R. L. Williams II, W. Ji, J. N. Howell, and R. R. Conatser Jr, “In Vivo Measurement of Human Tissue Compliance,” in *submitted, SAE Digital Human Modeling Conference, Seattle, WA, 2007*.
- [99] L. S. Taylor, A. L. Lerner, D. J. Rubens, and K. J. Parker, “A Kelvin-Voigt fractional derivative model for viscoelastic characterization of liver tissue,” in *ASME 2002 International Mechanical Engineering Congress and Exposition, 2002*, pp. 447–448.
- [100] A. Wineman, “Nonlinear viscoelastic solids—a review,” *Math. Mech. Solids*, vol. 14, no. 3, pp. 300–366, 2009.
- [101] J. R. Funk, G. W. Hall, J. R. Crandall, and W. D. Pilkey, “Linear and quasi-linear viscoelastic characterization of ankle ligaments,” *J. Biomech. Eng.*, vol. 122, no. 1, pp. 15–22, 2000.
- [102] S. Leeman and A. Peyman, “The Maxwell Model as a Soft Tissue Descriptor,” in *Acoustical Imaging*, M. Halliwell and P. N. T. Wells, Eds. Springer US, 2002, pp. 357–361.
- [103] A. Takacs, J. K. Tar, T. Haidegger, and I. J. Rudas, “Applicability of the Maxwell-Kelvin model in soft tissue parameter estimation,” in *Intelligent Systems and Informatics (SISY), 2014 IEEE 12th International Symposium on*, 2014, pp. 115–119.
- [104] M. A. Del Nobile, S. Chillo, A. Mentana, and A. Baiano, “Use of the generalized Maxwell model for describing the stress relaxation behavior of solid-like foods,” *J. Food Eng.*, vol. 78, no. 3, pp. 978–983, 2007.
- [105] Y. C. Fung and S. C. Cowin, “Biomechanics: mechanical properties of living tissues,” *J. Appl. Mech.*, vol. 61, p. 1007, 1994.
- [106] M. T. Ahmadian and A. A. Nikooyan, “Modeling and prediction of soft tissue directional stiffness using in-vitro force-displacement data,” *Int J Sci Res*, vol. 16, pp. 385–389, 2006.
- [107] M. A. Meyers and K. K. Chawla, *Mechanical behavior of materials*, vol. 2. Cambridge University Press Cambridge, 2009.
- [108] E. A. López-Guerra and S. D. Solares, “Modeling viscoelasticity through spring–dashpot models in intermittent-contact atomic force microscopy,” *Beilstein J. Nanotechnol.*, vol. 5, no. 1, pp. 2149–2163, 2014.

-
- [109] J. O. Smith, "Physical audio signal processing," *Stanf. Univ. Httpccrma Stanf. Edu~Jospasp Online Book Date Last Viewed*, vol. 10, p. 12, 2010.
- [110] N. G. McCrum, C. P. Buckley, and C. B. Bucknall, *Principles of polymer engineering*. Oxford University Press, 1997.
- [111] S. M. H. Ahmadzadeh and D. W. Hukins, "Feasibility of using mixtures of silicone elastomers and silicone oils to model the mechanical behaviour of biological tissues," *Proc. Inst. Mech. Eng. [H]*, p. 0954411914540138, 2014.
- [112] F. H. DeLand and W. A. North, "Relationship Between Liver Size and Body Size 1," *Radiology*, vol. 91, no. 6, pp. 1195–1198, 1968.
- [113] E. J. Chen, J. Novakofski, W. K. Jenkins, and W. O'Brien, "Young's modulus measurements of soft tissues with application to elasticity imaging," *Ultrason. Ferroelectr. Freq. Control IEEE Trans. On*, vol. 43, no. 1, pp. 191–194, 1996.
- [114] S. A. Glantz and B. K. Slinker, *Primer of applied regression and analysis of variance*. McGraw-Hill, Health Professions Division, 1990.
- [115] I. Brouwer, J. Ustin, L. Bentiery, A. Dhruv, and F. Tendick, "Measuring in vivo animal soft tissue properties for haptic modeling in surgical," in *Medicine meets virtual reality*, 2001, vol. 81, p. 69.
- [116] F. J. Carter, T. G. Frank, P. J. Davies, D. McLean, and A. Cuschieri, "Measurements and modelling of the compliance of human and porcine organs," *Med. Image Anal.*, vol. 5, no. 4, pp. 231–236, 2001.
- [117] I. Sakuma, Y. Nishimura, C. K. Chui, E. Kobayashi, H. Inada, X. Chen, and T. Hisada, "In vitro measurement of mechanical properties of liver tissue under compression and elongation using a new test piece holding method with surgical glue," in *Surgery Simulation and Soft Tissue Modeling*, Springer, 2003, pp. 284–292.
- [118] J. T. Iivarinen, R. K. Korhonen, and J. S. Jurvelin, "Experimental and numerical analysis of soft tissue stiffness measurement using manual indentation device—significance of indentation geometry and soft tissue thickness," *Skin Res. Technol.*, 2013.
- [119] K. J. Parker, S. R. Huang, R. A. Musulin, and R. M. Lerner, "Tissue response to mechanical vibrations for 'sonoelasticity imaging,'" *Ultrasound Med. Biol.*, vol. 16, no. 3, pp. 241–246, 1990.

-
- [120] F. K. B. Freyberger, M. Kuschel, R. L. Klatzky, B. Farber, and M. Buss, “Visual-haptic perception of compliance: Direct matching of visual and haptic information,” in *Haptic, Audio and Visual Environments and Games, 2007. HAVE 2007. IEEE International Workshop on*, 2007, pp. 5–10.
- [121] A. P. Field and G. Hole, *How to design and report experiments*. Sage publications London, 2003.
- [122] M. L. Rogers, W. B. Heath, C. C. Uy, S. Suresh, and D. B. Kaber, “Effect of visual displays and locations on laparoscopic surgical training task,” *Appl. Ergon.*, 2012.
- [123] F. A. Wichmann and N. J. Hill, “The psychometric function: I. Fitting, sampling, and goodness of fit,” *Atten. Percept. Psychophys.*, vol. 63, no. 8, pp. 1293–1313, 2001.
- [124] J. Berkson, “A statistically precise and relatively simple method of estimating the bio-assay with quantal response, based on the logistic function,” *J. Am. Stat. Assoc.*, vol. 48, no. 263, pp. 565–599, 1953.
- [125] M. Kuss, F. Jäkel, and F. A. Wichmann, “Bayesian inference for psychometric functions,” *J. Vis.*, vol. 5, no. 5, p. 8, 2005.
- [126] S. A. Klein, “Measuring, estimating, and understanding the psychometric function: A commentary,” *Atten. Percept. Psychophys.*, vol. 63, no. 8, pp. 1421–1455, 2001.
- [127] W. B. Tiest and A. M. Kappers, “An antisymmetric psychometric function on a logarithmic scale,” *Perception*, vol. 40, no. 1, pp. 99–100, 2011.
- [128] W. M. Bergmann Tiest, “Tactual perception of material properties,” *Vision Res.*, vol. 50, no. 24, pp. 2775–2782, 2010.
- [129] H. Z. Tan, X. D. Pang, and N. I. Durlach, “Manual resolution of length, force, and compliance,” *Adv. Robot.*, vol. 42, pp. 13–18, 1992.
- [130] L. Meli, C. Pacchierotti, and D. Prattichizzo, “Sensory subtraction in robot-assisted surgery: fingertip skin deformation feedback to ensure safety and improve transparency in bimanual haptic interaction,” *Biomed. Eng. IEEE Trans. On*, vol. 61, no. 4, pp. 1318–1327, 2014.
- [131] F. K. Freyberger and B. Färber, “Compliance discrimination of deformable objects by squeezing with one and two fingers,” in *Proc. EuroHaptics*, 2006, vol. 2006, pp. 271–276.

-
- [132] S. E. Zürich, “Exploration of Augmented Reality Technology for Surgical Training Simulators,” SWISS FEDERAL INSTITUTE OF TECHNOLOGY ZURICH, 1976.
- [133] A. Lecuyer, L. George, and M. Marchal, “Toward Adaptive VR Simulators Combining Visual, Haptic, and Brain-Computer Interfaces,” *Comput. Graph. Appl. IEEE*, vol. 33, no. 5, pp. 18–23, 2013.
- [134] A. Lecuyer, S. Coquillart, A. Kheddar, P. Richard, and P. Coiffet, “Pseudo-haptic feedback: can isometric input devices simulate force feedback?,” in *Virtual Reality, 2000. Proceedings. IEEE*, 2000, pp. 83–90.
- [135] F. Argelaguet, T. Sato, T. Duval, Y. Kitamura, and A. Lécuyer, “Collaborative Pseudo-Haptics: Two-User Stiffness Discrimination Based on Visual Feedback,” in *Haptics: Neuroscience, Devices, Modeling, and Applications*, Springer, 2014, pp. 49–54.
- [136] F. Crison, A. Lécuyer, A. Savary, D. Mellet-d’Huart, J.-M. Burkhardt, and J.-L. Dautin, “The use of haptic and pseudo-haptic feedback for the technical training of milling,” in *EuroHaptics Conference poster, Munich, Germany, 2004*.
- [137] D. A. Gomez Jauregui, F. Argelaguet, A.-H. Olivier, M. Marchal, F. Multon, and A. Lecuyer, “Toward ‘Pseudo-Haptic Avatars’: Modifying the Visual Animation of Self-Avatar Can Simulate the Perception of Weight Lifting,” *Vis. Comput. Graph. IEEE Trans. On*, vol. 20, no. 4, pp. 654–661, 2014.
- [138] “Multi-Fingered Palpation using Pseudo-Haptic Feedback.” [Online]. Available: http://www.academia.edu/7689147/Multi-Fingered_Palpation_using_Pseudo-Haptic_Feedback. [Accessed: 19-Nov-2014].
- [139] M. O. Ernst and H. H. Bühlhoff, “Merging the senses into a robust percept,” *Trends Cogn. Sci.*, vol. 8, no. 4, pp. 162–169, 2004.
- [140] I. Surgical, “The da Vinci surgical system,” *Intuitive Surg. Inc Sunnyvale CA Available Httpwww Intuitivesurgical Com*, 2013.
- [141] C. Basdogan, C.-H. Ho, M. Srinivasan, and others, “Virtual environments for medical training: graphical and haptic simulation of laparoscopic common bile duct exploration,” *Mechatron. IeeeAsme Trans. On*, vol. 6, no. 3, pp. 269–285, 2001.

-
- [142] H. K. Çakmak and U. Kühnapfel, *Animation and simulation techniques for vr-training systems in endoscopic surgery*. Springer, 2000.
- [143] S. Cotin, H. Delingette, and N. Ayache, “Real-time elastic deformations of soft tissues for surgery simulation,” *Vis. Comput. Graph. IEEE Trans. On*, vol. 5, no. 1, pp. 62–73, 1999.
- [144] J. Brown, S. Sorkin, J.-C. Latombe, K. Montgomery, and M. Stephanides, “Algorithmic tools for real-time microsurgery simulation,” *Med. Image Anal.*, vol. 6, no. 3, pp. 289–300, 2002.
- [145] F. L. Ferrufino, J. V. Cohen, E. B. Schaffner, F. C. Eulufi, F. P. Müller, J. M. Castillo, N. J. Cassis, and C. B. Wilson, “Simulation in Laparoscopic Surgery,” *Cir. Esp. Engl. Ed.*, vol. 93, no. 1, pp. 4–11, 2015.
- [146] O. A. van der Meijden and M. P. Schijven, “The value of haptic feedback in conventional and robot-assisted minimal invasive surgery and virtual reality training: a current review,” *Surg. Endosc.*, vol. 23, no. 6, pp. 1180–1190, 2009.

Appendix A:

A.1. Consent form

The participant should complete the whole of this sheet himself/herself

	Please confirm the statements by putting your initials in the box below
I have read and understood the participant information sheet	
I have had the opportunity to ask questions and discuss this study	
I have received satisfactory answers to all of my questions	
I have received enough information about the study	
I understand that I am free to withdraw from the study:- 1 At any time 2 Without having to give a reason for withdrawing	
I understand that any information I provide, including personal details, will be confidential, stored securely and only accessed by those carrying out the study.	
(When relevant) I understand that any information I give may be included in published documents but my identity will be protected by the use of pseudonyms	
I have no claim on any intellectual property that results from this research, with no further compensation to me.	
I will not disclose or discuss any aspect of this study of it with anyone else.	
I do not have any eyesight or hand impairments	
I agree to take part in this study	
Participant Signature	Date

Name of Participant	
Researcher Signature	Date
Name of Researcher	EVAN FAKHOURY

A.2. Chapter 4 information sheet

Participant information and consent form:

Please read carefully (Before taking part in the experiment):

- This experiment aims to assess the impact of visual information on the ability to discriminate softness of compliant objects.
- This experiment is five-fold, each lasting no longer than 50 minutes, divided into 5 independent sessions.
- In the first session, you will be using your index finger to indent silicone stimuli located behind a curtain so as to obstruct any visual feedback.
- In the second session, you will be using a stylus to indent silicone stimuli located behind a curtain so as to obstruct any visual feedback.
- In the third session, you will be using a stylus to indent silicone stimuli located directly in front of you. Hence direct visual feedback is available.
- In the fourth session, you will be using a stylus to indent silicone stimuli located inside a light box. A webcam will transmit a video feed in real-time to a computer screen in front of you. Hence, the visual feedback available is only through a 2D screen.
- In the fifth session, you will be watching video recording on a computer monitor of the sample being indented by someone else. In this session, you will only have indirect visual access and cannot indent the samples yourself. Any judgement regarding softness of the samples needs to be made using visual information gathered by observing the recordings.

-
- All sessions are 2AFC experiments, meaning that for each presented pair, a decision always needs to be made regarding which is softer. If unsure, then your best guess is acceptable.
 - Your results will be analysed and psychometric functions will be extracted based on your responses.
 - You can leave at any time.
 - Your name, email address, and phone number will be saved only be used for the purposes of administering the experiment; the information will not be passed to other parties, and that, unless you agree to allow us to keep the information to invite you to take part in future studies, the data will be destroyed after the study.
 - The results of the experiment cannot be used to identify the individuals who took part.
 - You do not have any claim over intellectual property rights that may emerge from the research.
 - You should not disclose anything about the experiment to others.
 - The research protocol has been carefully designed, is informed by similar experiments in the literature, and is necessary for the advancement of knowledge.
 - Your responses during the experiment (from which no individual or personal data can be identified) make relevant primary data and research evidence accessible to others for the stated period (10 years) after completing the research, following the RCUK's recommendations (RCUK Policy and Code of Conduct on the Governance of Good Research Conduct, section 2, July 2009).
 - Thank you for taking part in this study.

A.3. Chapter 5

Participant information and consent form:

Please read carefully (Before taking part in the experiment):

- This experiment aims to assess the decision making process when discriminating compliance using only visual cues.
- This experiment is two-fold, each lasting no longer than 50 minutes, divided into 2 independent sessions.

-
- You will observe compliant stimuli pairs being indented by a linear actuator, and then asked to determine the ‘softer’ stimulus of each pair. This will be repeated for several stimuli.
 - Your results will be analysed and psychometric functions will be extracted based on your responses.
 - You can leave at any time.
 - Your name, email address, and phone number will be saved only be used for the purposes of administering the experiment; the information will not be passed to other parties, and that, unless you agree to allow us to keep the information to invite you to take part in future studies, the data will be destroyed after the study.
 - The results of the experiment cannot be used to identify the individuals who took part.
 - You do not have any claim over intellectual property rights that may emerge from the research.
 - You should not disclose anything about the experiment to others.
 - The research protocol has been carefully designed, is informed by similar experiments in the literature, and is necessary for the advancement of knowledge.
 - Your responses during the experiment (from which no individual or personal data can be identified) make relevant primary data and research evidence accessible to others for the stated period (10 years) after completing the research, following the RCUK’s recommendations (RCUK Policy and Code of Conduct on the Governance of Good Research Conduct, section 2, July 2009).
 - Thank you for taking part in this study.

A.4. Chapter 6

Participant information and consent form:

Please read carefully (Before taking part in the experiment):

- This experiment aims to assess the accuracy at which humans discriminate softness of compliant objects using this robotic system.
- This experiment is a single session lasting no longer than 45 minutes.
- You will be presented with pairs of soft stimuli with various levels of compliance.

-
- Within each pair, a reference sample with fixed compliance is presented alongside a test sample that keeps changing.
 - The order of the samples within each pair is randomised.
 - Using the stylus, you will be asked to indent each sample within each pair while following the on-screen instructions regarding speed and exerted force.
 - You will need to use the screen in front of you to observe the indentation process as direct visual access is blocked.
 - After you indent both stimuli within a pair, simply state which sample felt ‘softer’. Sample on the left is labelled ‘1’ while sample on the right is labelled ‘2’.
 - You can leave at any time.
 - Your name, email address, and phone number will be saved only be used for the purposes of administering the experiment; the information will not be passed to other parties, and that, unless you agree to allow us to keep the information to invite you to take part in future studies, the data will be destroyed after the study.
 - The results of the experiment cannot be used to identify the individuals who took part.
 - You do not have any claim over intellectual property rights that may emerge from the research.
 - You should not disclose anything about the experiment to others.
 - The research protocol has been carefully designed, is informed by similar experiments in the literature, and is necessary for the advancement of knowledge.
 - Your responses during the experiment (from which no individual or personal data can be identified) make relevant primary data and research evidence accessible to others for the stated period (10 years) after completing the research, following the RCUK’s recommendations (RCUK Policy and Code of Conduct on the Governance of Good Research Conduct, section 2, July 2009).
 - Thank you for taking part in this study.

A.5. Chapter 7

Participant information and consent form:

Please read carefully (Before taking part in the experiment):

-
- This experiment aims to determine the visual boundary of illusion using a pseudo-haptic feedback system.
 - This experiment is a single session lasting no longer than 45 minutes.
 - You will be presented with soft stimuli with various levels of compliance.
 - Using the stylus, you will be asked to indent each stimulus while following the on-screen instructions regarding speed and exerted force.
 - You will need to use the screen in front of you to observe the indentation process as direct visual access is blocked.
 - After you indent a stimulus, you will be asked to give that a stimulus a ‘softness rating’ based on the softness of the reference stimulus. The reference is given a softness rating of 100. This value is unit-less.
 - You can leave at any time.
 - Your name, email address, and phone number will be saved only be used for the purposes of administering the experiment; the information will not be passed to other parties, and that, unless you agree to allow us to keep the information to invite you to take part in future studies, the data will be destroyed after the study.
 - The results of the experiment cannot be used to identify the individuals who took part.
 - You do not have any claim over intellectual property rights that may emerge from the research.
 - You should not disclose anything about the experiment to others.
 - The research protocol has been carefully designed, is informed by similar experiments in the literature, and is necessary for the advancement of knowledge.
 - Your responses during the experiment (from which no individual or personal data can be identified) make relevant primary data and research evidence accessible to others for the stated period (10 years) after completing the research, following the RCUK’s recommendations (RCUK Policy and Code of Conduct on the Governance of Good Research Conduct, section 2, July 2009).
 - Thank you for taking part in this study.

Appendix B: Protocols

B.1. Chapter 6 Experiment Protocol

The following protocol was developed and used for the recruited 12 participants:

- Please take a seat facing the computer screen.
- In this experiment, you will be comparing the softness of a series of pairs of compliant samples, and stating which you think is the softer sample.
- You will be able to see the samples on the computer screen in front of you. A webcam is attached to the experiment set-up so that you are able to observe what is occurring on the screen in real-time.
- The stylus in front of you is used to move the robot arm (show participant location of robot arm for clarity purposes)
- Once instructed to begin, hold the stylus in front of you using your dominant hand as you would a pen to write or tap on a surface.
- Highlighted in dotted green, the position of the tip of the stylus is displayed on the illustration to the right of the sample on the screen. Move the stylus from the docked position until the tip of the hemispherical stylus schematic reaches the ‘start’ position. The start position marks the position at which the indenter tip meets the surface of the sample.
- Once in that position, you can now indent the sample.
- Try to stay within the range of motion described by the limiting maximum indentation. Avoid going into the red shaded region.
- Follow the position, motion and speed of the moving dotted line. The dotted green line is a guide that should be used to regulate your indentation speed and depth. This ensures controlled, accurate and repeatable results.
- While indenting the sample at the prescribed pace and maintaining accurate position with respect to the moving bar, shift your focus to the sample you are indenting on the screen.
- You can indent the sample as many times as you need until you have a feel for it.

-
- Once you are done, move the indenter back up to the dotted hemispherical dock. This resets the indentation process and allows the second sample in that pair to be presented.
 - Use the same indentation process as the first sample to indent the second sample.
 - Return the hemispherical tip halo to its dock after completing the indentation of the second sample.
 - After both indentations are finished, please state the following: In your opinion, which was the softer sample of the two?
 - ‘1’ would be your response if you thought the first sample was softer. ‘2’ would be if you thought the second sample was the softer one.
 - If you are unsure, please ask for the pair to be presented again before you make your final decision.
 - After you give a decision, a new pair will randomly be selected, and you will be presented with the samples one after the other just like earlier.

B.2. Chapter 7 Experiment Protocol

The following protocol was developed and used for all twelve participants:

- Please take a seat facing the computer screen.
- In this experiment, you will be comparing the softness of a series of pairs of compliant samples, and stating which you think is the softer sample.
- You will be able to see the samples on the computer screen in front of you. A webcam is attached to the experiment set-up so that you are able to observe what is occurring on the screen in real-time.
- The stylus in front of you is used to move the robot arm (show participant location of robot arm for clarity purposes)
- Once instructed to begin, hold the stylus in front of you using your dominant hand as you would a pen to write or tap on a surface.
- Highlighted in dotted green, the position of the tip of the stylus is displayed on the illustration to the right of the sample on the screen. Move the stylus from the docked position until the tip of the hemispherical stylus schematic

reaches the 'start' position. The start position marks the position at which the indenter tip meets the surface of the sample.

- Once in that position, you can now indent the sample.
- Please note that this is the reference sample, and it is given a softness rating of 100.
- Try to stay within the range of motion described by the limiting maximum indentation. Avoid going into the red shaded region.
- Follow the position, motion and speed of the moving dotted line. The dotted line is a guide that should be used to regulate your indentation speed and depth. This ensures controlled, accurate and repeatable results.
- While indenting the sample at the prescribed pace and maintaining accurate position with respect to the moving bar, shift your focus to the sample you are indenting on the screen.
- You can indent the sample as many times as you need until you have a feel for it.
- Try to associate the softness of this reference sample to the value of 100.
- Once you are done, move the indenter back up to the dotted hemispherical dock. This resets the indentation process and allows the second sample in that pair to be presented.
- Use the same indentation process as the reference sample to indent the test sample.
- Return the hemispherical tip halo to its dock after completing the indentation of the second sample.
- Now, based on the 100 value of softness given to the reference sample, please assign a softness rating to the test sample. Softer implies a larger rating and harder implies a smaller rating value. For instance, if you feel the test sample is twice as soft as the reference, then you could say 200. If you feel it is half as soft, then you would say 50.
- There is no right or wrong answer, and there are no upper or lower limits on ratings.
- If you are unsure, please ask for both the reference and current test sample to be presented again before you make your final decision.

-
- After you provide a softness rating for the test sample, a new pair will randomly be selected, and you will be presented with the same reference sample as before followed by a test sample selected at random.

Appendix C: Regression Analysis

Data

Table 20. R squared and root mean square error between model fits and experimental data for all samples

SAMPLE	MAXWELL		VOIGT		KELVIN	
	R^2	$RSME$	R^2	$RSME$	R^2	$RSME$
1	0.99931	0.0037	0.99861	0.0053	0.99534	0.0098
2	0.99967	0.0026	0.99375	0.0114	0.99944	0.0034
3	0.9998	0.0020	0.99445	0.0108	0.99972	0.0024
4	0.99969	0.0025	0.99363	0.0115	0.99951	0.0032
5	0.99976	0.0022	0.99409	0.0111	0.99959	0.0029
6	0.99979	0.0021	0.99457	0.0107	0.99939	0.0036
7	0.99969	0.0026	0.99409	0.0112	0.99951	0.0032
8	0.99972	0.0024	0.99417	0.0110	0.99954	0.0031
9	0.99978	0.0022	0.99464	0.0107	0.99971	0.0025
10	0.99968	0.0026	0.99483	0.0105	0.99968	0.0026
11	0.99972	0.0024	0.9949	0.0104	0.99972	0.0024

Appendix D: Discussion Analysis

Table 21. Dunn's between-tasks post hoc tests with corrections

<i>Task 1</i>	<i>Task 2</i>	<i>Statistical significance?</i>
Finger pad only	Direct vision + tool	Yes
Finger pad only	2D + tool	Yes
Finger pad only	Tool only	Yes
Finger pad only	2D only	Yes
Finger pad only	Fixed depth 2D	Yes
Finger pad only	Fixed force 2D	Yes
Finger pad only	Pseudo-Haptics 2AFC	Yes
Finger pad only	Boundary of illusion	Yes
Boundary of illusion	Direct vision + tool	Yes
Boundary of illusion	2D + tool	Yes
Boundary of illusion	Tool only	Yes
Boundary of illusion	2D only	Yes
Boundary of illusion	Fixed depth 2D	Yes
Boundary of illusion	Fixed force 2D	Yes
Boundary of illusion	Pseudo-Haptics 2AFC	Yes
Pseudo-Haptics 2AFC	Direct vision + tool	Yes
Pseudo-Haptics 2AFC	2D + tool	No
Pseudo-Haptics 2AFC	Tool only	Yes
Pseudo-Haptics 2AFC	2D only	No
Pseudo-Haptics 2AFC	Fixed depth 2D	Yes
Pseudo-Haptics 2AFC	Fixed force 2D	Yes
Fixed force 2D	Direct vision + tool	No
Fixed force 2D	2D + tool	Yes
Fixed force 2D	Tool only	Yes
Fixed force 2D	2D only	Yes
Fixed force 2D	Fixed depth 2D	Yes
Fixed depth 2D	Direct vision + tool	Yes
Fixed depth 2D	2D + tool	Yes
Fixed depth 2D	Tool only	Yes
Fixed depth 2D	2D only	Yes
2D only	Direct vision + tool	Yes
2D only	2D + tool	No
2D only	Tool only	No
Tool only	Direct vision + tool	Yes
Tool only	2D + tool	No
2D + tool	Direct vision + tool	Yes

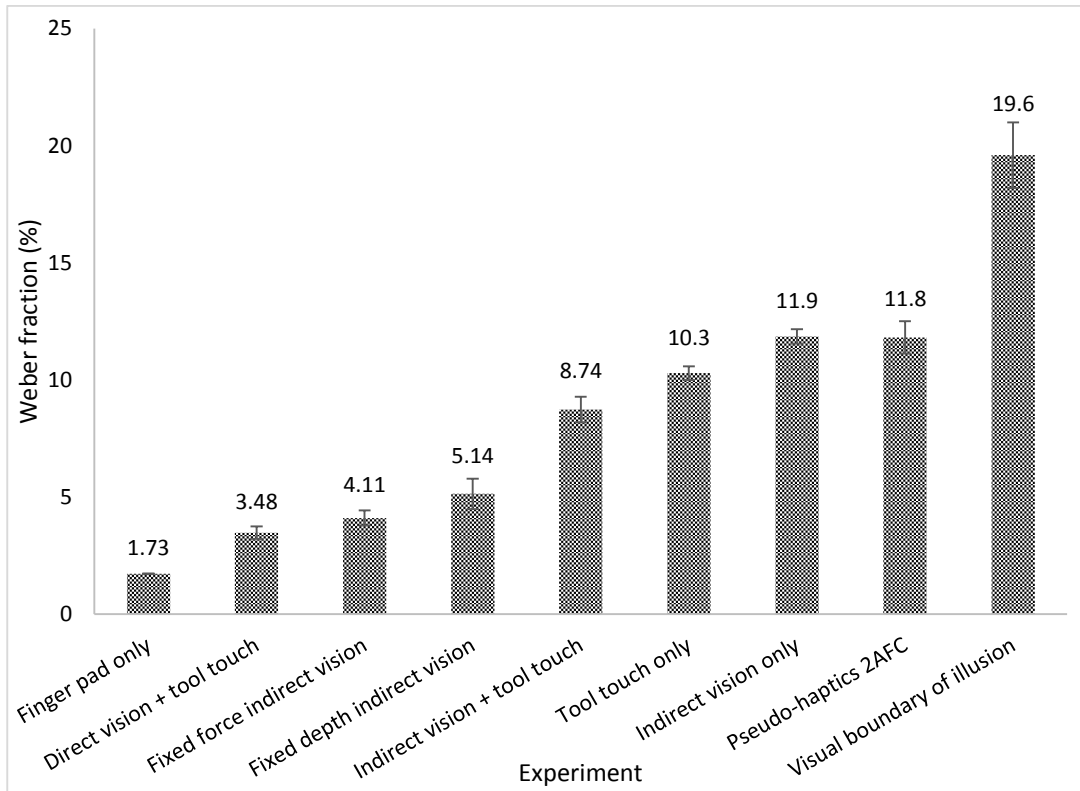


Figure 43. Average Weber fractions along with the standard error for all nine experiments conducted throughout the thesis